THESIS APPROVAL

GRADUATE SCHOOL, KASETSART UNIVERSITY

Master of Engineering (Materials Engineering)

DEGREE

Materials Engineering	Materials Engineering
FIELD	**DEPARTMENT**

TITLE: Preparation of Amphiphilic Polymer from Chemical Modification of Poly (γ-Glutamic Acid) (γ-PGA) for Use as a Sensing Material

NAME: Miss Nuorn Choothong

THIS THESIS HAS BEEN ACCEPTED BY

THESIS ADVISOR

(Miss Amornrat Lertworasirikul, D. Eng.)

THESIS CO-ADVISOR

(Assistant Professor Apirat Laobuthee, Ph.D.)

DEPARTMENT HEAD

(Assistant Professor Wisit Locharoenrat, M.Eng.)

APPROVED BY THE GRADUATE SCHOOL ON _____

DEAN

(Associate Professor Gunjana Theeragool, D.Agr.)

THESIS

PREPARATION OF AMPHIPHILIC POLYMER FROM CHEMICAL MODIFICATION OF POLY (γ-GLUTAMIC ACID) (γ-PGA) FOR USE AS A SENSING MATERIAL

NUORN CHOOTHONG

A Thesis Submitted in Partial Fulfillment of
the Requirements for the Degree of
Master of Engineering (Materials Engineering)
Graduate School, Kasetsart University
2012

Nuorn Choothong 2012: Preparation of Amphiphilic Polymer from Chemical Modification of Poly (γ-Glutamic Acid) (γ-PGA) for Use as a Sensing Material. Master of Engineering (Materials Engineering), Major Field: Materials Engineering, Department of Materials Engineering. Thesis Advisor: Miss Amornrat Lertworasirikul, D.Eng. 106 pages.

The aim of this research is to prepare sensitive and selective sensing materials based on poly (γ-glutamic acid), γ-PGA. Hydrophobic moieties, i.e. L-phenylalanine (L-PAE) and benzoxazine monomers (Bxs) were grafted onto γ-PGA. γ-PGA-*graft*-L-PAE having grafting degree of 30-50% showed thermoresponsive properties. The grafting degree of γ-PGA-*graft*-L-PAE had effect on thermoresponsive behavior. In aqueous solution, the copolymers with grafting degree about 49% showed thermoresponsive phenomenon at 80°C while the copolymers with grafting degree in range of 30-36% showed thermoresponsive properties when NaCl was added. Polymer concentration and polarity of solvent had effect on the thermoresponsive behavior. The clouding temperatures decreased as polymer concentration and NaCl concentration increased. The thermoresponsive phenomenon was reversible. Poly (γ-glutamic acid)-*graft*-3,4-dihydro-3-(2′-ethylhydroxyl)-6-methyl-1,3,2H-benzoxazine (γ-PGA-*graft*-Mt-Bx) and poly (γ-glutamic acid)-*graft*-3,4-dihydro-3-(2′-ethyl hydroxyl)-6-ethyl-1,3,2H-benzoxazine (γ-PGA-*graft*-Et-Bx)) were prepared by esterification reaction. The most attainable degree of conversion of γ-PGA-*graft*-Mt-Bx and γ-PGA-*graft*-Et-Bx were 30% and 25%, respectively. These graft copolymers showed a highly selective and sensitive recognition toward Cu (II) and Fe (III) ions in both aqueous and DMSO solutions. Dual responses, i.e. changes in color and solubility properties were observed in aqueous solution when the copolymers formed complexes with Cu (II) and Fe (III) ions. γ-PGA-*graft*-Mt-Bx showed higher adsorption efficiency than γ-PGA-*graft*-Et-Bx.

_____ / ___ / ___

Student's signature Thesis Advisor's signature

ACKNOWLEDGEMENTS

I am deeply indebted to my advisor, Dr. Amornrat Lertworasirikul for her advice, encouragement, and consistently valuable guidance throughout the duration of my graduate study and research. I would also like to thank my co-advisor, Assistant Professor Apirat Laobuthee for valuable suggestions and supports. Moreover, I would sincerely like to thank Professor Mitsuru Akashi, Associate Professor Toshiyuki Kida, Assistant Professor Michiya Matsusaki, Dr. Hiroaki Yoshida, and Mr. Masashi Matsumoto from Osaka University, Japan for their valuable comments and suggestions.

I would also greatfully thank Professor Suwabun Chirachanchai at The Petroleum and Petrochemical College, Chulalongkorn University for his kind support on using instruments such as freeze dryer, and Zeta nanosizer. In addition, I would like to thank all members in laboratory of Professor Suwabun for their kind helps in everything. Moreover, I would like to thank Assistant Professor Kiattawee Choowongkomon and members in his laboratory at Department of Biochemistry, Faculty of Science, Kasetsart University for their kindly supports on using freeze dryer and centrifuge.

I would like to thank all members of Amornrat's group and Apirat's group, Miss Apiwan Pumipichet, Miss Supamart Ngenruangroj, and Mr. Attapol Kaewvilai for their unconditional friendships. Moreover, I would also like to thank all staff at Department of Materials Engineering, Faculty of Engineering, Kasetsart University for their kind helps in everything.

I would like to thank my parents and my family for love, advice, encouragement, and especially financial support. Finally, thanks to all my friends for their love and generousness.

Nuorn Choothong

April, 2012

TABLE OF CONTENTS

Page

LIST OF TABLES

LIST OF FIGURES

LIST OF FIGURES (Continued)

LIST OF FIGURES (Continued)

LIST OF FIGURES (Continued)

LIST OF FIGURES (Continued)

LIST OF FIGURES (Continued)

LIST OF FIGURES (Continued)

LIST OF ABBREVIATIONS

γ-PGA	=	Poly (γ-glutamic acid)
L-PAE	=	L-Phenylalanine
Bxs	=	Benzoxazine monomers
Mt-Bx	=	3,4-Dihydro-3-(2′-ethylhydroxyl)-6-methyl-1,3,2H-benzoxazine
Et-Bx	=	3,4-Dihydro-3-(2′-ethyl hydroxyl)-6-ethyl-1,3,2H-benzoxazine
WSC	=	Water-soluble carbodiimide
T_{cloud}	=	Clouding temperature
^{o}C	=	Degree celcius
cm^{-1}	=	Per centimeter
ppm	=	Part per million
δ	=	Chemical shift
mmol	=	Millimole
g	=	Gram
mg	=	Milligram
mL	=	Millliter
min^{-1}	=	Per minute
μm	=	Micrometer
s	=	Second
M	=	Molar
%CD	=	Percentage of conversion degree or grafting degree
nm	=	Nanometer
λ_{max}	=	Maximum wavelength

PREPARATION OF AMPHIPHILIC POLYMER FROM CHEMICAL MODIFICATION OF POLY (γ-GLUTAMIC ACID) (γ-PGA) FOR USE AS A SENSING MATERIAL

INTRODUCTION

Our entire world is affected by variety of environmental problems. Some of the problems are acid rain, air pollution, global warming, hazardous waste, smog, water pollution, overpopulation, and rain forest destruction. These environment problems cause damage to human health. To solve these problems, the detection and removal techniques have become attractive research areas. Various technologies for the environmental detection have been developed, e.g. electrode sensors, gas sensors, pH sensors, thermal sensors, colorimetric sensors, and fluorescence microscopy. Selective, sensitive, and rapid sensing materials generated from biodegradable and biocompatible materials are required.

Poly (γ-glutamic acid) (γ-PGA) is a naturally occurring polyanionic polyamide. It is a major component of some Asian foods such as Natto, a Japanese fermented soya bean. This polymer is biodegradable and biocompatible. It has been applied in food, cosmetics, and medical fields (Lianga *et. al*., 2006; Shih *et. al.,* 2001; Takami, *et. al.,* 2005; Sung *et. al*., 2005). γ-PGA is a hydrophilic polymer. Its structure consists of a glutamic acid building block. The carboxylic acid side chains can be chemically modified to improve its functions. In this research, γ-PGA is chemically modified by grafting with hydrophobic moieties, i.e. L-phenylalanine ethyl ester (L-PAE) and benzoxazines (Bxs), at the carboxylic acid positions. The amphiphilic polymers thus obtained are expected to be useful for use as sensing materials for sensor devices.

This thesis is divided into two parts. The first part is related to chemically modification of the γ-PGA with L-phenylalanine ethyl ester (L-PAE). L-phenylalanine is a hydrophobic amino acid. It is reputed to exert anti-depressant properties. Poly(γ-

glutamic acid)-*graft*-L-phenylalanine (γ-PGA-*graft*-L-PAE) shows bioactivity, and it is biodegradable and nontoxic (Akagi *et al.,* 2005). Due to the amphiphilic characteristics of the copolymer, it has potential for use as a sensing material for biomedical and environmental fields. The copolymers with various grafting degrees are prepared. Their thermoresponsive properties are investigated and discussed.

The second part of the research is related to chemically modification of the γ-PGA with benzoxazines (Bxs). Bxs are heterocyclic compounds consisting of benzene and oxazine rings. They show inclusion properties, and can entrap metal ion (Chirachanchai *et al*., 2000). γ-PGA is a potential biosorbent for application in the removal and recovery of heavy metal (Sonny *et al.*, 2006). Combining of the benzoxazine into the γ-PGA structure is expected to yield a new type of material that can selectively trap the metal ions. Benzoxazines monomers are grafted into γ-PGA via an esterification reaction. Selectivity and sensitivity for metal ions is qualitatively and quantitatively studied.

OBJECTIVES

To synthesize amphiphilic polymers, i.e. poly(γ-glutamic acid)-*graft*-L-phenylalanine, poly (γ-glutamic acid)-*graft*-3,4-dihydro-3-(2′-ethylhydroxyl)-6-methyl-1,3,2H-benzoxazine, and poly (γ-glutamic acid)-*graft*-3,4-dihydro-3-(2′-ethyl hydroxyl)-6-ethyl-1,3,2H-benzoxazine, for use as sensing materials for thermo and colorimetric sensors

LITERATURE REVIEW

A sensor is a device that can detect and respond when the environmental quantity such as temperature, sound, light, force and pressure change. These quantity changes are translated to signal as an output. Stimuli-responsive polymers are polymers those change their structures and functions responding to the external physical and chemical conditions.

1. Thermoresponsive materials

One of the most important properties of thermoresponsive polymer is the presence of a critical solution temperature. Critical solution temperature is the temperature at which the transition phase of polymer solution occurred. If the presence of the phase transition of polymer solution is above this temperature, this polymer generally has a lower critical solution (LCST) (Gil *et al.*, 2004). Temperature responsive mechanism has been considerably investigated because it is relatively convenient and effective stimuli in many applications, especially for biomedical fields including drug delivery carriers, artificial muscles, biosensors, and scaffolds for tissue engineering. Thermoresponsive polymers are categorized into two types based on the difference in ability of intramolecular interaction. As for type I, the polymers are totally soluble in water at temperature below LCST since there is hydrogen bonding interaction between the polymer and water molecules. However, these interactions are broken at the temperature above LCST, and consequently the polymer chains collapse into globule conformation and then precipitate from the solution. For this type, an intramolecular coil-to-globule transition occurs before intermolecular aggregation through LCST, hence the collapse of individual polymer chains. Example of polymers those belong to type I are poly (N-isopropyl acrylamide) (PNIPAAm) and PNIPAAm-based copolymers, such as poly (N-isopropylacrylamide-co-2-hydroxyethylmethacrylate-6-hydroxyhexanoate), poly (N-isopropylacrylamide)-co-poly (ethylene glycol) methacrylate, poly (N-isopropyl acrylamide-co-methacrylic). PNIPAAm-based copolymers are well known and have received much

attention because they show LCSTs of approximately 30^{o}C, which are close to human body temperature.

Unlike type I, LCST transitions of type II are based on an amphiphilic balance or hydrophobic-hydrophilic balance of polymer. The hydrophilic/ hydrophobic balance can be adjusted by introducing hydrophilic or hydrophobic moieties on the polymer chain. During the LCST transition, the hydrophobic and hydrophilic balance of the copolymers is broken resulting in intermolecular aggregation. Example of polymers those belong to type II are block copolymers containing hydrophilic polyethylene oxide (PEO) segments, such as poly (ethylene oxide-b-propylene oxide) and poly (lactide-b-ethylene oxide).

Most thermoresponsive polymers reported so far are based on synthetic polymers which are non-biodegradable, lack of biocompatible and/or cytotoxic materials. Amino acid-based materials, e.g. elastin-like polypeptides, pegylated poly-L-glutamates, poly (asparagine) derivatives, have been remarkably developed to achieve the biodegradation and biocompatibility properties. Nonetheless, they are synthetic polypeptides or oligopeptides. Natural occurring polypeptides are expected to yield a novel thermoresponsive polymers those show excellent biocompatibility, biodegradation, useful bioactivity and nontoxicity.

Poly(γ-glutamic acid) (γ-PGA) is an anionic polypeptides produced by some Bacillus strains as a capsular or an extracellular viscous material. It is a main constituent of the sticky material in natto, Japanese fermented food made from soybeans. γ-PGA is water soluble, biodegradable and nontoxic for humans and the environment. Its utility has been proposed in the fields of cosmetics, medicine and water treatment. γ-PGA structure comprised of glutamic acid building block which its carboxylic acid side chains can be chemically modified to modulate its functions (Figure 1).

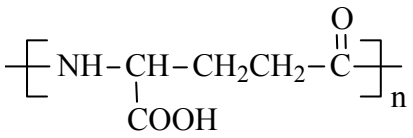

Figure 1 Chemical structure of γ-PGA.

In 2004, Shimokuri (Shimokuri *et al*., 2004) modified γ-PGA with propyl group via esterification to produce a biodegradable polymer that shows thermoresponsive properties by controlling the hydrophobic-hydrophilic balance of the polymer chain. The results indicated that none of the samples showed thermosensitivity in pure water. On the other hand, they showed a clouding behavior upon heating when NaCl was added. The clouding temperature (LCST) could be controlled by a change of the NaCl concentration and polymer concentration.

In 2005, Akagi (Akagi et al., 2005) prepared amphiphilic grafted copolymer from γ-PGA and L-PAE (Figure 3). L-PAE is a non-polar amino acid (Figure 2). It is used in healthy, pharmaceutical and food products (Buruiana et al., 2010)

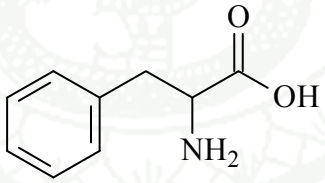

Figure 2 Chemical structure of L-PAE.

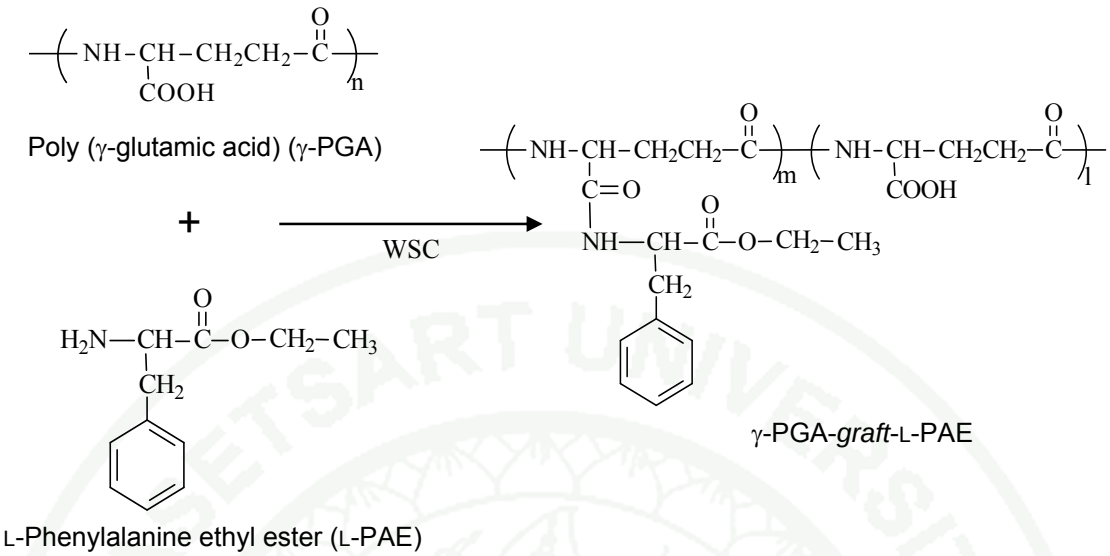

Figure 3 Schematic illustration of γ-PGA-*graft*-L-PAE.

L-PAE was a hydrophobic moiety. It was grafted onto the γ-PGA hydrophilic backbone. The degree of L-PAE grafting depended on amount of water-soluble carbodiimide (WSC) used during the synthesis process. This grafted copolymer could be prepared in the form of nanoparticles and applied as a protein carrier. An in vitro cytotoxicity testing of this copolymer showed that γ-PGA-*graft*-L-PAE nanoparticles did not induce any cytotoxicity against HL-60 cells and could be used as protein carriers without significant cytotoxic effect. γ-PGA-*graft*-L-PAE was able to be hydrolyzed to glutamic acid by γ-glutamic transpeptidase (γ-GTP). Figure 4 shows the SEM images of the enzymatic degradation. After degradation for 2-4 h, their spherical shape size was gradually lost. With the further degradation, this graft copolymer disappeared completely (Akagi et al., 2005). Due to the bioactivity, biodegradability and nontoxicity of γ-PGA-*graft*-L-PAEs together with their amphiphilic characteristics, the copolymers has potential to be used as a thermoresponsive polymer for biomedical and environmental fields.

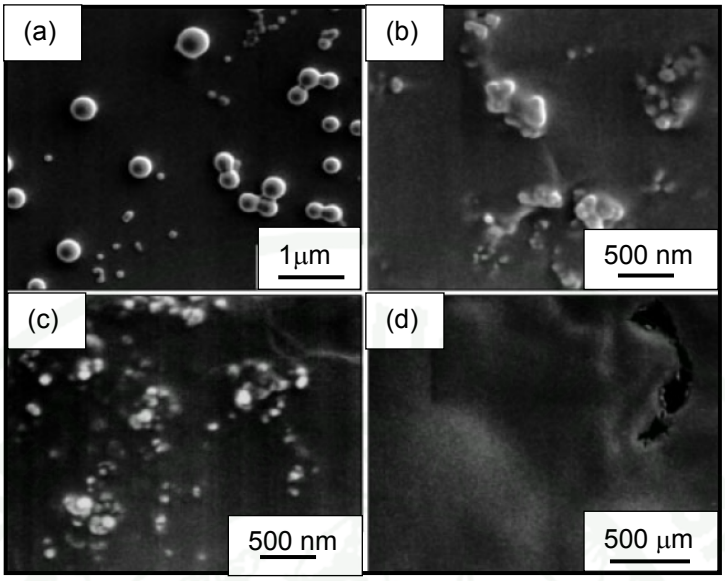

Figure 4 SEM images of γ-PGA-*graft*-L-PAE following enzymatic degradation with γ-GTP; (a) before degradation, (b) after 2h of degradation, (c) after 4 h of degradation, and (d) after 6 h of degradation.

2. Colorimetric materials

In recent year, methods for selective and sensitive detection of metal ions have received a great attention. A number of metal ions sensors have been developed, for example, colorimetric sensor. The colorimetric sensor is generally well known, and commonly used for routine analysis. Colorimetric sensors that provide immediately change in optical have been interested due to their simplicity, rapidity, high sensitivity and ease of detection by human eye. The colorimetric sensors of metal ions are based on a specific chemical reaction or complex formation between the sensor molecule and target species. Therefore, suitable material for using as a substrate of the colorimetric sensor should be a compound that can interact with the metal ions.

γ-PGA and their derivatives are not useful only in drug delivery and tissue engineering fields but also useful in environmental application. McLean (McLean *et al*., 1990) reported that γ-PGA could bind several metal ions such as Ni (II), Cu (II), Mn (III) and Cr (III).

In 2008, Mamdolna (Mamdolna *et al.*, 2008) reported a complex formation between γ-PGA and lead (II) ions. The complex formation was generated by the cross-linked of the carboxylic functional groups of linear γ-PGA chain and lead (II) ions. This copolymer could form stable nanoparticles and has a potential for wastewater treatment.

In 2009, Inbaraj (Inbaraj et al., 2009) used γ-PGA as a natural adsorbent for the mercury (II) adsorption. From this study, γ-PGA interacted with mercury (II) by using their carboxylic acid and amide functional groups. Additionally, γ-PGA binded with mercury (II) could be recovered by using acid solution (pH 2). The reused γ-PGA showed small loss in adsorption efficiency during five cycles of operation.

Hikichi (Hikichi *et al*., 1990) used ^{1}H and ^{13}C-NMR methods to obtain polymer-metal complex structure. The ^{1}H-NMR results are shown in Figure 5. Peak at α-proton was broaden when Cu (II) ions was added to γ-PGA solution. The authors concluded that the oxygen atom of the side chain carboxyl group of γ-PGA binds to Cu (II) ions in aqueous solution at neutral pH and at room temperature. In addition, the results obtained from ^{13}C-NMR spectra suggested that the complex formation was occurred by the oxygen atom of the side-chain carboxyl group and probably also the nitrogen atom of amide group interacted with Cu (II).

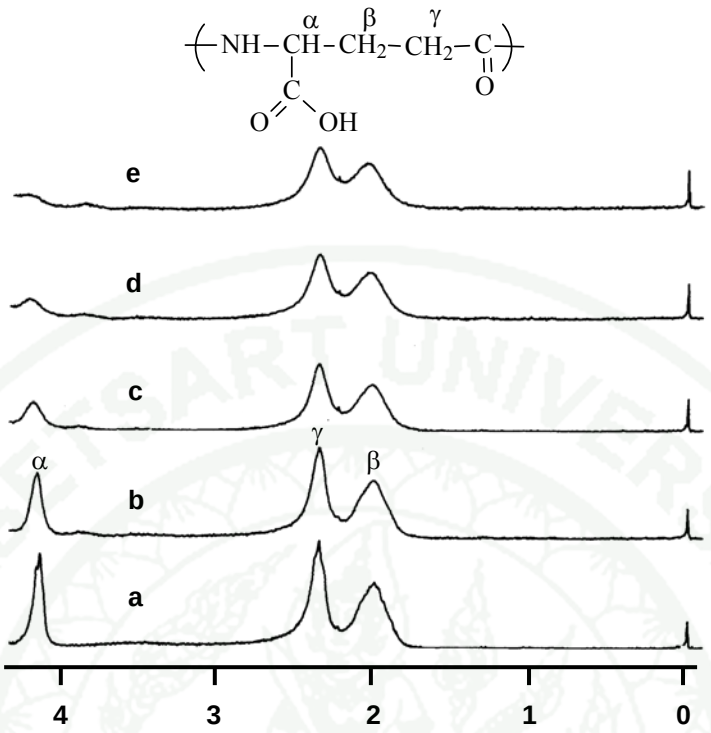

Figure 5 ^{1}H-NMR spectra of γ-PGA in D_2O at various Cu (II) concentration at room temperature amd neutral pH with (a) $f = 0$, (b) $f = 5 \times 10^{-3}$, (c) $f = 1 \times 10^{-2}$, (d) $f = 2 \times 10^{-2}$, and (e) $f = 5 \times 10^{-2}$.

Although γ-PGA shows potential for development to be a sensing material for metal ions, the selectivity and efficiency should be improved.

Supramolecular compounds or host-guest compounds are the most complexes used in colorimetric sensors. The host molecules can either be acyclic molecules such as cholic acid or cyclic compounds such as cyclodextrin, crown ether and calixarenes while the guest molecules can be neutral molecules, cations, and anions depending on the host cavity. The specific interactions between host and guest molecules bring about an inclusion phenomenon which relates to many potential applications especially for use as ions extraction material in environmental application. Benzoxazines (Bx), heterocyclic compounds consisting of benzene and oxazine ring, is one of materials that show supramolecular properties, and have been received much attention in the past few decades.

In 1999, Chirachanchai (Chirachanchai *et al.,* 2000) focused on the supramolecular properties of bis (3,4-dihydro-2H-3-methyl-1,3-benzoxazinyl) isopropane, BA-m (Figure 6) and proposed this compound as a novel ion extraction material. This research studied the ionophore reaction between BA-m with ions of alkaline and alkaline earth metals. The ion extraction phenomenon was observed by using the Pedersen's technique in liquid-liquid system at room temperature. From Figure 7, BA-m showed the extraction ability with various metal ions via molecular assembly by using their oxygen and nitrogen atoms. The amount of entrapped ion increased as a monomer concentration increased (Figure 8).

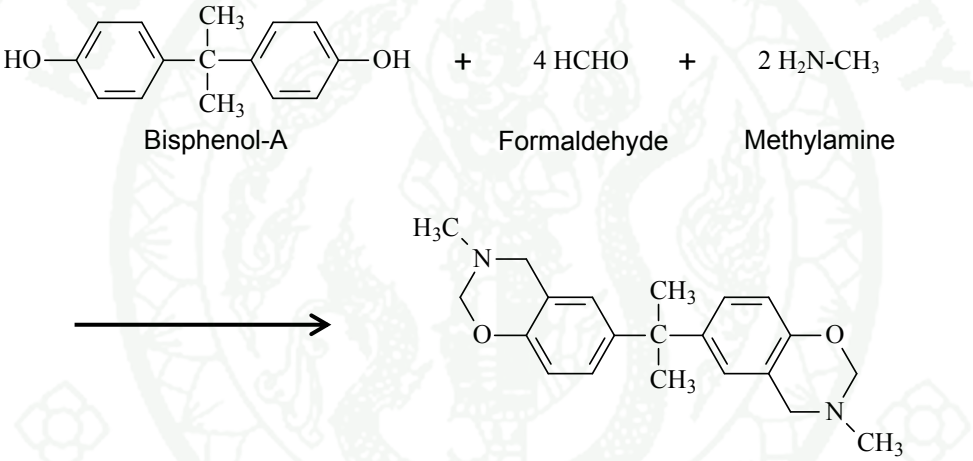

Figure 6 Preparation of BA-m.

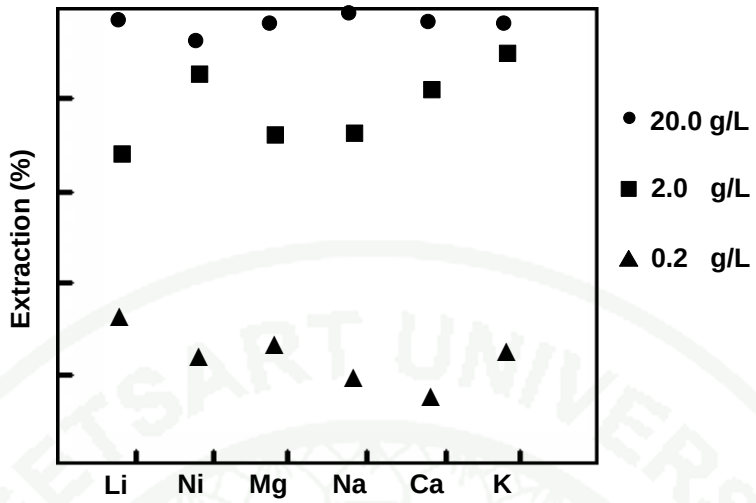

Figure 7 The ion extraction efficiently of bis (3,4-dihydro-2H-3-methyl-1,3-benzoxazinyl) isopropane, BA-m with various concentrations in dichloromethane solution.

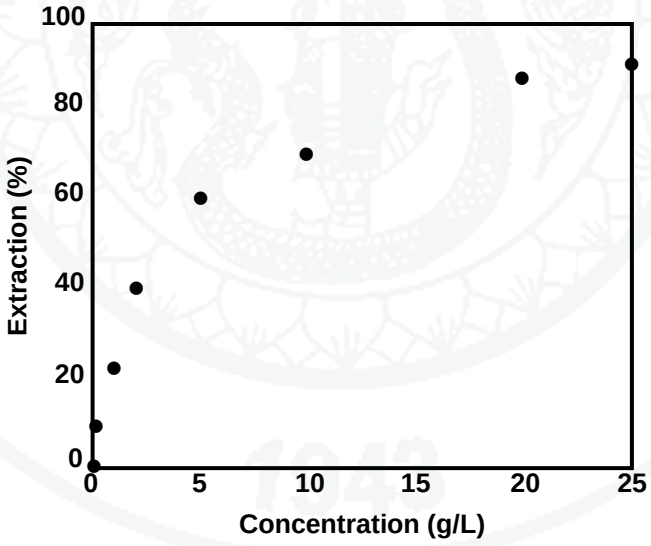

Figure 8 The ion extraction efficiency of the Ca^{2+} ion as a function of the bis (3,4-dihydro-2H-3-methyl-1,3-benzoxazinyl) isopropane, BA-m monomer concentration in dichloromethane solution.

In addition, the efficiency of ions extraction of BA-m was compared with essential inclusion compounds such as 18-crown-6, calix [4] arene, calix [6] arene,

and calix [8] arene for the lithium (Figure 9) (Yamagishi et al., 1996). The results showed that the extraction efficiency of the Bx is the highest at nearly 80%.

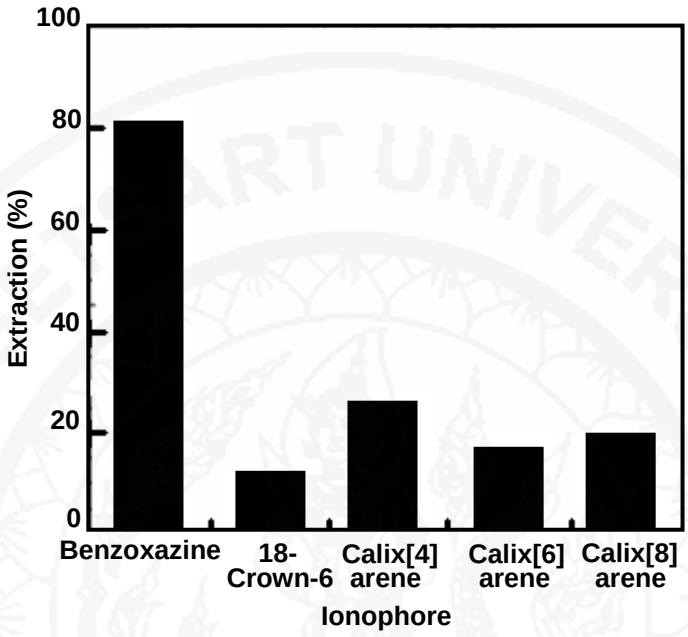

Figure 9 Comparison of the ion extraction efficiency of the bis (3,4-dihydro-2H-3-methyl-1,3-benzoxazinyl) isopropane, BA-m monomer with 18-crown-6, calyx [4] arene, calyx [6] arene, and calyx [8] arene.

MATERIALS AND METHODS

Materials

Poly (γ-glutamic acid) (γ-PGA, $\overline{M_w}$ = 200,000-500,000) was obtained from Wako Pure Chemical Industries (Japan). L-Phenylalanine ethylester hydrochlorides (L-PAE), sodium hydrogen carbonate ($NaHCO_3$) and dimethyl sulfoxide (DMSO, GC grade 99.5%) were obtained from Sigma-Aldrich (China). 1-Ethyl-3-(3-dimethylaminopropyl) carbodiimide or water soluble carbodiimide (WSC) was purchased from Wako Pure Chemical Industries (Japan). Sodium chloride (NaCl) was obtained from AnalaR (English). WSC and NaCl were dried at 50°C for 3 hours before used. Acetonitrile (CH_3CN) was purchased from LABSCAN (Thailand). Sulfuric acid was purchased from Carlo Erba. Analytical grade of copper (II) sulfate hexahydrate ($CuSO_4 \cdot 6H_2O$), nickel (II) chloride hexahydrate ($NiCl_2 \cdot 6H_2O$), cobalt (II) nitrate hexahydrate ($Co(NO_3)_2 \cdot 6H_2O$, zinc (II) chloride ($ZnCl_2$), and iron (III) nitrate ($Fe(NO_3)_3 \cdot 9H_2O$) were purchased from Ajax (New Zealand). All purchased chemicals were used without further purification. Benzoxazines (3,4-dihydro-3-(2′-ethylhydroxyl)-6-methyl-1,3,2H-benzoxazine, Mt-Bx, and 3,4-dihydro-3-(2′-ethyl hydroxyl)-6-ethyl-1,3,2H-benzoxazine, Et-Bx) were synthesized by following the method reported by Kaewvilai (Kaewilai et al., 2012). Cellulose dialysis membrane (MWCO: 10,000) was purchased from Dimethyl/Por® (Japan). Ultra-pure water was used for an investigation of thermoresponsive properties.

Instruments

Fourier transform infrared (FT-IR) spectra were recorded on a Bruker Alpha-E spectrometer. ^{1}H-nuclear magnetic resonance (^{1}H-NMR) spectra were recorded on a Varian Mercury-400 spectrometer with working frequency 400 MHz. Particle size distribution and surface charge were measured by using a Zetasizer Nano ZS (Malvern Instruments, U.K.).

Clouding temperature was determined from changes of the transmittance at 500 nm against temperature using JASCO V-550 UV/VIS spectrophotometer. Metal-ions-responsive properties were investigated by using Shimadzu UV-1700 spectrophotometer.

Methods

1. Chemically modification of poly (γ-glutamic acid) (γ-PGA) with L-phenylalanine (L-PAE)

1.1 Synthesis of poly (γ-glutamic acid)-*graft*-L-phenylalanine (γ-PGA-*graft*-L-PAE)

γ-PGA-*graft*-L-PAE was synthesized by using γ-PGA and L-PAE as reactants, and using WSC as a catalyst. The synthesis reaction of γ-PGA-*graft*-L-PAE was shown in Figure 10.

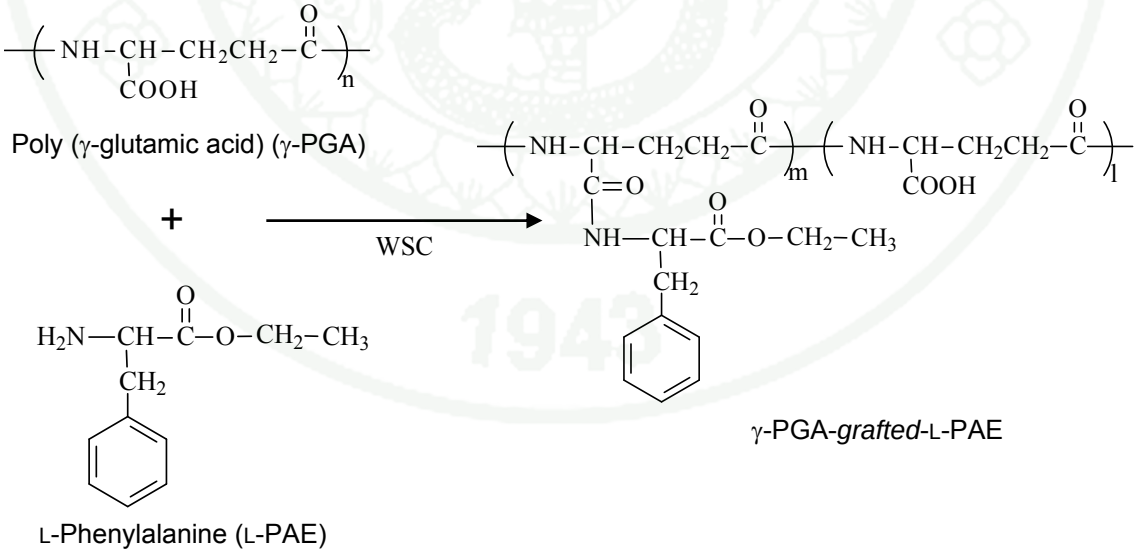

Figure 10 Schematic illustration of γ-PGA-*graft*-L-PAE.

γ-PGA (606.3 mg, 4.7 mmol of glutamic acid repeating units) was dissolved in 0.1 M $NaHCO_3$ (100 mL) in an erlenmeyer flask at 4 °C for 15 minutes. WSC (96-3604 mg, 0.5-19.6 mmol) were then added in each of the solution by following the conditions in Table 1. The mixtures were stirred at 4 °C for 30 minutes. After that L-PAE (1080 mg, 4.7 mmol) was added and stirred at 4 °C for 1 hour. These mixtures were stirred overnight at room temperature. The solutions were dialyzed through dialysis tube. The distilled water was changed every 30 minutes during the first 8 hours, and then 12 hours for 7 days. The purified product solutions were dried by freeze dryer for 3 days.

Table 1 Amount of chemicals for synthesis of γ-PGA-*graft*-L-PAE.

Sample	γ-PGA		WSC		L-PAE	
	mmol	mg	mmol	mg	mmol	mg
1	4.7	606.3	0.5	96	4.7	1080
2	4.7	606.3	1.2	230	4.7	1080
3	4.7	606.3	3.5	671	4.7	1080
4	4.7	606.3	3.8	728	4.7	1080
5	4.7	606.3	4.7	901	4.7	1080
6	4.7	606.3	9.4	1802	4.7	1080
7	4.7	606.3	14.1	2703	4.7	1080
8	4.7	606.3	19.6	3604	4.7	1080

1.2 Characterization of γ-PGA-*graft*-L-PAE

The chemical structures of the obtained γ-PGA-*graft*-L-PAE were characterized by FT-IR and ^{1}H-NMR spectroscopies. The samples for FT-IR technique were measured with 32 scans at a resolution 16 cm^{-1} over the range from 4000 to 600 cm^{-1}. ^{1}H-NMR technique was measured in dimethyl sulfoxide-d_6 (DMSO-d_6) and ^{1}H-NMR chemical shift in parts per million (ppm) were recorded from 0.00 ppm to 9.00 ppm using tetramethylsilane (TMS) as an internal standard.

Particle size of γ-PGA-*g*raft-L-PAE were determined by dynamic light scattering (DLS) method. The γ-PGA-*graft*-L-PAE suspension was filtered through Millipore nylon filters (pore size 0.4μm) to eliminate dust and large contaminants.

Thermoresponsive behaviors of γ-PGA-*graft*-L-PAE samples were investigated by eye detection and UV-Vis spectroscopy. Polymer solutions were heated to 80 °C, and then cooled to 0 ^{o}C, alternatively. The UV-Vis spectroscopy were performed using heating and cooling rates of 0.5 $^{o}C \cdot min^{-1}$. The temperature dependence of the light transmittance with a wavelength of 500 nm was monitored, and clouding temperature (T_{cloud}) was determined as the temperature at which transmittance decreased to half of its initial value. The polymer solutions were centrifuged to remove aggregates before measurement.

2. Chemically modification of poly (γ-glutamic acid) (γ-PGA) with benzoxazine monomers (Bxs).

2.1 Synthesis of poly (γ-glutamic acid)-*graft* -benzoxazine monomers (γ-PGA-*graft*-Bxs)

3,4-Dihydro-3-(2′-ethyl hydroxyl)-6-methyl-1,3,2H-benzoxazine (Mt-Bx) and 3,4-dihydro-3-(2′-ethyl hydroxyl)-6-ethyl-1,3,2H-benzoxazine (Et-Bx) were used to graft onto γ-PGA backbone. γ-PGA-*graft*-Mt-Bx and γ-PGA-*graft*-Et-Bx were synthesized via the esterification reaction as shown in Figure 11 and Figure 12, respectively.

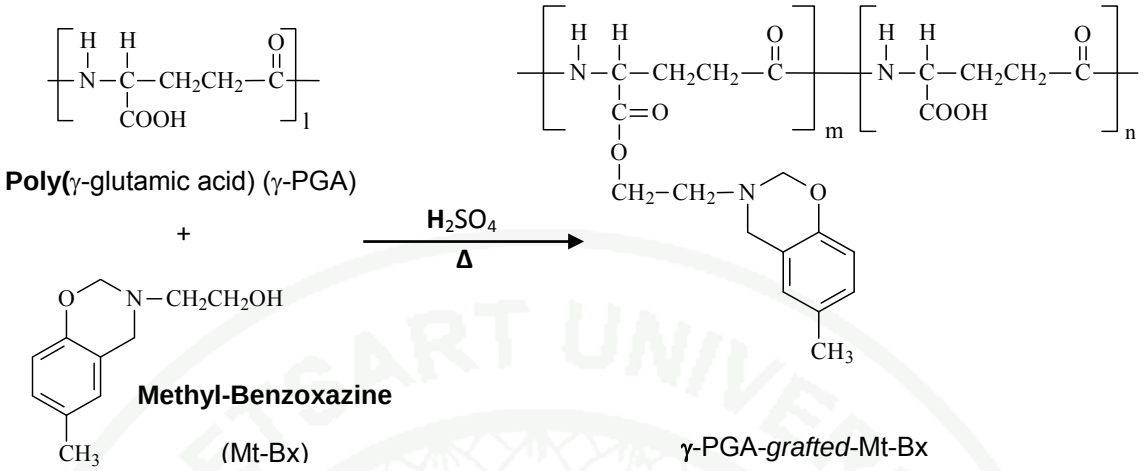

Figure 11 Schematic illustration of γ-PGA-*graft*-Mt-Bx synthesis.

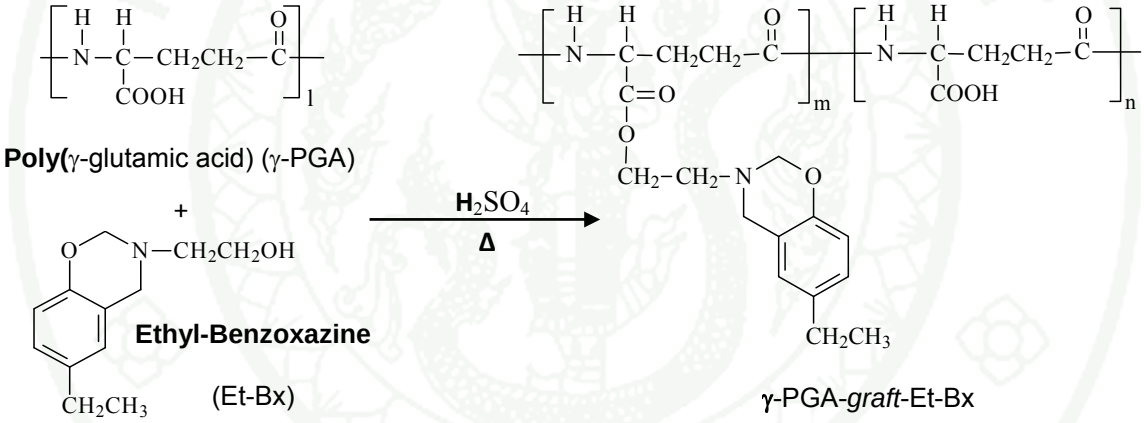

Figure 12 Schematic illustration of γ-PGA-*graft*-Et-Bx synthesis.

γ-PGA (1.0 g, 2.0 mmol) was dispersed in CH_3CN (100 mL) inside a two-neck round bottom flask equipped with a magnetic stir bar, a condenser and a dropping funnel. After that, 80 mL of acetonitrile solution of Mt-Bx (1.5 g, 7.75 mmol) or Et-Bx (1.5 g, 7.75 mmol) was slowly drip-fed into the slurry. The mixture was further refluxed and vigorously stirred at 80°C. The optimum reaction time was determined by using FT-IR spectra. The solid products were purified by washed several times with distilled water and acetone, and then dried in an oven overnight at 60°C.

2.2 Study on metal-ions-responsive properties of γ-PGA-*graft*-Bxs

The responsivenesses of γ-PGA-*graft*-Mt-Bx and γ-PGA-*graft*-Et-Bx toward Cu (II), Co (II), Ni (II), Zn (II) and Fe (III) ions were primary investigated in aqueous solution. Aqueous solutions of $CuSO_4$, Co $(NO_3)_2$, $NiCl_2$, $ZnCl_2$ and Fe $(NO_2)_3$ were used in this study. The γ-PGA-*graft*-Mt-Bx powder (1.0 mg) or γ-PGA-*graft*-Et-Bx powder (2.0 mg) was added to each metal ion solution (1.00 mM for γ-PGA-*graft*-Mt-Bx and 5.00 mM for γ-PGA-*graft*-Et-Bx). The mixed solutions were detected visually and were also UV-visible spectrophotometer.

The metal-ions responsive properties were quantitatively studied by photometric titration method in a DMSO solution. Different volumes of DMSO solution of γ-PGA-*graft*-Mt-Bx (0.02 mM) or γ-PGA-*graft*-Et-Bx (0.008 mM) (Table 2) were added to each metal salt solution (0.40 mM). The mixed solutions were then adjusted with DMSO to attain a total volume of 10.00 mL.

Table 2 Volume of γ-PGA-*graft*-Bx used in photometric titration method.

No. of test	0.02 mM γ-PGA-*graft*-Mt-Bx	0.008 mM γ-PGA-*graft*-Et-Bx	No. of test	0.02 mM γ-PGA-*graft*-Mt-Bx	0.008 mM γ-PGA-*graft*-Et-Bx
1	0.025	0.100	11	0.275	1.600
2	0.050	0.200	12	0.300	1.800
3	0.075	0.300	13	0.325	2.000
4	0.100	0.400	14	0.350	2.500
5	0.125	0.500	15	0.375	3.000
6	0.150	0.600	16	0.400	3.500
7	0.175	0.800	17	0.450	4.000
8	0.200	1.000	18	0.500	4.500
9	0.225	1.200	19	0.550	5.000
10	0.250	1.400			

RESULTS AND DISCUSSION

1. Study on thermoresponsive properties of γ-PGA-*graft*-L-PAEs

1.1 Preparation and characterization of γ-PGA-*graft*-L-PAEs

The γ-PGA-*graft*-L-PAEs obtained after freeze drying were white foam-like materials (Figure 13).

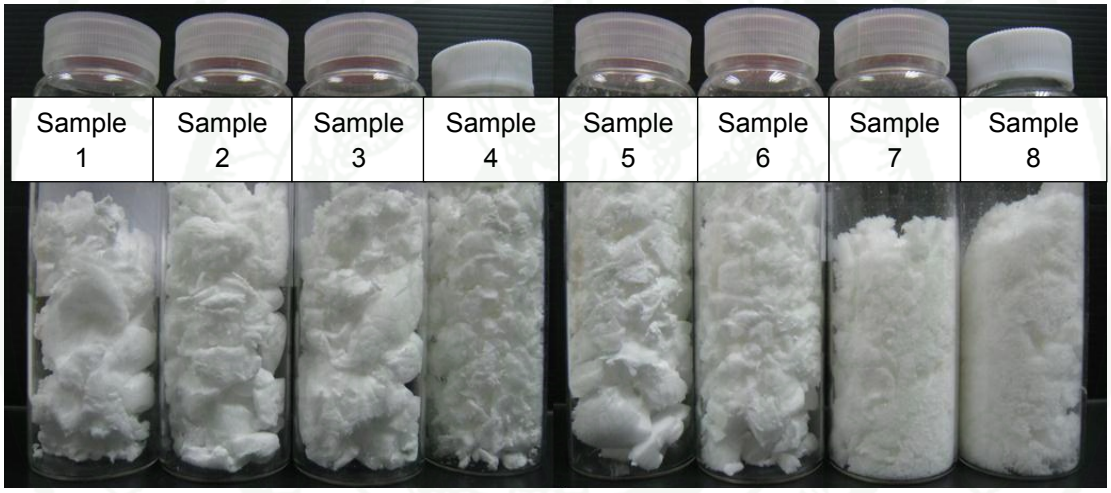

Figure 13 Appearances of γ-PGA-*graft*-L-PAEs (sample 1-8)

The FT-IR spectra of γ-PGA, L-PAE and γ-PGA-*graft*-L-PAEs were shown in Figure 14. The absorption peaks at 3280 cm^{-1} and 1580 cm^{-1} indicated the amide bonds, and peaks at 3072-3028 cm^{-1} and 1445 cm^{-1} showed the presence of aromatic rings in structures of the copolymers. For sample number 4-8, the appearance of absorption peak at around 1630-1640 cm^{-1} was clearly observed. The results indicated that an increasing of WSC content in synthesis process had effect on an increasing of amide bonds in the obtained copolymers. Since L-PAE was grafted onto γ-PGA via the amide bond, the obtained spectra of the copolymers revealed that a grafting degree increased as WSC content increased.

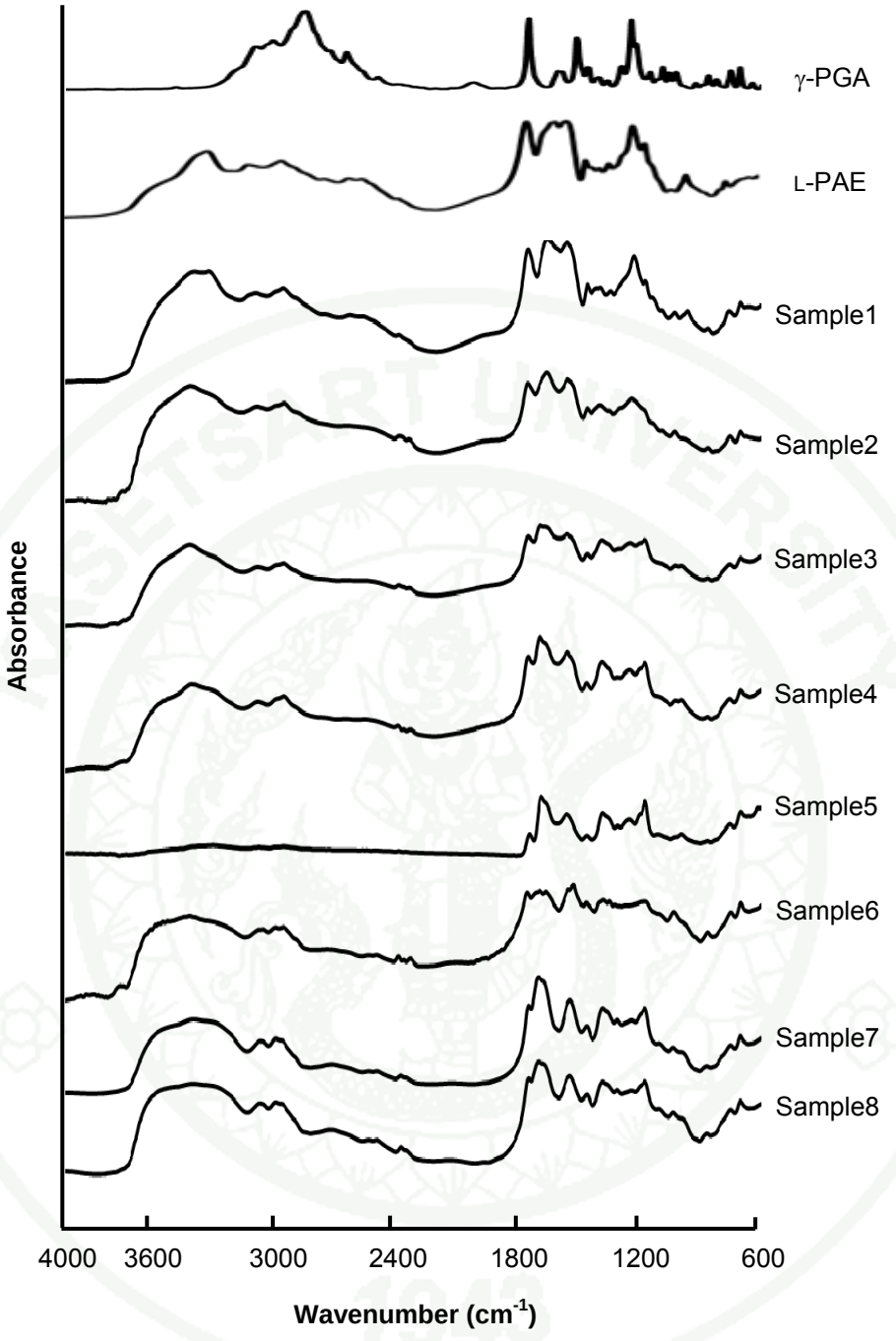

Figure 14 FT-IR spectra of γ-PGA, L-PAE and γ-PGA-*graft*-L-PAEs.

^{1}H-NMR technique was used to confirm the chemical structures of γ-PGA-*graft*-L-PAEs. Figure 15 showed ^{1}H-NMR spectra of γ-PGA-*graft*-L-PAEs comparing with those of γ-PGA and L-PAE.

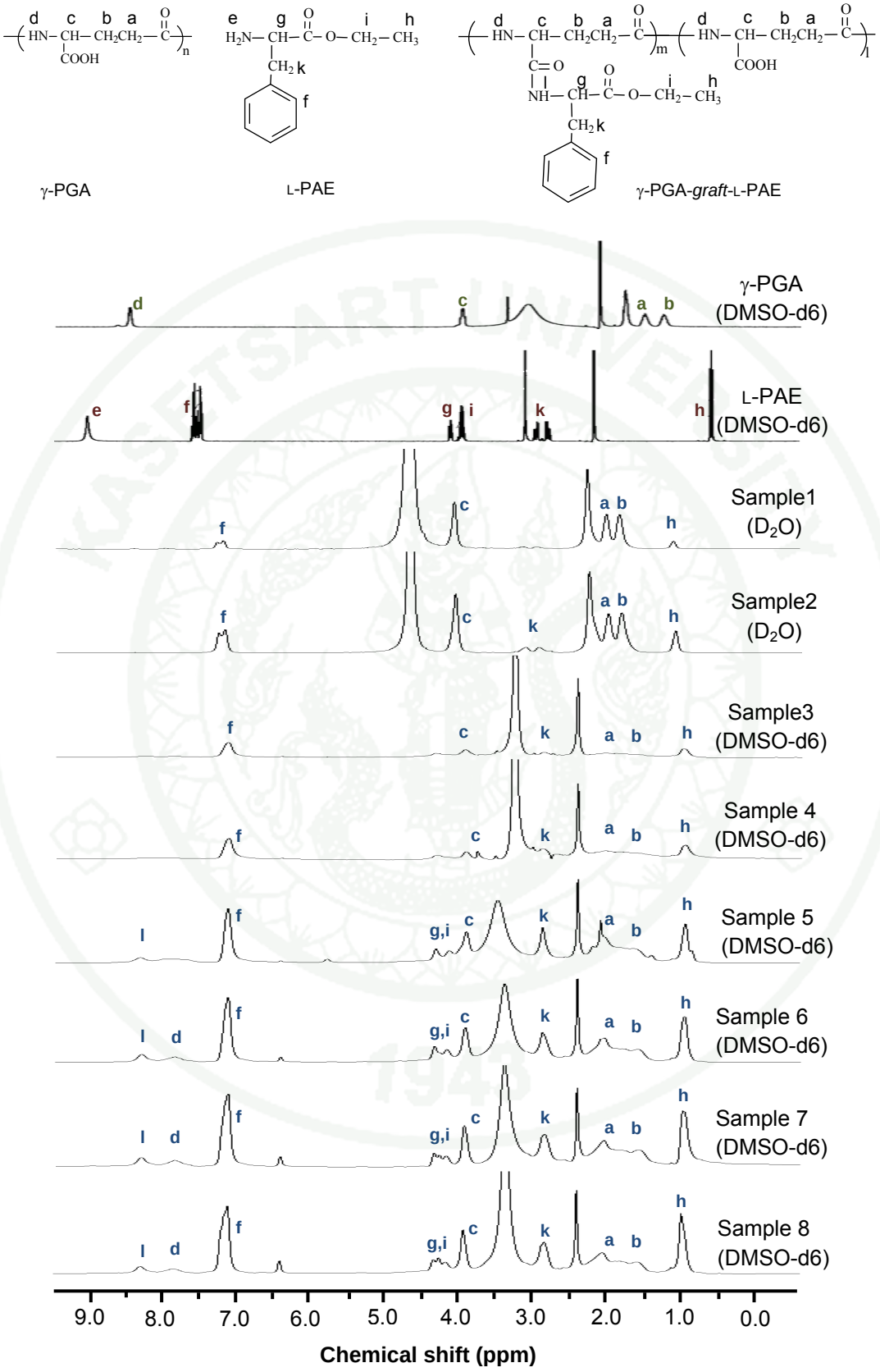

Figure 15 ^{1}H-NMR spectra of γ-PGA, L-PAE and γ-PGA-*graft*-L-PAEs.

γ-PGA-*graft*-L-PAE obtained from synthesis conditions 1 and 2 were insoluble in deuterated dimethyl sulfoxide (DMSO-d6). NMR measurements of those two samples were performed in D_2O while other samples were measured by using DMSO-d6 as a solvent. ^{1}H-NMR results were shown as follows.

γ-PGA: ^{1}H-NMR (DMSO-d_6, δ in ppm): 1.6-2.2 (4H, -CHC$\underline{H}_2$C$\underline{H}_2$CO-), 4.0-4.3 (1H, -NH-C$\underline{H}$(COOH)-CH_2-), 8.5-9.0 (1H, -N$\underline{H}$-CH(CO_2H)-CH_2-)

L-PAE: ^{1}H-NMR (DMSO-d_6, δ in ppm): 1.1-1.2 (3H, -COO-CH_2C$\underline{H}_3$-), 3.0-3.3 (2H, H_2N-CH($COOC_2H_5$)-C$\underline{H}_2$-C_6H_5) , 4.1-4.2 (2H, -COO-C$\underline{H}_2$$CH_3$), 4.2-4.3 (1H, H_2N-C$\underline{H}$($COOC_2H_5$)-CH_2-C_6H_5), 7.2-7.4 (5H, -C_6H_5), 8.5-8.7 (2H, -NH_2)

γ-PGA-*graft*-L-PAE conditions 1-2: ^{1}H-NMR (D_2O, δ in ppm): 1.0-1.2 (3H, -COO-CH_2C$\underline{H}_3$), 1.6-2.4 (4H, -CHC$\underline{H}_2$C$\underline{H}_2$CO), 2.7-3.2 (2H, -HN-CH($COOC_2H_5$)-C$\underline{H}_2$-C_6H_5), 3.9-4.2 (1H, -NH-C$\underline{H}$(CO_2H)-CH_2), 7.0-7.4 (5H, -C_6H_5)

γ-PGA-*graft*-L-PAE conditions 3-8: ^{1}H-NMR (DMSO-d_6, δ in ppm): 0.9-1.2 (3H, -COO-CH_2C$\underline{H}_3$), 1.4-2.5 (4H, -CHC$\underline{H}_2$C$\underline{H}_2$CO), 2.7-3.0 (2H, -HN-CH($COOC_2H_5$)-C$\underline{H}_2$-C_6H_5), 3.8-4.0 (1H, -NH-C$\underline{H}$(CO_2H)-CH_2), 4.0-4.5 (2H, -CO_2-C$\underline{H}_2$$CH_3$, 1H, -NH-C$\underline{H}$($CO_2H$)-$CH_2$), 7.0-7.4 (5H, -$C_6H_5$), 7.6- 8.0 (1H, -N$\underline{H}$-CH($CO_2H$)-$CH_2$), 8.2-8.4 (H, -CONH-CH-)

In addition, ^{1}H-NMR technique was carried out to calculate the total amount of L-PAE grafted onto γ-PGA backbone, or the grafting degree. Ratios of the integral area of the chemical shift at 7.20-7.40 ppm (aromatic protons) of L-PAE to the integral area of methylene protons, 1.0-2.6 ppm, at γ-PGA backbone was calculated.

It was found that the grafting degree was affected by the amount of WSC used in the synthesis process. That is grafting degree increased as amounts of WSC increased (Figure 16). The reaction mechanism (Figure 17) was proposed by following the mechanism reported by Naoki (Naoki et al., 1995).

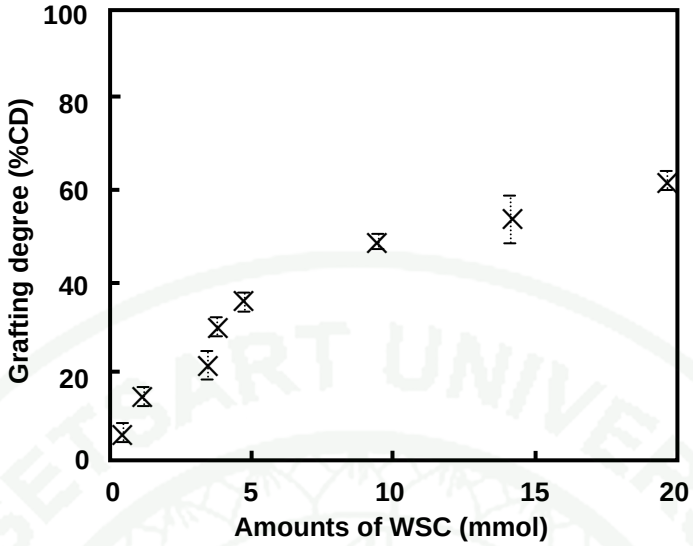

Figure 16 The relations between the amounts of WSC and grafting degree of γ-PGA-*graft*-L-PAEs.

From Figure 17, carbodiimide molecule reacts with a proton to form carbocation (1). This carbocation will be hydrolyzed by water into the urea derivative (2). The carbocation can react with an ionized carboxyl group to form *O*-acrylisourea compound (3). As a result of reprotonation at the site of Schiff base, *O*-acrylisourea compound change into a carbocation (4). In the reaction with water, this carbocation (4) transfer to the urea derivative (2). Since the ionized carboxyl group is a very strong base, its reaction with carbocation (4) may produce carboxylic anhydride (8). When an amine is present, the quickly form of the amide (7) was occurred. Moreover, the carbocation (4) will react with a water molecule or an amine to produce carboxylate (6) or amide (7), respectively. In addition, a few amine molecules can react directly with carbocation (4) to form amide (7) without anhydride formation. As shown in the mechanism, total amount of WSC does not react with γ-PGA and L-PAE. It was lost by the side reactions with water, hence the dependence of grafting degree on the amount of WSC.

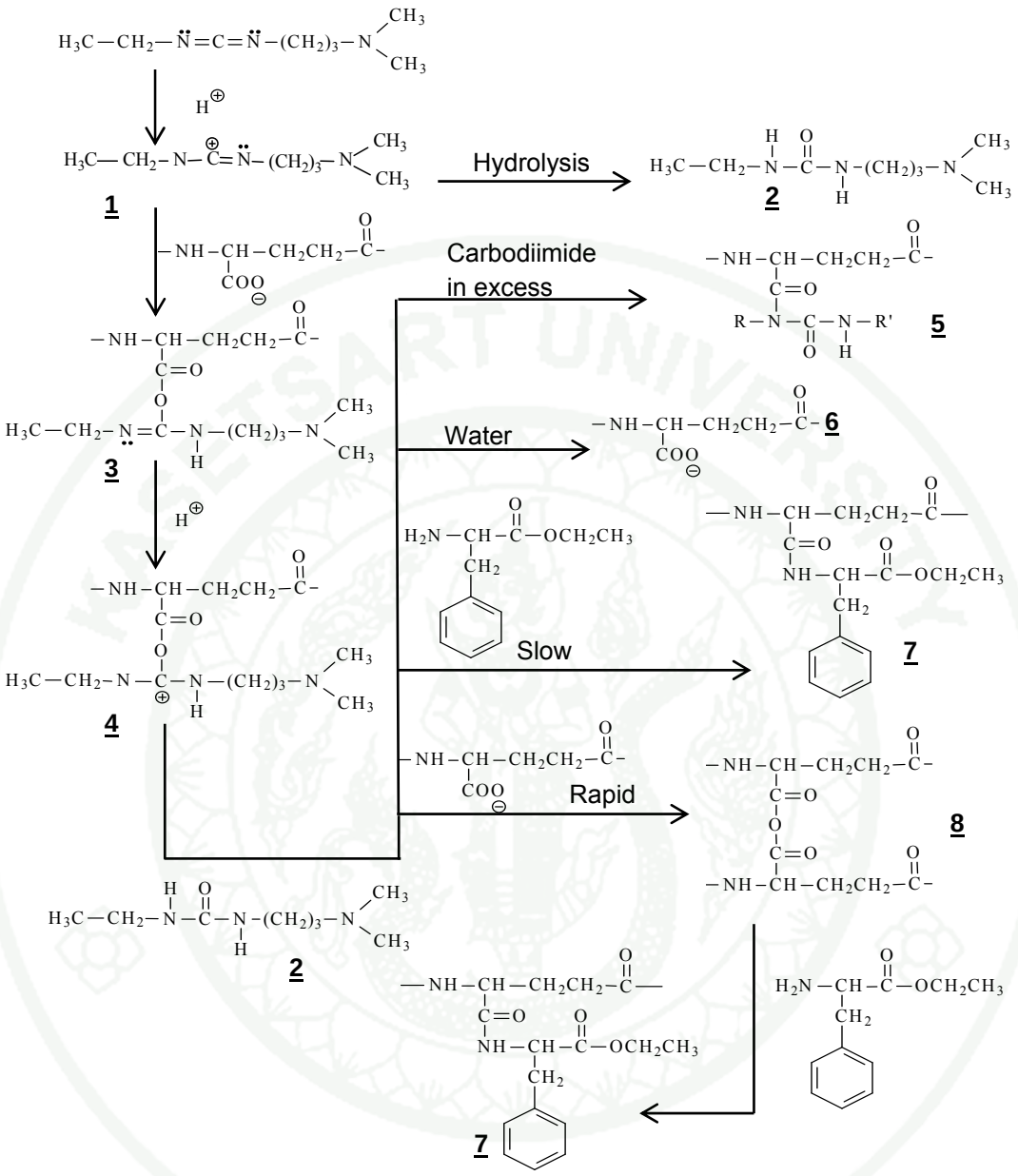

Figure 17 Proposed reaction mechanisms of the amide formation between carboxylic acid of γ-PGA and amine of L-PAE in an aqueous media in the presence of water soluble carbodiimide (WSC).

1.2 Thermosensitivity of γ-PGA-*graft*-L-PAEs

Solubility of the copolymers was tested by varying a concentration from 0.1-1.0 mg/mL. The copolymers having grafting degree about or less than 15% were completely dissolved in the ultrapure water while those having grafting degree higher than 15% were partially dissolved (Table 3). The solubility of the copolymers decreased when hydrophobicity of the chain increased.

Table 3 Solubility test of γ-PGA-*graft*-L-PAEs.

Sample	%CD	Concentration (mg/mL)									
		0.1	**0.2**	**0.3**	**0.4**	**0.5**	**0.6**	**0.7**	**0.8**	**0.9**	**1.0**
1	**7±1**	●	●	●	●	●	●	●	●	●	●
2	**15±2**	●	●	●	●	●	●	●	●	●	●
3	**22±2**	●	●	●	●	●	●	●	●	●	X
4	**30±1**	●	●	●	●	●	●	●	X	X	X
5	**36±1**	●	●	●	●	●	●	X	X	X	X
6	**49±1**	●	●	●	●	X	X	X	X	X	X
7	**54±4**	●	●	X	X	X	X	X	X	X	X
8	**62±2**	●	●	X	X	X	X	X	X	X	X

● Soluble X Insoluble

The graft copolymers are amphiphilic polymers that can self-agrregate in aqueous solution and could form nanoparticles due to their amphiphilic characteristic (Akagi *et al.*, 2005). Particle sizes of the copolymers in aqueous solutions at various concentrations are shown in Figure 18 and summarized in Table 4. The size of γ-PGA-*graft*-L-PAEs with grafting degrees of 7-62% at concentration of 0.2 mg/mL are in rang of 30-393 nm.

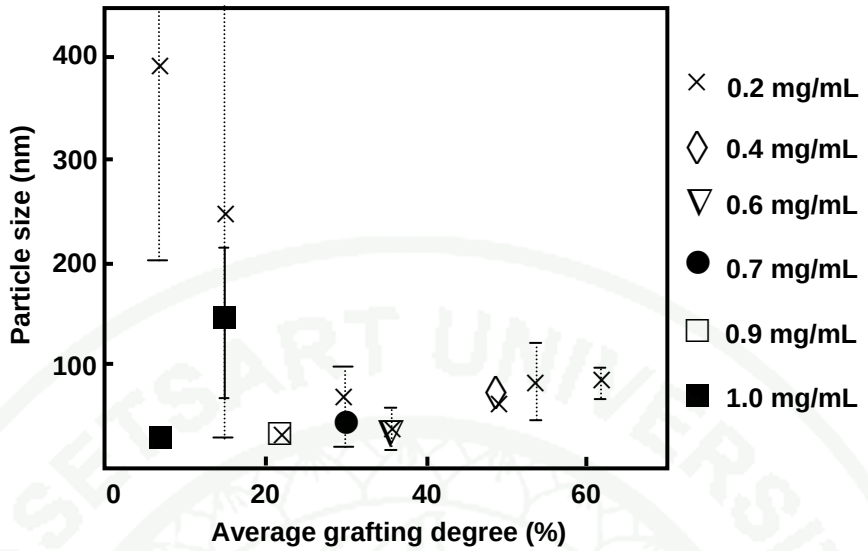

Figure 18 Particle sizes of γ-PGA-*graft*-L-PAE with grafting degree of 7-62% in aqueous solutions at room temperature.

Table 4 Particle size of γ-PGA-*graft*-L-PAEs in aqueous solutions.

Sample	%CD	Particle size (Mean±SD, nm)								
		Concentration (mg/mL)								
		0.2	**0.3**	**0.4**	**0.5**	**0.6**	**0.7**	**0.8**	**0.9**	**1.0**
1	**7±1**	393±186	–	–	–	–	–	–	–	27±4
2	**15±2**	245±281	–	–	–	–	–	–	–	144±74
3	**22±2**	30±0.4	–	–	–	–	–	–	32±5	X
4	**30±1**	65±31	–	–	–	–	42±17	X	X	X
5	**36±1**	38±21	–	–	–	35±4	X	X	X	X
6	**49±1**	58±1	–	68±0.3	X	X	X	X	X	X
7	**54±4**	81±1	X	X	X	X	X	X	X	X
8	**62±2**	83±6	X	X	X	X	X	X	X	X

- No data, X insoluble

Particle size of the copolymers with low grafting degree (7-15%) is bigger than that of the copolymers with higher grafting degree. This could be explained that the copolymer with low grafting degree has lower hydrophobic segments. The interactions among the polymer chains and water molecules are very strong. Their structures are expanded. Therefore, the particle sizes are larger (Figure 19 (a)). On the other hand, when grafting degree increases, the graft copolymer has more hydrophobic parts and could form smaller particles because their hydrophobic interactions are dominant (Figure 19 (b)).

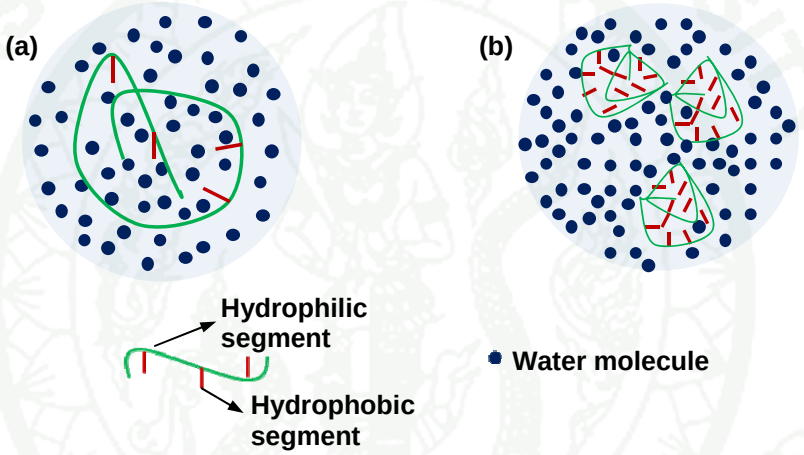

Figure 19 Illustration of γ-PGA-*graft*-L-PAE in aqueous solution at concentration of 0.2 mg/mL at room temperature (a) grafting degree = 7-15%, (b) grafting degree = 22-62%.

When polymer concentration increases, the size of the copolymers with relatively low grafting degree (≤ 15%) are drastically decreases (Figure 18). On the other hand, concentration of the polymer has lower effect on particle size of the copolymers when grafting degree is in ranging of 22-49%. According to the obtained results, the particle size depends on both the polymer concentration and the grafting degree.

A preliminary detection on thermosensitivity properties of γ-PGA-*graft*-L-PAE was carried out by observation of change in clarity of the polymer solutions during

heating and cooling. Aqueous solutions of the copolymers having grafting degree of 7-49% (sample 1-6) were heated to 80°C and cooled in an ice bath alternatively. The clarity of the solutions did not change during heating and cooling. However, the light transmittance of the copolymer with grafting degree of 49% (sample 6) trended to decrease when temperature increased (Figure 20) while transmittance values of those having grafting degree of 7-36% (sample 1-5) were consistent. The clouding temperature (T_{cloud}) of sample 6 was around 80°C. These results indicated that the grafting degree had effect on thermoresponsive behavior.

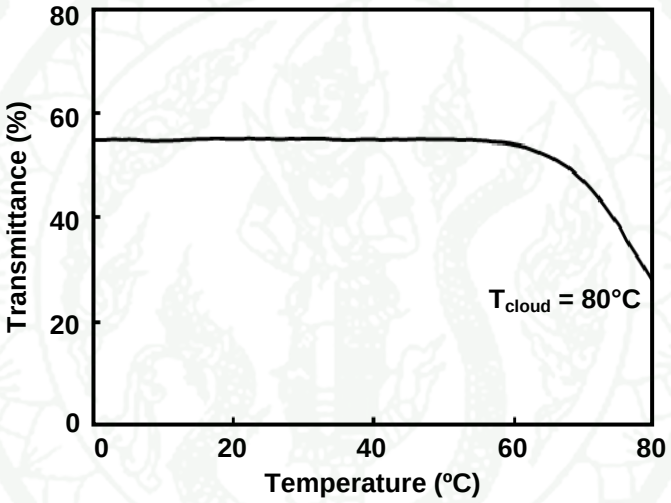

Figure 20 Effect of temperature on light transmittance of γ-PGA-*graft*-L-PAE with grafting degree of 49% (sample 6). The measurement was performed at heating rate of 0.5°C·min^{-1}. The solutions were centrifuged before measurement.

In general, amphiphilic polymer shows different behavior in solvent of different polarity. Shimokuri (Shimokuri *et al.*, 2005) found that thermoresponsive behavior of γ-PGA propylates could not be found in pure water but it could be observed when NaCl was added. Here, it was found that the presence of NaCl affected the clarity of the solutions of copolymer with grafting degree of 30-49% (sample 4-6) upon heating and cooling (Figure 21). These results revealed that γ-

PGA-*graft*-L-PAEs with the grafting degree of 30-49% had suitable hydrophilic and hydrophobic balance for thermoresponsive properties in NaCl solution.

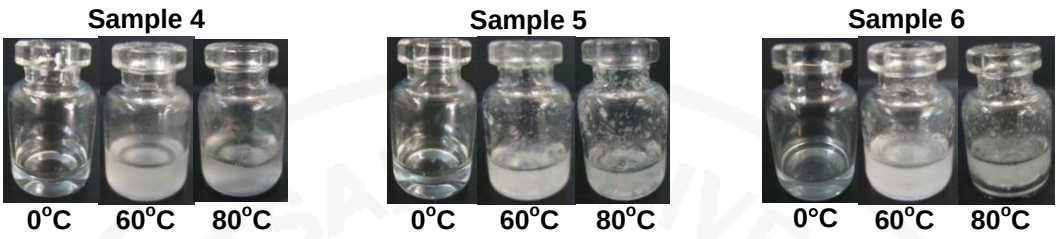

Figure 21 Thermoresponsive behavior of γ-PGA-*graft*-L-PAEs in 4M NaCl solutions (5 mg/mL) without centrifugation.

Particle sizes of the copolymers in 4M NaCl solution at various concentrations are investigated. The results are shown in Figure 22 and summarized in Table 5. The size of γ-PGA-*graft*-L-PAEs with grafting degrees of 7-49% in 4M NaCl at concentration of 0.2 mg/mL are in range of 62-405 nm.

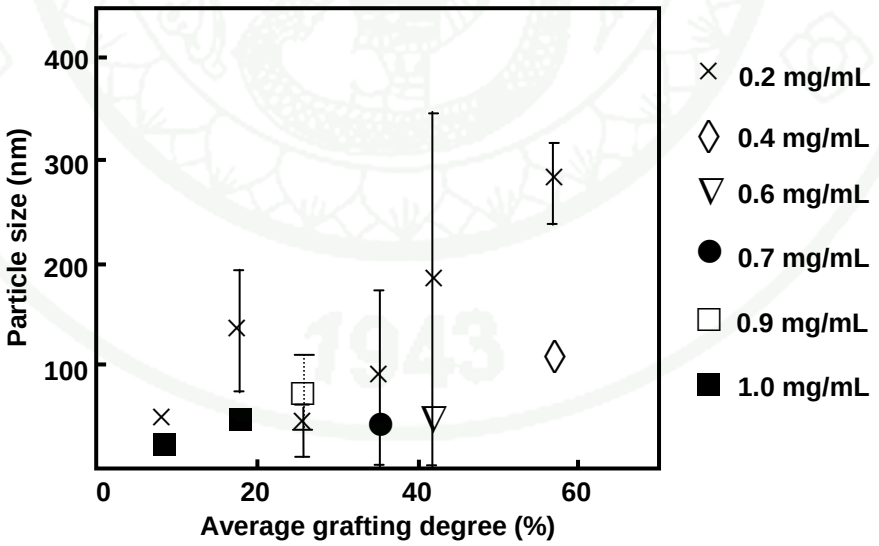

Figure 22 Particle sizes of γ-PGA-*graft*-L-PAEs with grafting degree of 7-49% in 4M NaCl at room temperature.

Table 5 Particle size of γ-PGA-*graft*-L-PAEs in 4 M NaCl solution.

Sample	%CD	Particle size (Mean±SD, nm)								
		Concentration (mg/mL)								
		0.2	**0.3**	**0.4**	**0.5**	**0.6**	**0.7**	**0.8**	**0.9**	**1.0**
1	**7±1**	68±13	–	–	–	–	–	–	–	33±4
2	**15±2**	192±95	–	–	–	–	–	–	–	64±19
3	**22±2**	62±55	–	–	–	–	–	–	105±55	X
4	**30±1**	129±138	–	–	–	–	56±3	X	X	X
5	**36±1**	264±284	–	–	–	73±20	X	X	X	X
6	**49±1**	405±56	–	159±9	X	X	X	X	X	X

- No data X insoluble

Unlike aqueous solution, the size of the copolymers with grafting degree of 7-15% in 4M NaCl are smaller. This is because NaCl promoted the dehydration effect. The polymer structures are compact. On the other hand, sizes of the copolymers with higher grafting degree are bigger. This could be explained that the copolymers with high grafting degree have more bulky side chains so their sizes are bigger. Moreover, the hydrophobic interaction is promoted in the presence of NaCl, and lead to an aggregation of the particles. Therefore, the sizes of the copolymers become larger when the polymers have more hydrophobic segments.

The effect of temperature on the particle size of the copolymers with grafting degree of 30-49% was investigated (Figure 23). The particle size increases as the temperature increases. This is because high temperature enhances the dehydration effect. An aggregation is easily occurs hence an increase of the particle size (Figure 24).

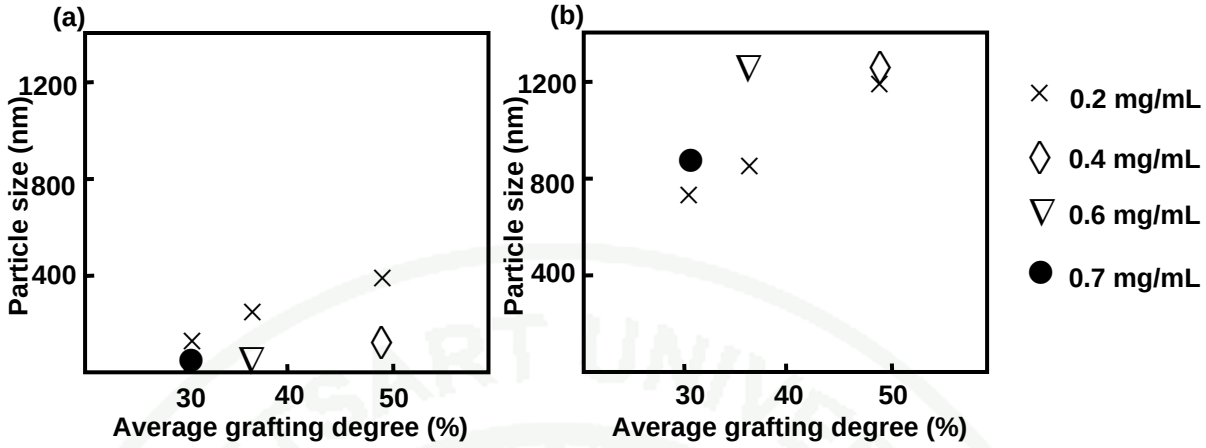

Figure 23 Particle sizes of γ-PGA-*graft*-L-PAEs with grafting degree of 30-49% in 4M NaCl at different polymer concentration (a) at room temperature, and (b) at 60 °C.

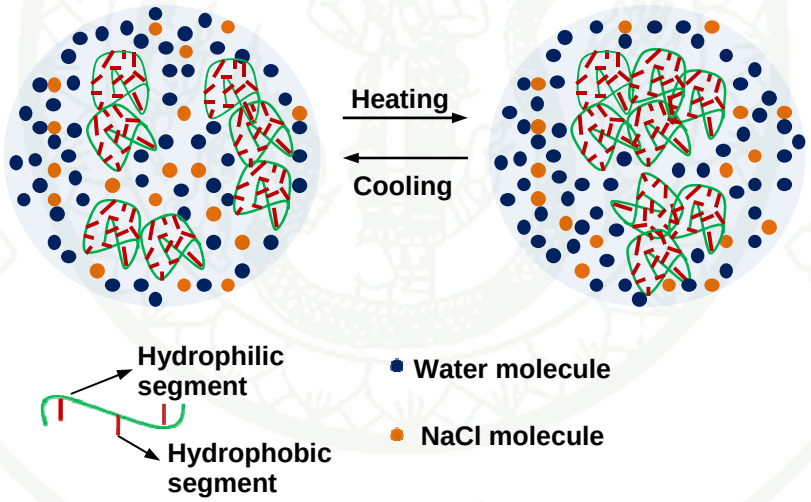

Figure 24 Schematic illustration of thermoresponsive phenomenon of γ-PGA-*graft*-L-PAE in NaCl solution.

Effect of NaCl concentration on clouding temperatures of the copolymers was investigated by UV-visible spectroscopy. The copolymers with different grafting degree showed response at different temperatures (Table 6).

Table 6 Clouding temperatures (T_{cloud}) of γ-PGA-*graft*-L-PAEs in NaCl solution.

NaCl (M)	Grafting degree (%)					
	7±1	**15±2**	**22±2**	**30±1**	**36±1**	**49±1**
0	–	–	–	–	–	80°C
1	–	–	–	–	–	–
2	–	–	–	–	76°C	–
4	–	–	–	57°C	70°C	–

– No thermoresponsive phenomenon

The measurement was performed at heating rate of $0.5^{o}C \cdot min^{-1}$

The copolymers with grafting degree of 30% and 36% (sample 4, 5) did not show thermoresponsive behavior in aqueous solutions but they showed this phenomenon when NaCl was added. The reason is because of the dehydration effect as mentioned above. The clouding temperatures of copolymers with grafting degree 30-36% are in range of 57-76 °C. When NaCl concentration increases, the dehydration effect is stronger. Aggregation occurred at lower temperature. That is why the clouding temperature was shifted to lower temperature.

Besides polarity of the solvent, polymer concentration also had effect on thermosensitivity properties. Effect of polymer concentration on clouding temperatures was investigated by fixing the NaCl concentration at 4M (Table 7). The clouding temperatures trended to decrease as the polymer concentration increased. This might be explained from the results of the particle size which presents in Figure 23.

Table 7 Effect of polymer concentration on clouding temperature (T_{cloud}) of γ-PGA-*graft*-L-PAEs in 4M NaCl solution.

Polymer concentration (mg/ml)	Grafting degree (%)					
	7±1	**15±2**	**22±2**	**30±1**	**36±1**	**49±1**
1	X	X	X	X	X	X
5	X	X	X	57°C	70°C	X
10	X	X	X	47°C	59°C	76°C

X: No thermoresponsive phenomenon

The measurement was performed at heating rate of $0.5^{o}C \cdot min^{-1}$

According to the results shown in Figure 23, the particle size trended to increase when polymer concentration increase. Since the aggregation of the particle was easily occurred at high polymer concentration during heating, the clouding temperature was shifted to lower temperature when the polymer concentration increased.

It is noticeable that light transmittance in response to temperature curve showed hysteresis phenomena during the heating and cooling processes (Figure 25). The phase separation of the copolymer to form aggregations in NaCl solution was reversible (Figure 26). The clouding temperatures observed in each cycle were invariant at around 60°C. Once the aggregations were formed during heating, the temperature response was affected by strong hydrophobic interactions among the polymer chain, and therefore the transmittance was not recovery to the initial point.

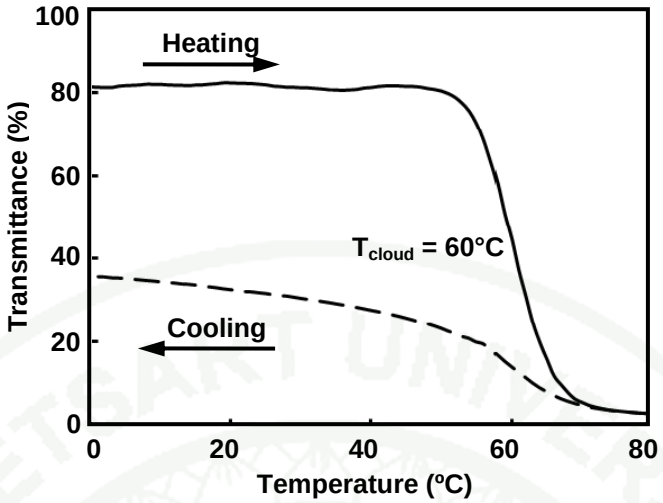

Figure 25 Clouding temperature hysteresis curve of 10 mg/mL of γ-PGA-*graft*-L-PAE with grafting degree of 36% (sample 5) in heating and cooling cycle (heating/cooling rate = 0.5°C·min^{-1}).

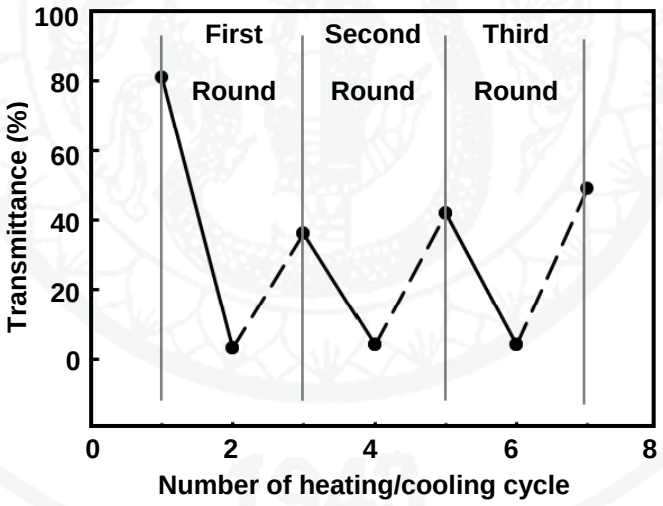

Figure 26 Reversible change of light transmittance in response to temperature for 10 mg/mL of γ-PGA-*graft*-L-PAE in 4M NaCl solutions (grafting degree of 36%, heating/cooling rate = 0.5°C·min^{-1}).

2. Chemically modification of poly (γ-glutamic acid) (γ-PGA) with benzoxazine derivatives (Bxs).

2.1 Study on γ-PGA-*graft*-Mt-Bx

2.1.1 Synthesis and characterization of γ-PGA-*graft*-Mt-Bx

FT-IR spectra of γ-PGA-*graft*-Mt-Bxs synthesized at various reaction times were shown in Figure 27. The peaks found in γ-PGA spectrum at 3283, 1640 cm^{-1} indicated an amide bond and absorption peak at 1730 cm^{-1} refer to carbonyl groups. The characteristic peaks of Mt-Bx were observed at 1494, 1118 and 870 cm^{-1}, referring to the oxazine ring (trisubstituted on benzene), ether aromatic (Ar-O-C) and benzene ring out of plane, respectively. The characteristic peaks of the γ-PGA-*graft*-Mt-Bxs products appear at 1732, 1499, 1117 and 870 cm^{-1} which assigned for carbonyl bond, ozaxine ring (trisubstituted stretching), ether aromatic (Ar-O-C) and benzene ring out of plane, respectively. The FT-IR spectra revealed that the formation of the product already started at 15 min.

To determine the optimum reaction time, the ratio of absorbance between the carbonyl group (C=O) at 1732 cm^{-1} and the oxazine ring (trisub) at 1499 cm^{-1}, and that of the absorbance between the carbonyl group (C=O) at 1732 cm^{-1} and the ether bond (C-O) at 1117 cm^{-1} were evaluated. Figure 28 shows that the optimum reaction time for γ-PGA-g-Bx product was 2 hours.

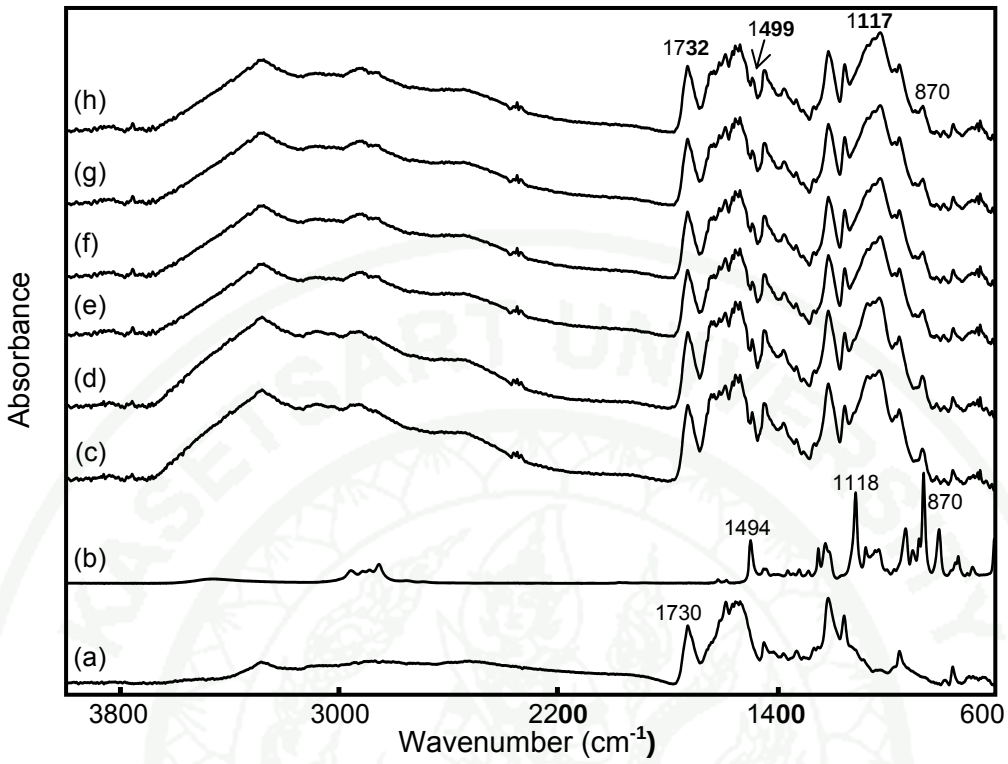

Figure 27 FT-IR spectra of (a) γ-PGA, (b) Mt-Bx, and γ-PGA-*graft*-Mt-Bx after synthesized for (c) 15 min, (d) 1 h, (e) 2 h, (f) 4 h, (g) 6 h, and (h) 8 h.

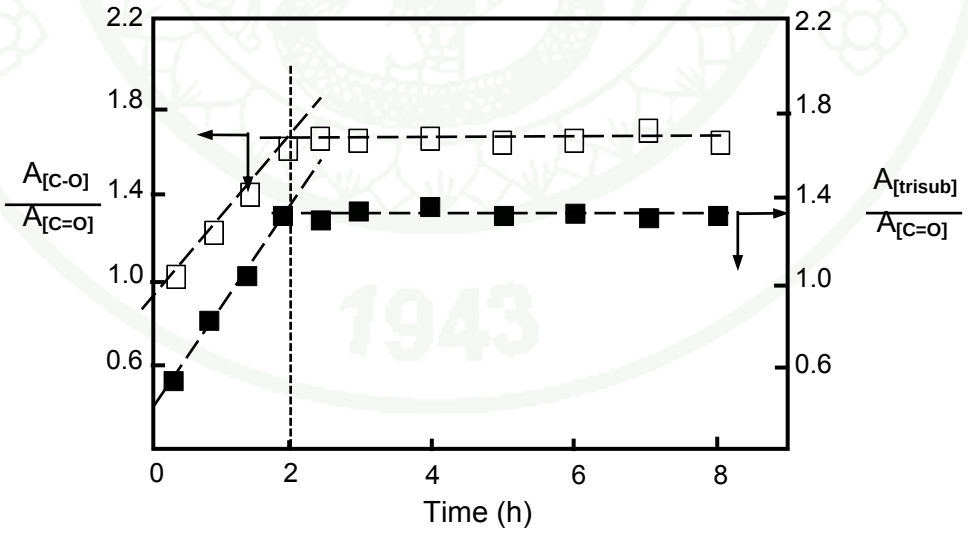

Figure 28 Peak absorbance ratios of ether and carbonyl (□), and oxazine ring and carbonyl (■) at various reaction times of γ-PGA-*graft*-Mt-Bx synthesis.

The structure of γ-PGA-*graft*-Mt-Bx synthesized with the reaction time of 2 h was further confirmed by ^{1}H-NMR spectrum (Figure 29). The ^{1}H-NMR result was shown as follow.

γ-PGA-*graft*-Mt-Bx: ^{1}H-NMR (DMSO-d6, δ in ppm): 1.62-2.35 (4H, -CH-C<u>H</u>$_2$C<u>H</u>$_2$-CO-), 2.84-3.08 (2H, -C<u>H</u>$_2$-N(C<u>H</u>$_2$)-O-), 4.10-4.45 (1H, -NH-C<u>H</u>(CO$_2$CH$_2$)-CH$_2$-), 7.96-8.43 (1H, -N<u>H</u>-CH(CO$_2$CH$_2$)-CH$_2$-), and 6.49-7.22 (3H, -O-C-C<u>H</u>C<u>H</u>CC<u>H</u>C-CH$_2$-N-).

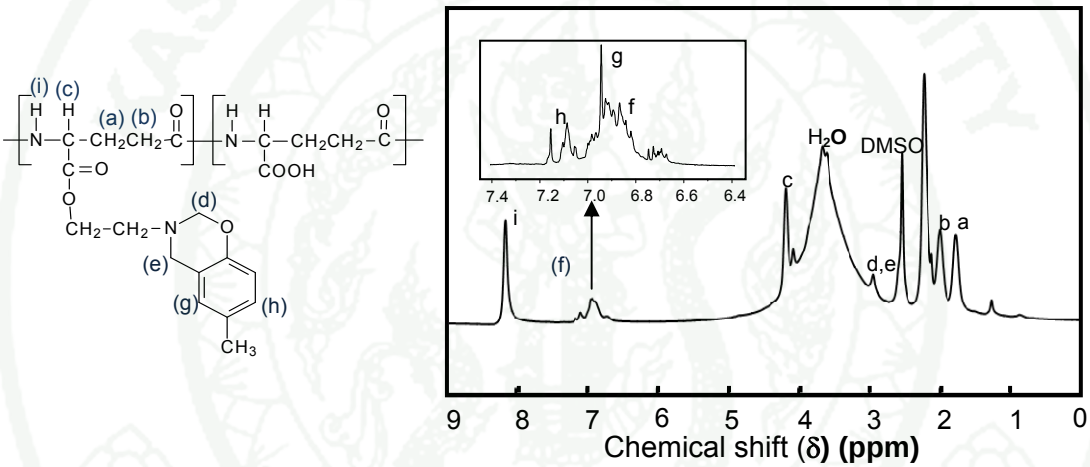

Figure 29 ^{1}H-NMR spectrum of γ-PGA-*graft*-Mt-Bx synthesized with reaction time of 2h in DMSO-d6.

The integration ratio of the methylene proton (1.62-2.35 ppm) of γ-PGA and aromatic proton (6.49-7.22 ppm) of benzoxazine was evaluated to estimate the degree of benzoxazine grafting. The grafting degree of sample synthesized with a reaction time of 2 h was 30%.

2.1.2 Metal-ions-responsive test of γ-PGA-*graft*-Mt-Bx

2.1.2.1 Metal (II) ion responsive properties

Responsive properties of γ-PGA-*graft*-Mt-Bx toward Cu (II), Co (II), Ni (II), and Zn (II) ions were studied. Preliminary studies of the metal-ion responsive properties of the γ-PGA-*graft*-Mt-Bx solution was evaluated from the color transition by visual observation (Figure 30).

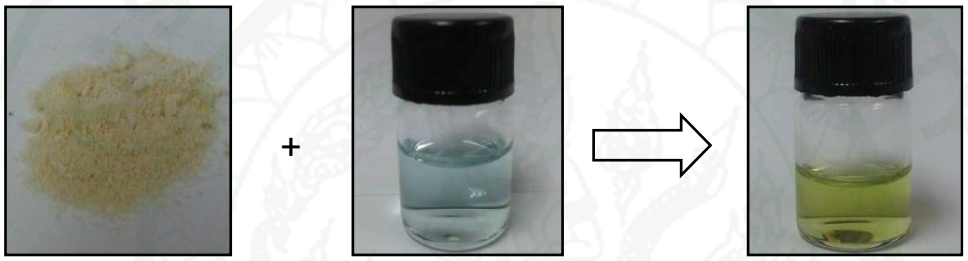

Figure 30 Change in color of aqueous solution of Cu(II) ion when γ-PGA-*graft*-Mt-Bx was added.

When γ-PGA-*graft*-Mt-Bx powder was added to each aqueous solution of metal (II) ions, only the aqueous solution of Cu (II) ions was changed from clear to yellow. In addition, it was surprising that some portion of the γ-PGA-*graft*-Mt-Bx disappeared in the Cu (II) aqueous solution. It is expected that γ-PGA-*graft*-Mt-Bx may form a complex with Cu (II) ions, so that the solubility properties were changed. To clarify this phenomenon, the liquid portion separated by centrifugation or filtration was examined by UV-visible spectrometer. Figure 31 shows that UV spectrum of the liquid portion is different from that of Cu (II) aqueous solution and the maximum absorption spectra of γ-PGA-*graft*-Mt-Bx-Cu (II) complex appeared at 415 nm. Changes in color and solubility properties appeared when γ-PGA-*graft*-Mt-Bx formed a complex with Cu(II) ions. These two phenomena were detected with the naked eye.

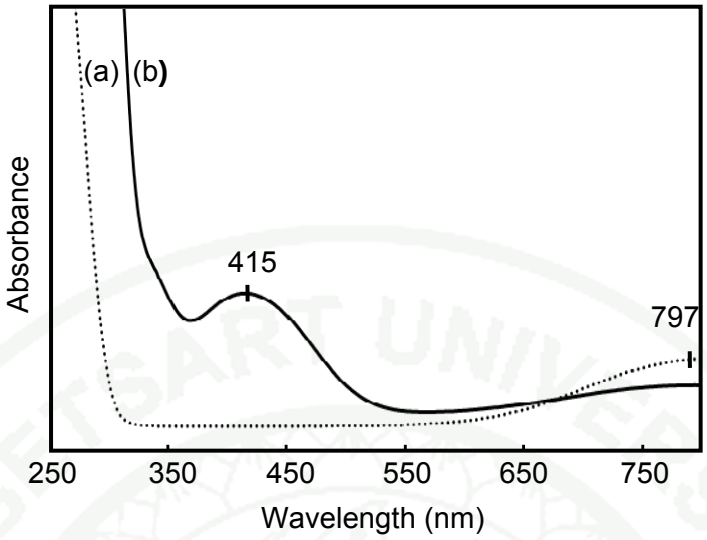

Figure 31 UV-visible absorption spectra of (a) aqueous solution of Cu (II) ions, and (b) γ-PGA-*graft*-Mt-Bx-Cu (II) complex in an aqueous solution.

While the liquid portion was investigated and finally found that the complex between γ-PGA-*graft*-Mt-Bx exists in the aqueous solution, the precipitate was investigated by dissolving them in DMSO and then characterizing by UV-visible. The maximum absorption peaks (λ_{max}) of the γ-PGA-*graft*-Mt-Bx precipitate, γ-PGA-*graft*-Mt-Bx and Cu (II) ions in the DMSO solutions were observed at 410, 278, and 272 nm, respectively (Figure 32). The shift of the λ_{max} indicated that the precipitate was also complex between the γ-PGA-*graft*-Mt-Bx and Cu (II) ions. The reason why the complex exists in the precipitate form might be due to the fact that Bx were not uniformly graft onto γ-PGA backbone or the high molecular weight portion of the γ-PGA-*graft*-Mt-Bx were formed complex and therefore this portion could not dissolve in water.

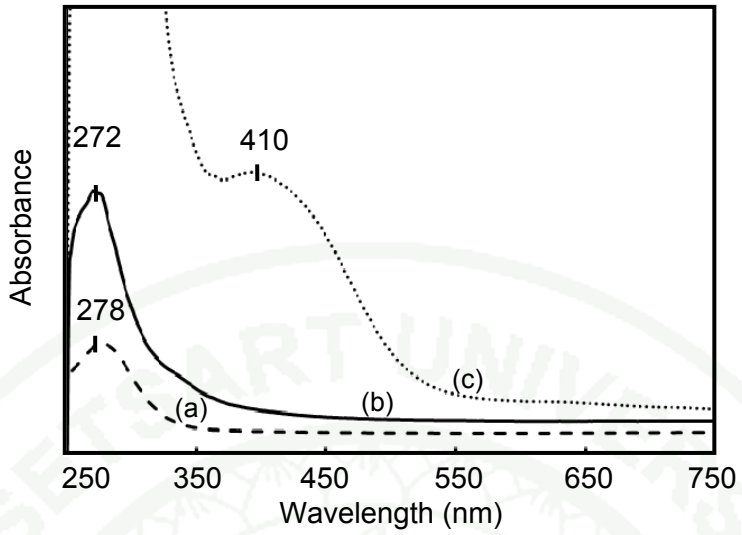

Figure 32 UV-Vis absorption spectra of (a) γ-PGA-*graft*-Mt-Bx, (b) Cu (II) ions, and (c) γ-PGA-*graft*-Mt-Bx precipitate in DMSO solution.

To clarify these phenomena, Cu (II) sulfate and γ-PGA-*graft*-Mt-Bx were dissolved in the DMSO. The yellow solution was obtained after adding the clear solution of the Cu (II) ions into a clear solution of γ-PGA-*graft*-Mt-Bx (Figure 33). This color transition phenomenon was further confirmed by UV-visible spectra.

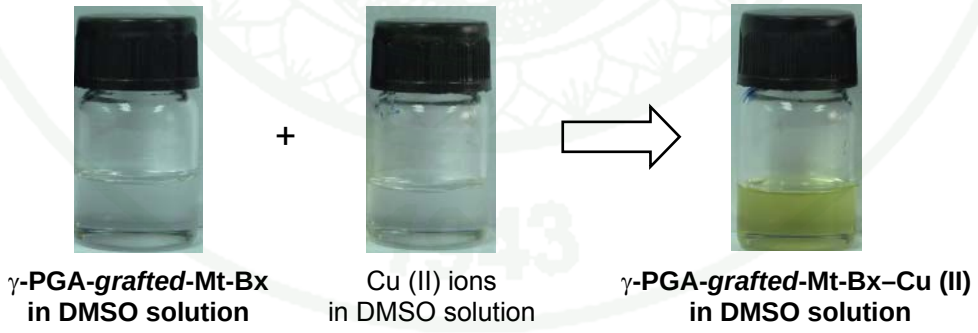

Figure 33 Change in color of γ-PGA-*graft*-Mt-Bx solution after mixing with Cu (II) ions in a DMSO solution.

From Figure 34, the maximum absorption peaks of γ-PGA-*graft*-Mt-Bx and Cu (II) ions present at 278 and 272 nm, respectively. After the complex formation between γ-PGA-*graft*-Mt-Bx and Cu (II) ions was formed, the maximum absorption

peak was shifted to 410 nm. The obtained results indicated that γ-PGA-*graft*-Mt-Bx showed sensitivity to Cu (II) ions in both water and DMSO solutions.

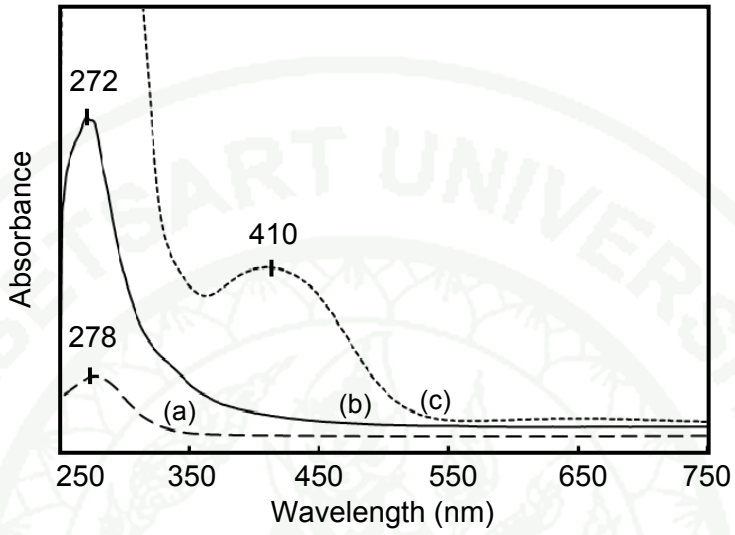

Figure 34 UV-Vis absorption spectra of (a) γ-PGA-*graft*-Mt-Bx, (b) Cu (II) ions, and (c) mixed solution of γ-PGA-*graft*-Mt-Bx with Cu (II) in DMSO solutions.

Qualitative analysis to determine the ratio of γ-PGA-*graft*-Mt-Bx to Cu (II) ions was carried out by using a photometric titration method. In this study, different amounts of the γ-PGA-*graft*-Mt-Bx solution was added to the Cu (II) ions solution. The ratio of γ-PGA-*graft*-Mt-Bx to Cu (II) ions was evaluated from the absorbance at 410 nm. Figure 35 shows the results obtained from the photometric titration method. It was found that the absorbance increases as quantity of the polymer increases during the first period, after that it becomes constant after the amount of the polymer solution exceeds 0.26 mL. By calculation, the ratio of γ-PGA-*graft*-Mt-Bx to Cu (II) ions was 1:390. This means that 1 molecule of γ-PGA-*graft*-Mt-Bx can trap 390 ions of Cu (II) ions.

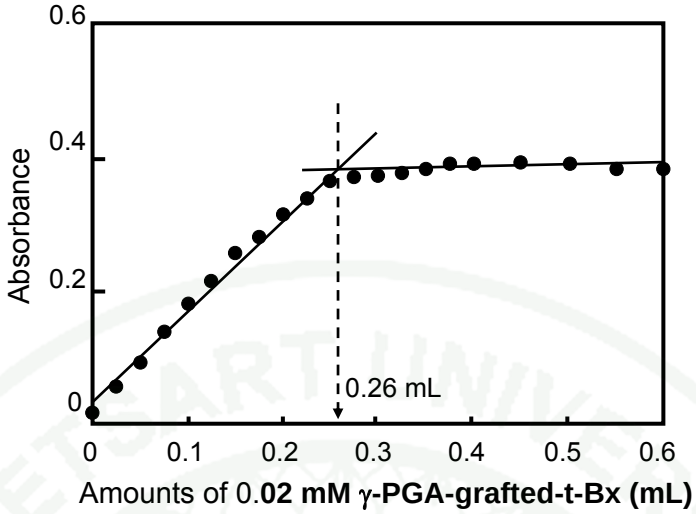

Figure 35 The relationship between the maximum absorbance at wavelength at 410 nm and the amount of 0.02 mM of γ-PGA-*graft*-Mt-Bx solution from photometric titration method.

2.1.2.2 Iron (III) ions responsive properties

From preliminary studies of the iron (III) responsive properties of the γ-PGA-*graft*-Mt-Bx solution was evaluated from the color transition by visual observation (Figure 36). After the γ-PGA-*graft*-Mt-Bx was added into the aqueous solution of iron (III) nitrate, color of the solution was changed from clear to purple. This color transition phenomenon was further examined by using UV-visible spectrophotometer.

Figure 36 Change in color of aqueous solution of Fe (II) ion when γ-PGA-*graft*-Mt-Bx was added.

It was surprising that some portion of the γ-PGA-*graft*-Mt-Bx disappeared in the iron (III) aqueous solution. It is expected that γ-PGA-*graft*-Mt-Bx may form a complex with iron (III) ions, so that the solubility properties were changed. To clarify this phenomenon, the liquid portion separated by centrifugation or filtration was examined by UV-visible spectrometer. Figure 37 shows that UV spectrum of the liquid portion is different from that of iron (III) aqueous solution. The maximum absorption spectra of the iron (III) ion solution and γ-PGA-*graft*-Mt-Bx-iron (III) complex appeared at 285 and 508 nm, respectively. Changes in color and solubility properties appeared when γ-PGA-*graft*-Mt-Bx formed a complex with iron (III) ions. These two phenomena were detected with the naked eye.

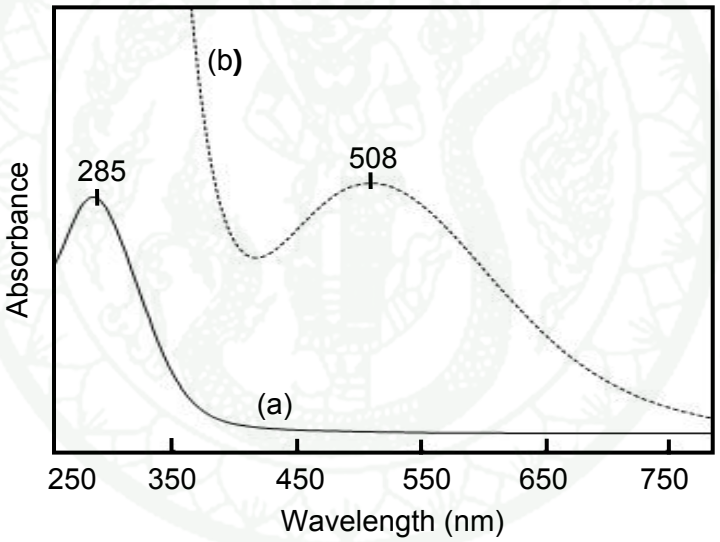

Figure 37 UV-visible absorption spectra of (a) aqueous solution of iron (III) ions, and (b) γ-PGA-*graft*-Mt-Bx-iron (III) complex in an aqueous solution.

While the liquid portion was investigated and finally found that the complex between γ-PGA-*graft*-Mt-Bx exists in the aqueous solution, the precipitate was investigated by dissolving them in DMSO and then characterizing by UV-visible. The maximum absorption peaks (λ_{max}) of the γ-PGA-*graft*-Mt-Bx precipitate, γ-PGA-*graft*-Mt-Bx and iron (III) ions in the DMSO solutions were observed at 460, 273, and 320 nm, respectively (Figure 38). The shift of the λ_{max} indicated that the precipitate

was also complex between the γ-PGA-*graft*-Mt-Bx and iron (III) ions. The reason why the complex exists in the precipitate form might be due to the fact that Bx were not uniformly graft onto γ-PGA backbone or the high molecular weight portion of the γ-PGA-*graft*-Mt-Bx were formed complex, and therefore this portion could not dissolve in water.

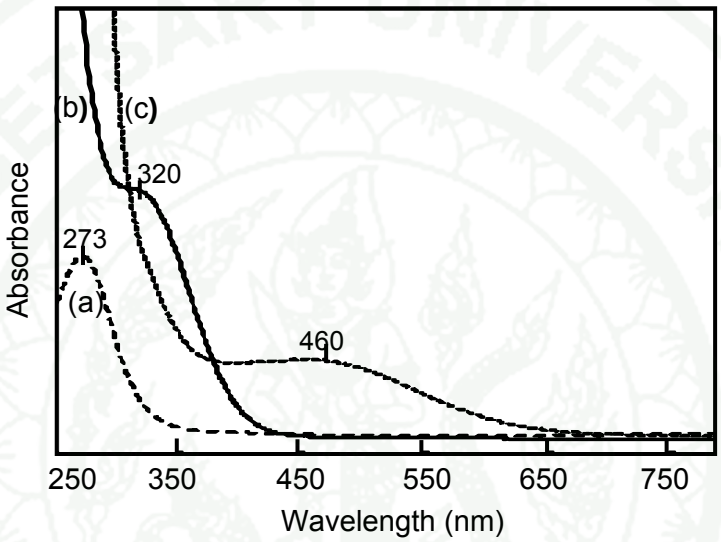

Figure 38 UV-Vis absorption spectra of (a) γ-PGA-*graft*-Mt-Bx, (b) iron (III) ions, and (c) γ-PGA-*graft*-Mt-Bx precipitate in DMSO solution.

To clarify these phenomena, iron (III) nitrate and γ-PGA-*graft*-Mt-Bx were dissolved in the DMSO. The color of the mixture changed from clear to purple (Figure 39). This color transition phenomenon was further confirmed by using UV-visible spectrophotometer.

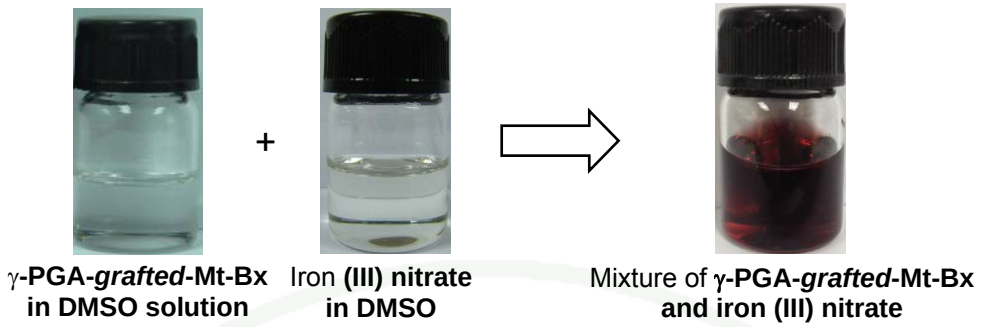

Figure 39 Change in color of γ-PGA-*graft*-Mt-Bx solution after mixing with iron (III) nitrate in a DMSO solution.

Figure 40 shows that the maximum absorption peaks of γ-PGA-*graft*-Mt-Bx and iron (III) ions in DMSO present at 273 and 320 nm, respectively. After the complex formation between γ-PGA-*graft*-Mt-Bx and iron (III) ions was formed, the maximum absorption peak was shifted to 501 nm. The obtained results indicated that γ-PGA-*graft*-Mt-Bx showed sensitivity to iron (III) ions in both water and DMSO solutions.

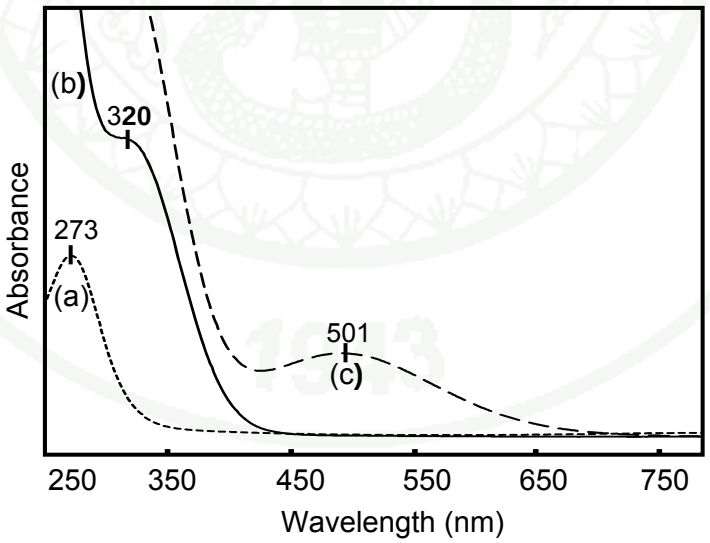

Figure 40 UV-Vis absorption spectra of (a) γ-PGA-*graft*-Mt-Bx, (b) iron (III) ions, and (c) mixed solution of γ-PGA-*graft*-Mt-Bx with iron (III) in DMSO solutions.

Qualitative analysis to determine the ratio of the polymer to iron (III) ions was carried out by using a photometric titration method. In this study, different amounts of the γ-PGA-*graft*-Mt-Bx solutions were added to the iron (III) ions solution. The ratio of γ-PGA-*graft*-Mt-Bx to iron (III) ions was evaluated from the absorbance at 501 nm. Figure 41 shows the results obtained from the photometric titration method. It was found that the absorbance increases as quantity of the polymer increases during the first period, after that it becomes constant after the amount of the polymer solution exceeds 0.46 ml. By calculation, the ratio of γ-PGA-*graft*-Mt-Bx to Fe (III) ions was 1:217. This means that 1 molecule of γ-PGA-*graft*-Mt-Bx can trap 217 ions of Fe (III) ions.

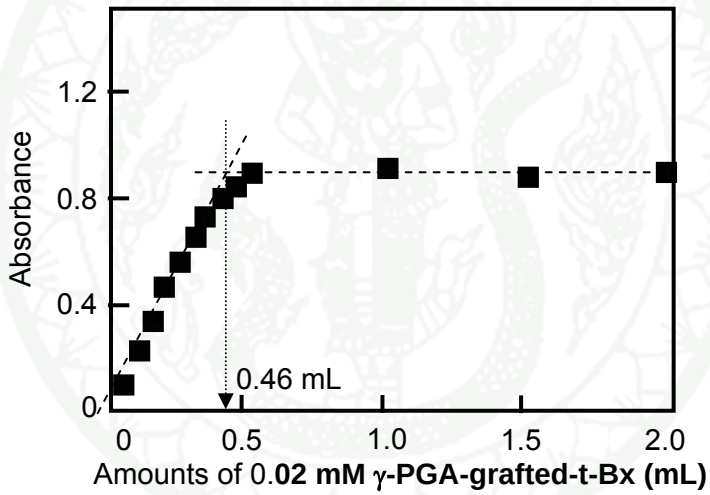

Figure 41 The relationship between the maximum absorbance at wavelength 510 nm and the amount of 0.02 mM of γ-PGA-*graft*-Mt-Bx solution from photometric titration method.

2.2 Study on γ-PGA-*graft*-Et-Bx

2.2.1 Synthesis and characterization of γ-PGA-*graft*-Et-Bx

The FT-IR spectra were used to determine the chemical structure of γ-PGA-*graft*-Et-Bx synthesized at various reaction times (Figure 42). γ-PGA showed the characteristic peaks at 3283, 1640 (amide bond), and 1730 cm^{-1} (carbonyl group). The absorption peaks of ethyl-Bx appeared at 1504 cm^{-1} (oxazine ring, trisubstituted on benzene), 1120 cm^{-1} (ether aromatic, Ar-O-C), and 871 cm^{-1} (benzene ring out of plane). It was found that the characteristic peaks of the product appeared at 1733, 1517, 1164 and 901 cm^{-1} which correspond to the carbonyl bond, oxazine ring (trisubstituted on benzene), ether aromatic (Ar-O-C) and benzene ring out of plane, respectively. The FT-IR spectra showed that the formation of the product already started at 15 min.

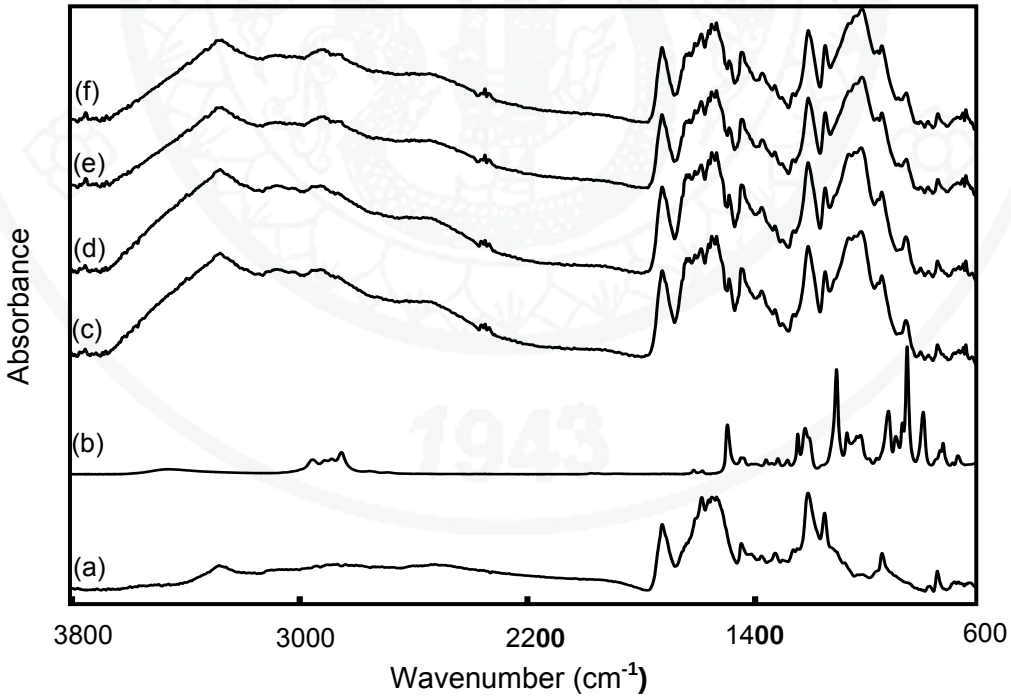

Figure 42 FT-IR spectra of (a) γ-PGA, (b) Et-Bx, and γ-PGA-*graft*-Et-Bx after synthesized for (c) 15 min, (d) 1 h, (e) 2 h, and (f) 4 h.

To determine the optimum reaction time, the ratio of absorbance between the carbonyl group (C=O) at 1733 cm^{-1} and the oxazine ring (trisub) at 1517 cm^{-1}, and that of the absorbance between the carbonyl group (C=O) at 1733 cm^{-1} and the ether bond (C-O) at 1164 cm^{-1} were evaluated. Figure 43 shows that the optimum reaction time for γ-PGA-*graft*-Et-Bx product was 15 min. However, γ-PGA-*graft*-Et-Bx used for the further studies was synthesized by using the reaction time equal to 2 h.

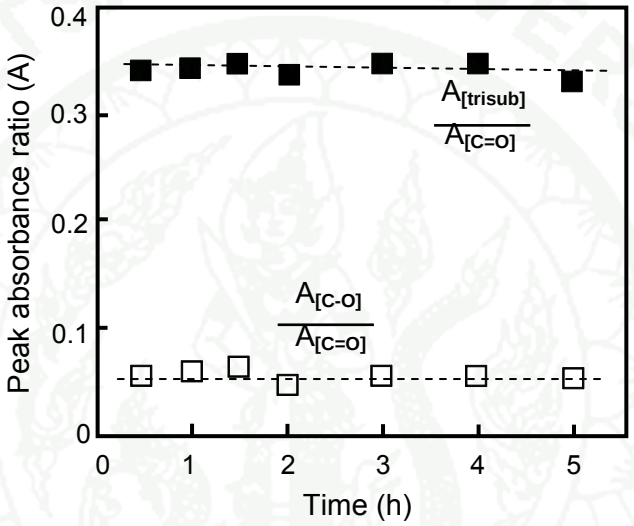

Figure 43 Peak absorbance ratios of ether and carbonyl (□), and oxazine ring and carbonyl (■) at various reaction times of γ-PGA-*graft*-Et-Bx synthesis.

The ^{1}H-NMR spectrum of γ-PGA-*graft*-Et-Bx was shown in Figure 44. The ^{1}H-NMR results were shown as follows.

γ-PGA-*graft*-Et-Bx: ^{1}H-NMR (DMSO-d6, δ in ppm): 0.97-1.21 (5H, -(C_2H_5)-CH_2CH_3), 1.46-2.41 (4H, -CH-C$\underline{H}_2$C$\underline{H}_2$-CO), 2.90-2.92 (2H, C$\underline{H}_2$-N(C$\underline{H}_2$)-O-), 4.12-4.23(1H, -NH-C$\underline{H}$(CO_2CH_2)-CH_2), 6.58-7.31 (3H, -O-C-C$\underline{H}$C$\underline{H}$CC$\underline{H}$C-CH_2-N-), and 8.04-8.28 (1H, -N$\underline{H}$-CH(CO_2CH_2)-CH_2).

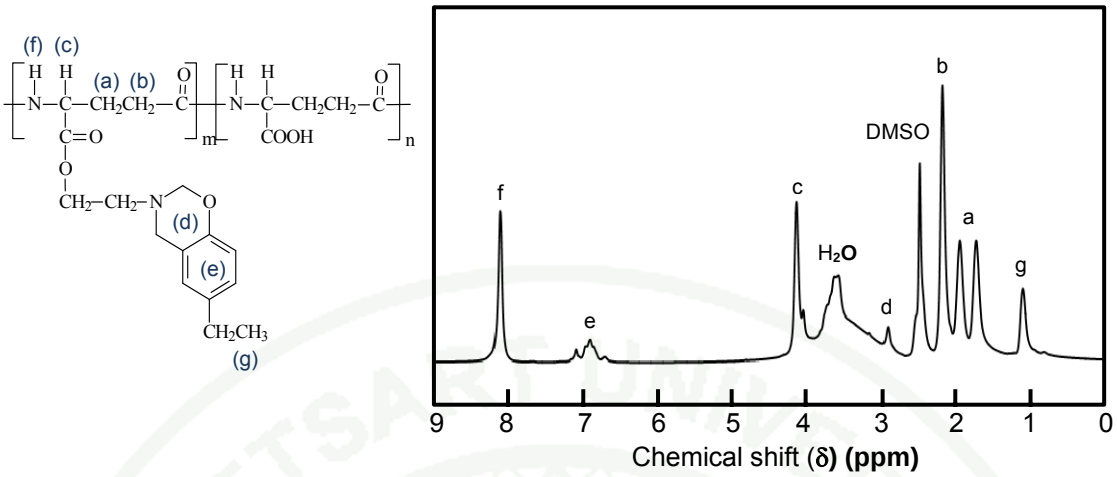

Figure 44 ^{1}H-NMR spectrum of γ-PGA-*graft*-Et-Bx in DMSO-d6.

The integration ratio of the amide proton (8.04-8.28 ppm) of γ-PGA and the aromatic proton (6.58-7.31 ppm) of Et-Bx was evaluated in the order to calculate the degree of grafting. The degree of Et-Bx grafting was 25%.

2.2.2 Metal-ions-responsive test of γ-PGA-*graft*-Et-Bx

2.2.2.1 Metal (II) ion responsive properties

Responsive properties of γ-PGA-*graft*-Et-Bx toward Cu (II), Co (II), Ni (II), and Zn (II) ions were studied. Preliminary studies of the metal-ion responsive properties of the γ-PGA-*graft*-Mt-Bx solution was evaluated from the color transition by visual observation (Figure 45).

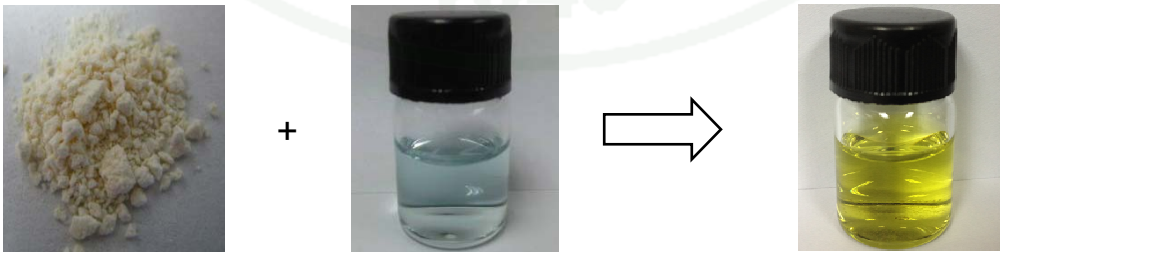

γ-PGA-*grafted*-Et-Bx | The aqueous solution of Cu (II) | **γ-PGA-*grafted*-ethyl-Bx-iron(III) complex in aqueous solution**

Figure 45 Change in color of aqueous solution of Cu(II) ion when γ-PGA-*graft*-Et-Bx was added.

When γ-PGA-*graft*-Et-Bx powder was added to each aqueous solution of metal (II) ions, only the aqueous solution of Cu (II) ions was changed from clear to yellow. In addition, it was surprising that some portion of the γ-PGA-*graft*-Et-Bx disappeared in the Cu (II) aqueous solution. It is expected that γ-PGA-*graft*-Et-Bx may form a complex with Cu (II) ions, so that the solubility properties were changed. To clarify this phenomenon, the liquid portion separated by centrifugation or filtration was examined by UV-visible spectrometer. Figure 46 shows that UV spectrum of the liquid portion is different from that of Cu (II) aqueous solution and the maximum absorption spectra of γ-PGA-*graft*-Mt-Bx-Cu (II) complex appeared at 397 and 797 nm. Changes in color and solubility properties appeared when γ-PGA-*graft*-Mt-Bx formed a complex with Cu (II) ions. These two phenomena were detected with the naked eye.

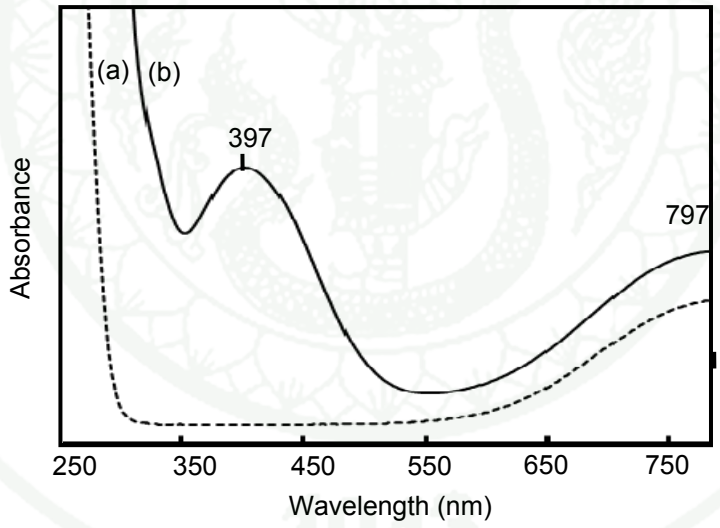

Figure 46 UV-visible absorption spectra of (a) aqueous solution of Cu (II) ions, and (b) γ-PGA-*graft*-Et-Bx-Cu (II) complex in an aqueous solution.

While the supernatant was investigated and finally found that the complex between γ-PGA-*graft*-Et-Bx exists in the aqueous solution, the precipitate was investigated by dissolving them in DMSO and then characterizing by UV-visible. The λ_{max} of the γ-PGA-*graft*-Et-Bx precipitate, γ-PGA-*graft*-Et-Bx and Cu (II) ions in the DMSO solutions were observed at 401, 280, and 272 nm, respectively (Figure 47).

The shift of the λ_{max} indicated that the precipitate was also complex between the γ-PGA-*graft*-Et-Bx and Cu (II) ions. The reason why the complex exists in the precipitate form might be due to the fact that Bx were not uniformly graft onto γ-PGA backbone or the high molecular weight portion of the γ-PGA-*graft*-Et-Bx were formed complex and therefore this portion could not dissolve in water.

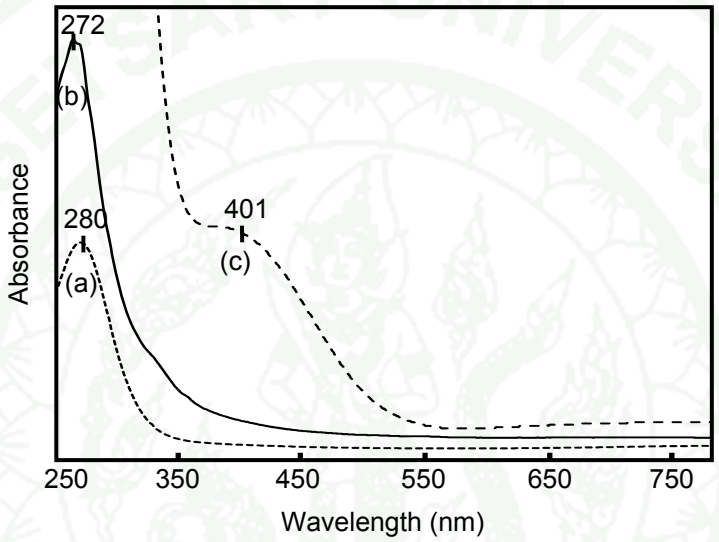

Figure 47 UV-Vis absorption spectra of (a) γ-PGA-*graft*-Et-Bx, (b) Cu (II) ions, and (c) γ-PGA-*graft*-Et-Bx precipitate in DMSO solution.

To clarify these phenomena, Cu (II) sulfate and γ-PGA-*graft*-Et-Bx were dissolved in the DMSO. The yellow solution was obtained after adding the clear solution of the Cu (II) ions into a clear solution of γ-PGA-*graft*-Et-Bx (Figure 48). This color transition phenomenon was further confirmed by UV-visible spectra.

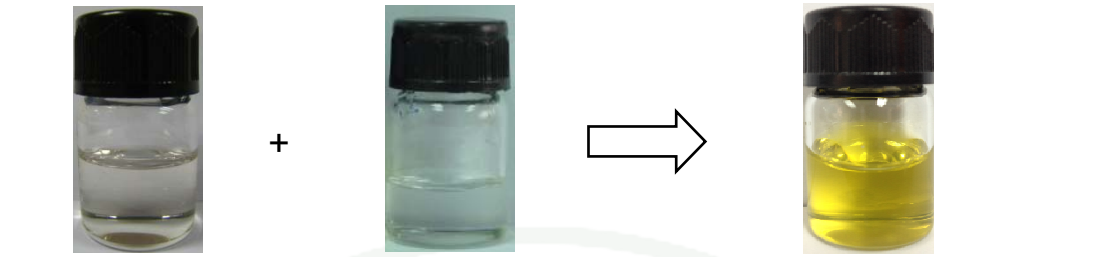

Figure 48 Change in color of γ-PGA-*graft*-Et-Bx solution after mixing with Cu (II) ions in a DMSO solution.

Figure 49 shows that the maximum absorption peaks of γ-PGA-*graft*-Et-Bx and Cu (II) ions present at 280 and 272 nm, respectively. After the complex formation between γ-PGA-*graft*-Et-Bx and Cu (II) ions was formed, the maximum absorption peak was shifted to 401 nm. The obtained results indicated that γ-PGA-*graft*-Et-Bx showed sensitivity to Cu (II) ions in both water and DMSO solutions.

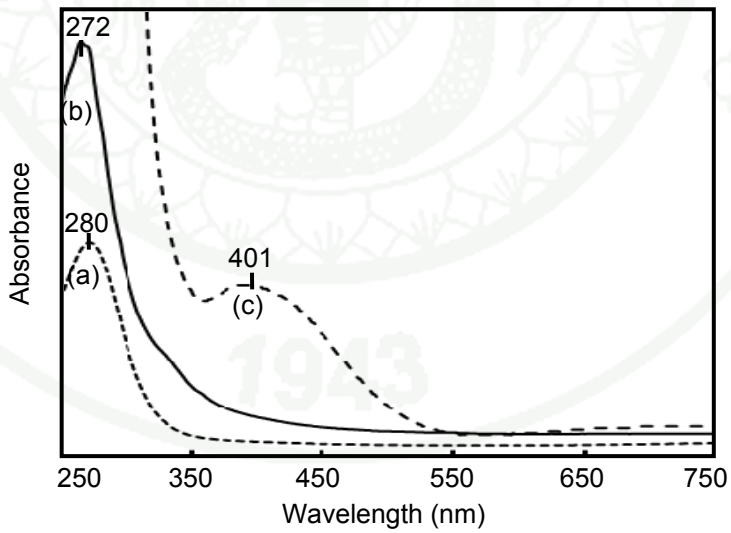

Figure 49 UV-Vis absorption spectra of (a) γ-PGA-*graft*-Et-Bx, (b) Cu (II) ions, and (c) mixed solution of γ-PGA-*graft*-Et-Bx with Cu (II) in DMSO solutions.

Qualitative analysis to determine the ratio of γ-PGA-*graft*-Et-Bx to Cu (II) ions was carried out by using a photometric titration method. Different amounts of

the γ-PGA-*graft*-Et-Bx solution were added to the Cu (II) ions solution. The ratio of γ-PGA-*graft*-Et-Bx to Cu (II) ions was evaluated from the absorbance at 401 nm. Figure 50 shows the results obtained from the photometric titration method. It was found that the absorbance increases as quantity of the polymer increases during the first period, after that it becomes constant after the amount of the polymer solution exceeds 0.82 mL. By calculation, the ratio of γ-PGA-*graft*-Et-Bx to Cu (II) ions was 1:305. This means that 1 molecule of γ-PGA-*graft*-Et-Bx can trap 305 ions of Cu(II) ions.

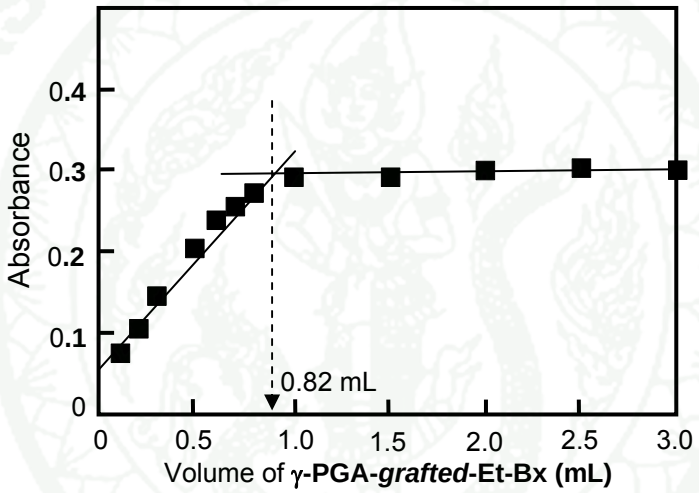

Figure 50 The relationship between the maximum absorbance at wavelength at 401 nm and the amount of 0.008 mM of γ-PGA-*graft*-Et-Bx solution from photometric titration method.

2.2.2.2 Iron (III) ion responsive properties

The iron (III) ions responsive properties of γ-PGA-*graft*-Et-Bx were primary investigated with naked eye (Figure 51). After the γ-PGA-*graft*-Et-Bx was added into the aqueous solution of iron (III) nitrate, color of the solution was changed from clear to purple. This color transition phenomenon was further examined by using UV-visible spectrophotometer.

Figure 51 Change in color of aqueous solution of iron(III) nitrate after mixing with γ-PGA-*graft*-Et-Bx.

It was surprising that some portion of the γ-PGA-*graft*-Et-Bx disappeared in the iron (III) aqueous solution. It is expected that γ-PGA-*graft*-Et-Bx may form a complex with iron (III) ions, so that the solubility properties were changed. To clarify this phenomenon, the liquid portion separated by centrifugation or filtration was examined by UV-visible spectrometer. Figure 52 shows that UV spectrum of the supernatant is different from that of iron (III) aqueous solution. The maximum absorption spectra of the aqueous solution of iron (III) nitrate, γ-PGA-*graft*-Et-Bx-iron (III) complex appeared at 294 and 520 nm, respectively. Changes in color and solubility properties appeared when γ-PGA-*graft*-Mt-Bx formed a complex with iron (III) ions. These two phenomena were detected with the naked eye. γ-PGA-*graft*-Mt-Bx modified by this study is thus designated as a dual-response sensing material.

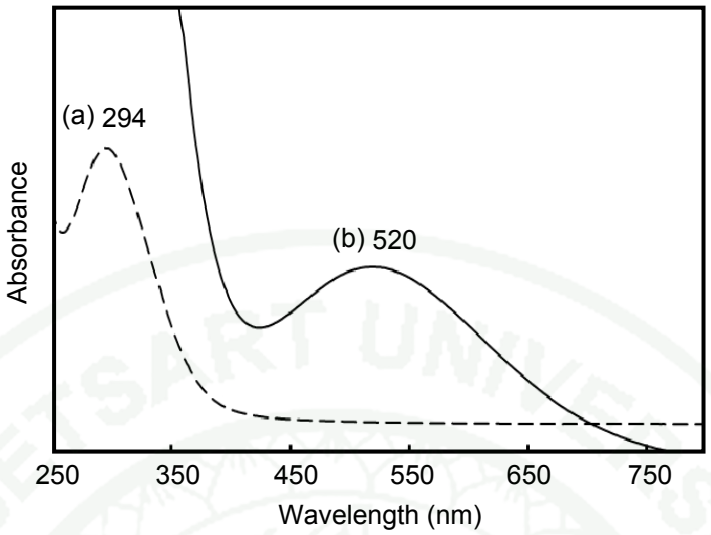

Figure 52 UV-visible absorption spectra of (a) aqueous solution of iron (III) nitrate, and (b) γ-PGA-*graft*-Et-Bx-iron (III) complex in an aqueous solution.

While the liquid portion was investigated and finally found that the complex between γ-PGA-*graft*-Et-Bx exists in the aqueous solution, the precipitate was investigated by dissolving them in DMSO and then characterizing by UV-visible. λ_{max} of the γ-PGA-*graft*-Et-Bx precipitate, γ-PGA-*graft*-Et-Bx and iron (III) ions in the DMSO solutions were observed at 470, 275, and 316 nm, respectively (Figure 53). The shift of the λ_{max} indicated that the precipitate was also complex between the γ-PGA-*graft*-Et-Bx and iron (III) ions. The reason why the complex exists in the precipitate form might be due to the fact that Et-Bx were not uniformly graft onto γ-PGA backbone or the high molecular weight portion of the γ-PGA-*graft*-Et-Bx were formed complex and therefore this portion could not dissolve in water.

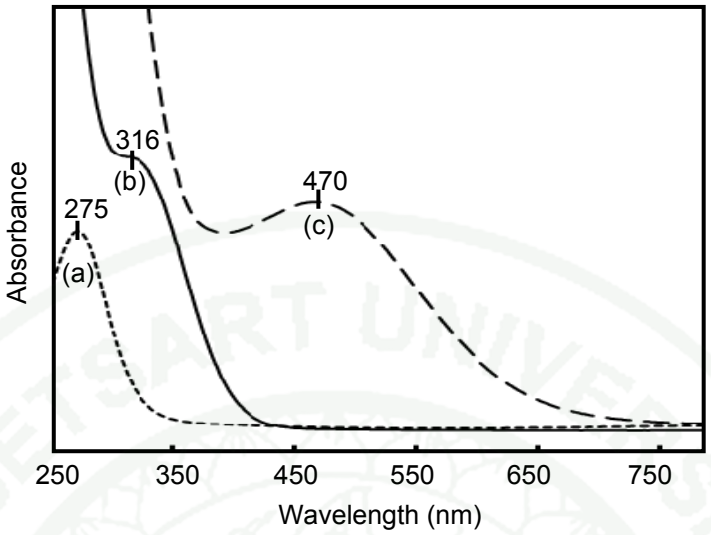

Figure 53 UV-Vis absorption spectra of (a) γ-PGA-*graft*-Et-Bx, (b) iron (III) ions, and (c) γ-PGA-*graft*-Et-Bx precipitate in DMSO solution.

To clarify these phenomena, iron (III) nitrate and γ-PGA-*graft*-Et-Bx were dissolved in the DMSO. The color of the mixture changed from clear to purple (Figure 54). This color transition phenomenon was further confirmed by using UV-visible spectrophotometer.

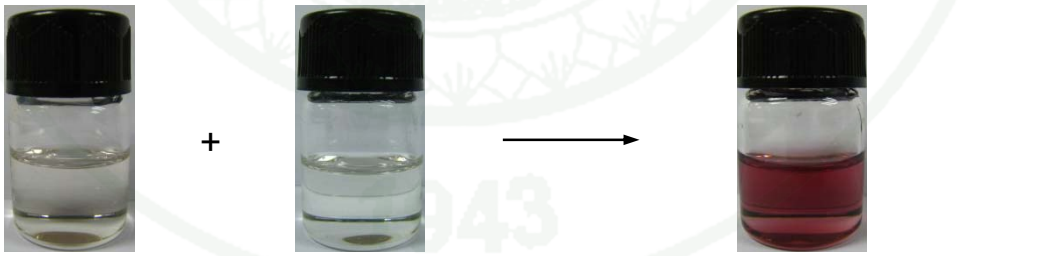

Figure 54 Change in color of γ-PGA-*graft*-Et-Bx solution after mixing with iron (III) nitrate in a DMSO solution.

Figure 55 shows UV spectra of solution of γ-PGA-*graft*-Et-Bx in DMSO, iron (III) nitrate in DMSO and the mixed solution of γ-PGA-*graft*-Et-Bx and iron (III) nitrate in DMSO. The maximum absorption peak was shifted to 503 nm after the

complex between the γ-PGA-*graft*-Et-Bx and iron (III) ions was formed. The obtained results indicated that γ-PGA-*graft*-Et-Bx showed sensitivity to iron (III) ions in both water and DMSO solutions.

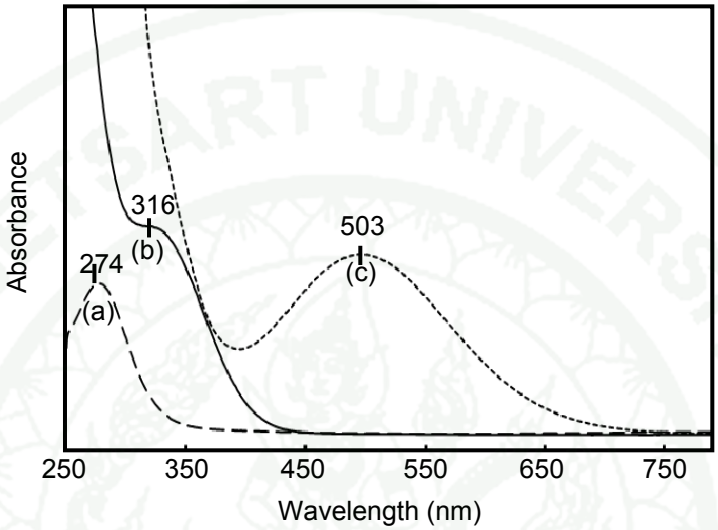

Figure 55 UV-Vis absorption spectra of (a) solution of γ-PGA-*graft*-Et-Bx in DMSO, (b) iron (III) nitrate in DMSO, and (c) mixture of γ-PGA-*graft*-Et-Bx and iron (III) nitrate in DMSO solution.

The qualitative analysis to determine a ratio of the polymer to iron (III) ions in the complex was carried out by using a photometric titration method. The solution of the γ-PGA-*graft*-Et-Bx and iron (III) ions were prepared by using DMSO as a solvent. In this study, different amount of the polymer solution was added into the iron (III) ions solution. The ratio of γ-PGA-*graft*-Et-Bx complexed with iron(III) ions was evaluated from the absorbance at λ_{max} of the complex at 501 nm. Figure 56 shows the result obtained from the titration method. It was found that the absorbance increase as quantity of the polymer in the solution increased at the beginning, and then it is started to be constant after the polymer solution was add more than 1.63 mL. Calculation based on these results revealed that the ratio of γ-PGA-*graft*-Et-Bx to the iron (III) ion was 1:154.

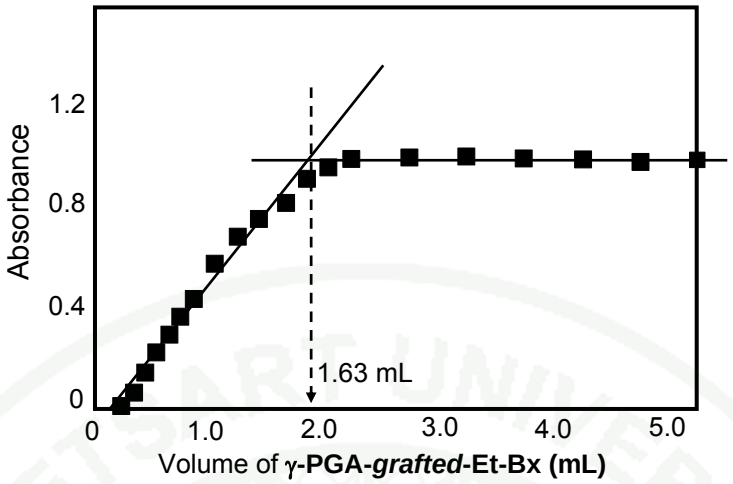

Figure 56 Relationship between absorbance at 501 nm and volume of γ-PGA-*graft*-Et-Bx solution (0.008 mmole) from photometric titration method.

CONCLUSIONS

Amphiphilic polymers composed of γ-PGA as a hydrophilic backbone and L-PAE as a hydrophobic segment were successfully prepared. The grafting degree was varied by the amount of WSC. 0.5-19.6 mmol of WSC gave the copolymer with grafting degree in range of 7-62%. The grafting degree increased as amounts of WSC increased. The solubility of the copolymers decreased when hydrophobicity of the chain increased. The particle size of copolymers depended on the grafting degree and the polymer concentration. The copolymers with grafting degree about 49% in aqueous solution showed thermoresponsive phenomenon at 80^{o}C. On the other hand, the copolymers with grafting degree in range of 30-49% showed thermoresponsive behavior when NaCl was added. The clouding temperatures depended on polymer and NaCl concentrations. The clouding temperature decreased as polymer concentration and NaCl concentration increased. Reversible thermoresponsive behavior could be observed.

γ-PGA-*graft*-Mt-Bx and γ-PGA-*graft*-Et-Bx were successfully prepared by esterification reaction. The most attainable grafting degree of γ-PGA-*graft*-Mt-Bx and γ-PGA-*graft*-Et-Bx were 30 and 25%, respectively. γ-PGA-*graft*-Mt-Bx and γ-PGA-*graft*-Et-Bx showed selective colorimetric sensing properties toward Cu(II) and Fe (III) ions. For Cu (II) ions, the color of the solution changed from clear to yellow in both aqueous solution and DMSO solution. For Fe (III) ions, the color of the solution changed from clear to purple in both aqueous solution and DMSO solution. The stoichiometric ratio of γ-PGA-*graft*-Mt-Bx to Cu (II) and Fe (III) ions were 1:390 and 1:217, respectively. The ratio of γ-PGA-*graft*-Et-Bx to Cu (II) and Fe (III) ions were 1:305 and 1:154, respectively. Since changes in color of the solution and solubility properties are obviously observed by human eyes when γ-PGA-*graft*-Bx either form complex with Cu (II) or Fe (III) ions, the γ-PGA-*graft*-Bx is designated as a novel dual-response sensing material.

LITERATURE CITED

Akagi, T., T. Kaneko, T. Kida, and M. Akashi. 2005. Preparation and characterization of biodegradable nanoparticles based on poly (γ-glutamic acid) with L-phenylalanine as a protein carrier. **Journal of Controlled Release** 108: 226-236.

Akagi, T., M. Higashi, T. Kaneko, T. Kida, and M. Akashi. 2005. In vitro enzymatic degradation of nanoparticles prepared from hydrophobically-modified poly (γ-glutamic acid). **Macromolecular Bioscience** 5: 598-602.

Akagi, T., M. Higashi, T. Kaneko, T. Kida, and M. Akashi. 2005. Hydrolytic and enzymatic degradation of nanoparticles based on amphiphilic poly (γ-glutamic acid)-graft-L-phenylalanine copolymers. **Biomacromolecules** 7:297-303.

Attaphon, K., R. Sawittree, W. Worawat, V. Chatchai, S. Songwut, K. Nattamon, and L. Apirat. 2012. The effect of alkali and Ce(III) ions on the response properties of benzoxazine supramolecules prepared via molecular assembly. **Molecules** 17:511-526.

Bodnar, M., A.L. Kjøniksen, R. M. Molnar, J.F. Hartmann, L. Daroczi, B. Nystromb, and J. Borbely. 2008. Nanoparticles formed by complexation of poly-gamma-glutamic acid with lead ions. **Journal of Hazardous Materials** 153: 1185-1192.

Buruiana, E. C., M. Murariu, and T. Buruiana. 2010. Copolyacrylates with phenylalanine and anthracene entities prepared by ATRP and microwave irradiation. **Journal of Luminescence** 130: 1794-1801.

Chirachanchai, S., A. Laobuthee, S. Phongtamrug, W. Siripatanasarakit, and H. Ishida. 2000. A novel ion extraction material using host-guest properties of oligobenzoxazine local structure and benzoxazine monomer molecular assembly. **Journal of Applied polymer Science** 77: 2561-2568.

Chirachanchai, S., A. Laobuthee, S. Phongtamrug, W. Siripatanasarakit, and H. Ishida. 2000. A novel ion extraction material using host-guest properties of oligobenzoxazine local structure and benzene monomer molecular assembly. **Journal of Applied Polymer Science** 77: 2561-2794.

Gil, E. S., and S. M. Hudson. 2004. Stimuli-reponsive polymers and their bioconjugates. **Progress in Polymer Science** 29: 1173-1222.

Inbaraj, B. S., J. S. Wang, J. F. Lu, F. Y. Siao, and B. H. Chen. 2009. Adsorption of toxic mercury (II) by an extracellular biopolymer poly (γ-glutamic acid). **Bioresource Technology** 100: 200-207.

Lianga, H. F., C. T. Chenb, S. C. Chena, R. A. Kulkarnia, Y. L. Chiua, M. C. Chena, and H. W. Sunga. 2006. Paclitaxel-loaded poly(g-glutamic acid)-poly(lactide) nanoparticles as a targeted drug delivery system for the treatment of liver cancer. **Biomaterials** 27: 2051–2059.

Mclean, R. J. C., D. Beauchemin, L. Clapham, and T. J. Beveridge. 1990. Metal-binding characteristics of the gamma-glutamyl capsular polymer of *Bacillus licheniformis* ATCC 9945. **Applied and Environmental Microbiology** 56: 3671-3677.

Naoki, N. and I. Yoshito. 1995. Mechanism of amide formation by carbodiimide for conjugation in aqueous media, **Bioconjugate Chemistry** 6: 123-130.

Shih, I. L., and Y. Ts. Van. 2001. The production of poly-(γ-glutamic acid) from microorganisms and its various applications. **Bioresource Technology**, 79: 207-225.

Shimokuri, T., T. Kaneko, and M. Akashi. 2004. Specific thermosensitive volume change of biopolymer gels derived from propylated poly (γ-glutamate)s. **Journal of Polymer Science: Part A: Polymer Chemistry** 42: 4492-4501.

Shimokuri, T., T. Kaneko, T. Serizawa, and M. Akashi. 2004. Preparation and thermosensitivity of naturally occurring polypeptide poly (γ-glutamic acid) derivatives modified by propyl groups. **Macromolecular Bioscience** 4: 407-411.

Sonny, S. M., C. C. Theodore, M. D. Christopher, and A. I. Alexander. 2006. A heavy metal biotrap for wastewater remediation using poly-γ-glutamic acid. **Biotechnology Progress** 22: 523–531.

Sung, M. H., C. Park, C. J. Kim, H. Poo, K. Soda, and M. Ashiuchi. 2005. Natural and edible biopolymer poly-γ-glutamic acid: synthesis, production, and applications. **The Chemical Record** 5: 352-366.

Takami, A., H. Mariko, K. Tatsuo, K. Toshiyuki, and A. Mitsuru. 2005. In vitro enzymatic degradation of nanoparticles prepared from hydrophobically-modified poly (γ-glutamic acid). **Macromolecular Bioscience** 5: 598–602.

Takami, A., H. Mariko, K. Tatsuo, K. Toshiyu ki, and A. Matsuru. 2005. Hydrolytic and enzymatic degradation of nanoparticles based on amphiphilic poly(γ-glutamic acid)-graft-L-phenylalanine copolymers. **Biomacromolecules** 7: 297-303.

Takami, A., K. Tatsuo, K. Toshiyuki, and A. Mitsuru. 2005. Preparation and characterization of biodegradable nanoparticles based on poly(γ-glutamic acid) with L-phenylalanine as a protein carrier. **Journal of Controlled Release** 108: 226– 236.

Yamacehi, T. A., K. Tani, K. Shirano, S. I. Ishida, and Y. Nakamoto. 1996. Metal cation extraction properties of linear all-ortho phenolic oligomers. **Journal of Polymer Science: Part A Polymer Chemistry** 34: 687-693.

APPENDICES

Appendix A

FT-IR spectra and ^{1}H-NMR spectra

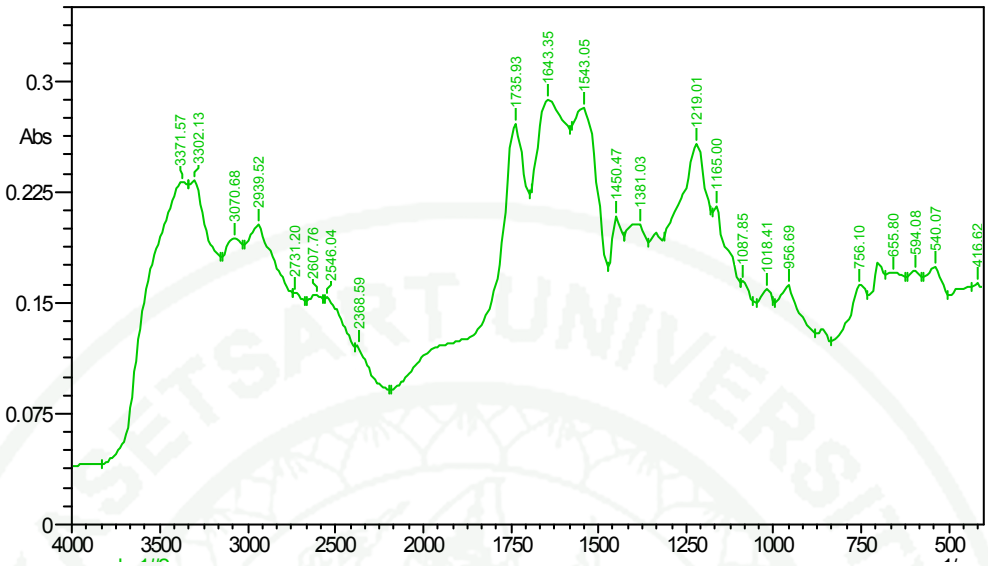

Appendix Figure A1 FT-IR spectrum of γ-PGA-*graft*-L-PAE with grafting degree of 7%.

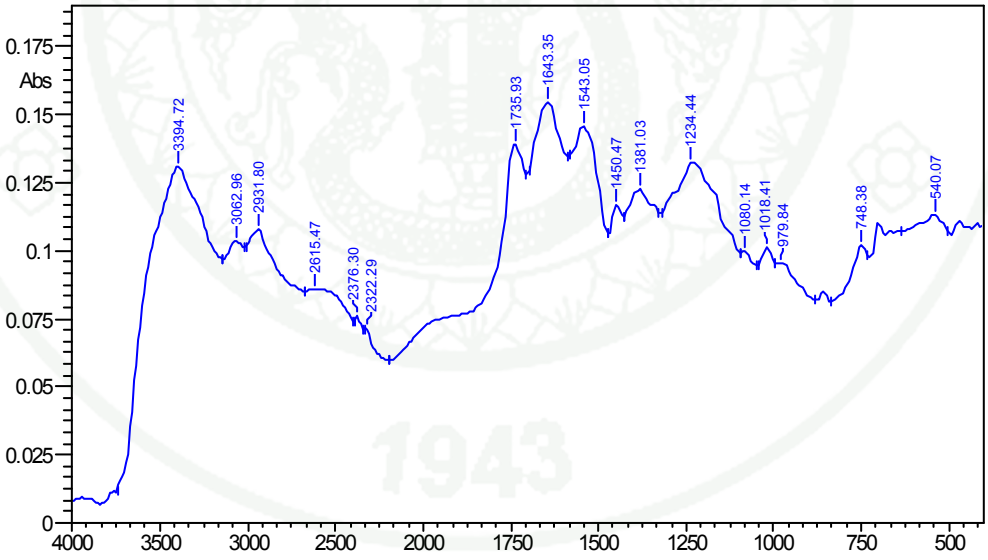

Appendix Figure A2 FT-IR spectrum of γ-PGA-*graft*-L-PAE with grafting degree of 15%.

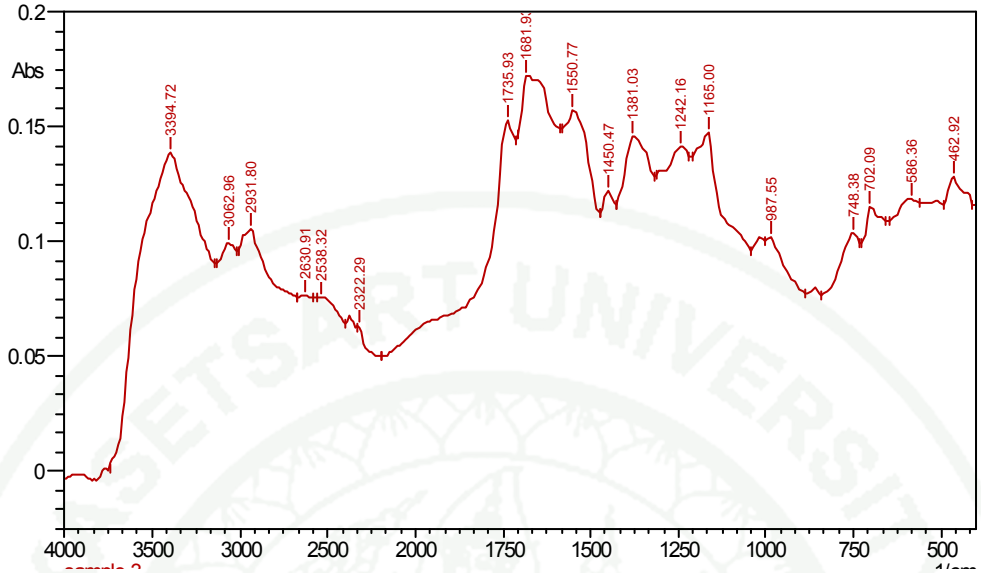

Appendix Figure A3 FT-IR spectrum of γ-PGA-*graft*-L-PAE with grafting degree of 22%.

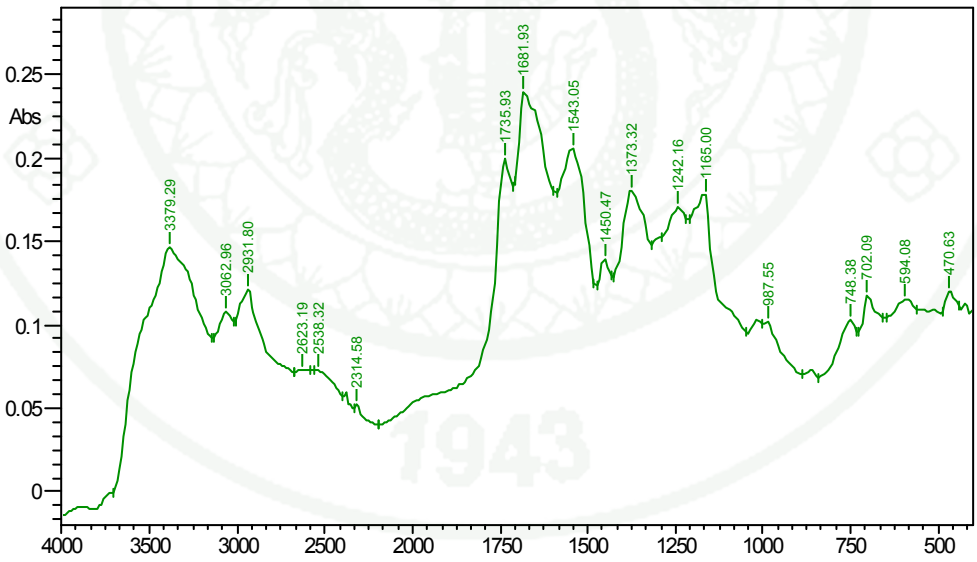

Appendix Figure A4 FT-IR spectrum of γ-PGA-*graft*-L-PAE with grafting degree of 30%.

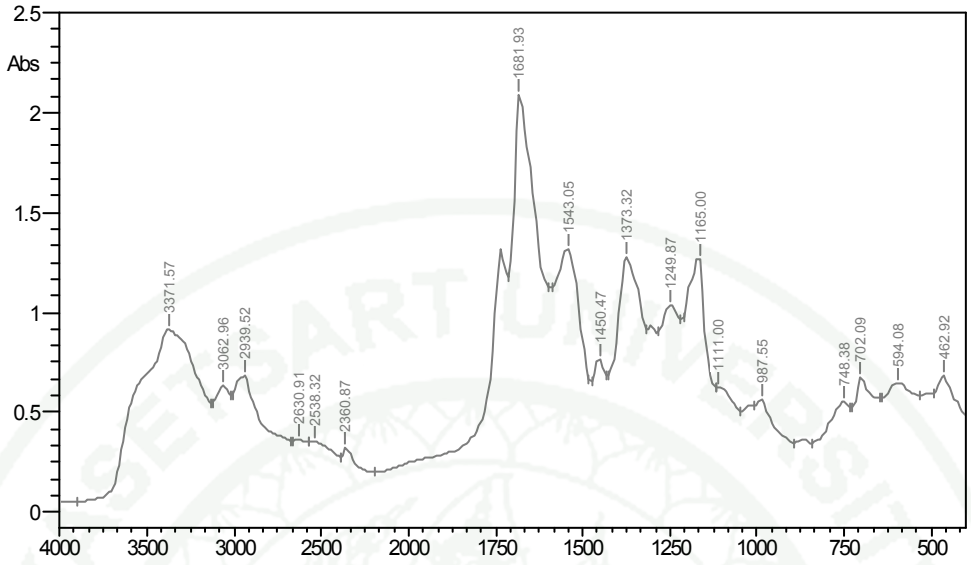

Appendix Figure A5 FT-IR spectrum of γ-PGA-*graft*-L-PAE with grafting degree of 36%.

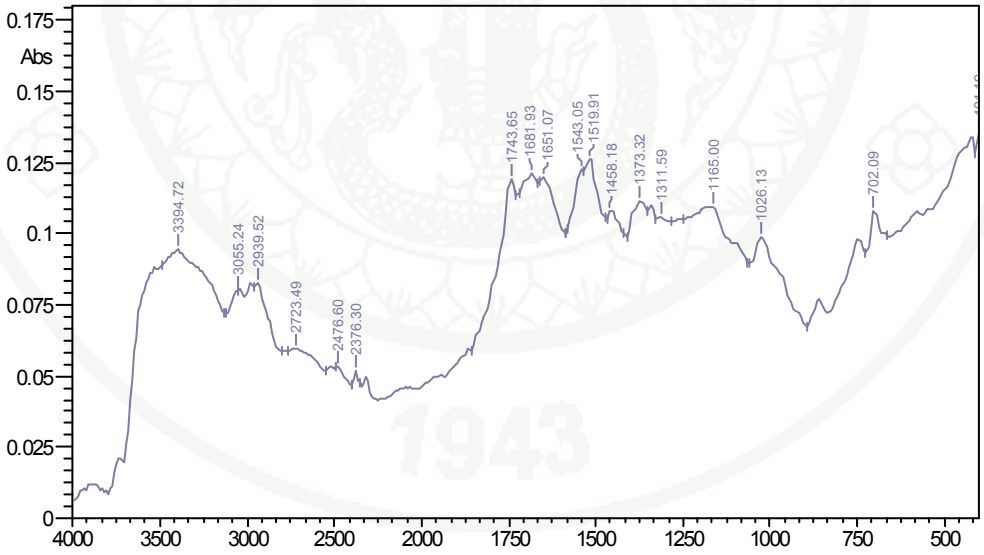

Appendix Figure A6 FT-IR spectrum of γ-PGA-*graft*-L-PAE with grafting degree of 49%.

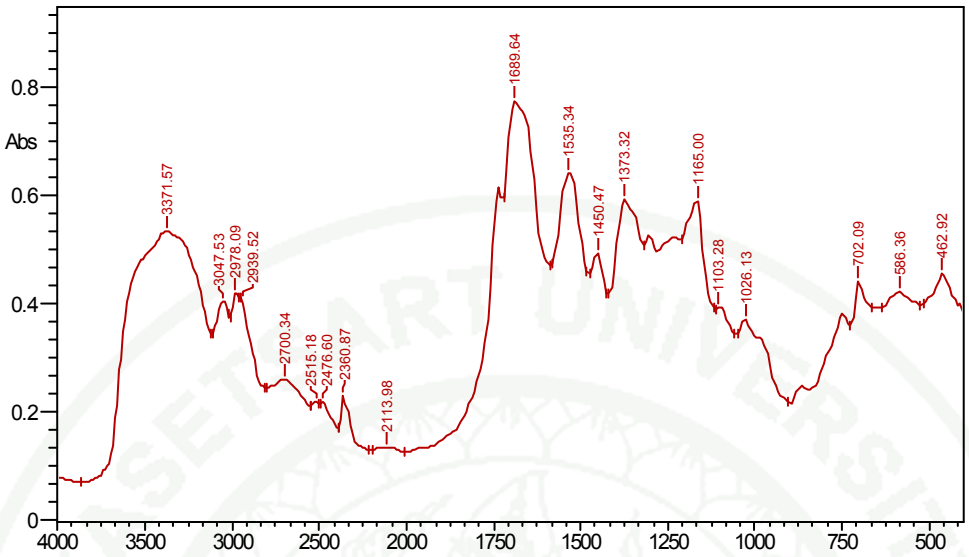

Appendix Figure A7 FT-IR spectrum of γ-PGA-*graft*-L-PAE with grafting degree of 54%.

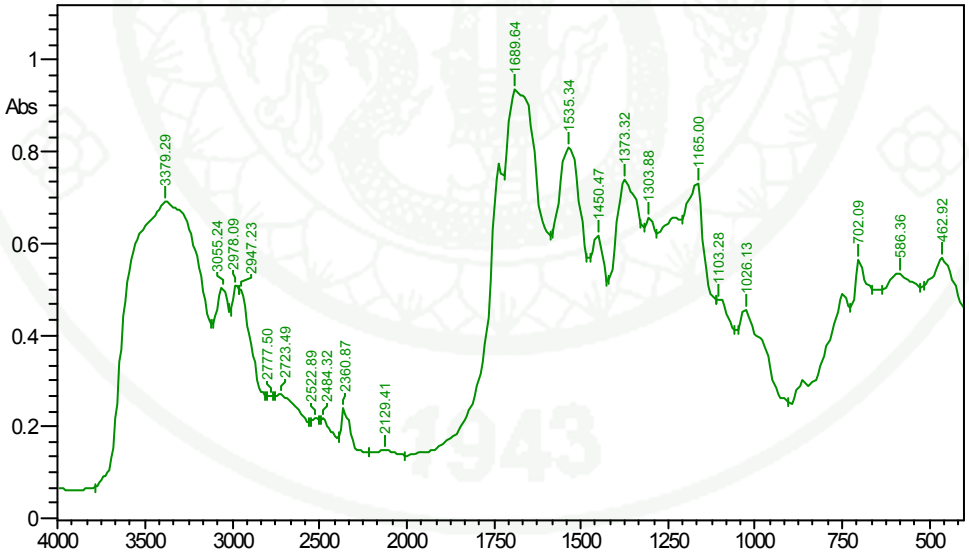

Appendix Figure A8 FT-IR spectrum of γ-PGA-*graft*-L-PAE with grafting degree of 62%.

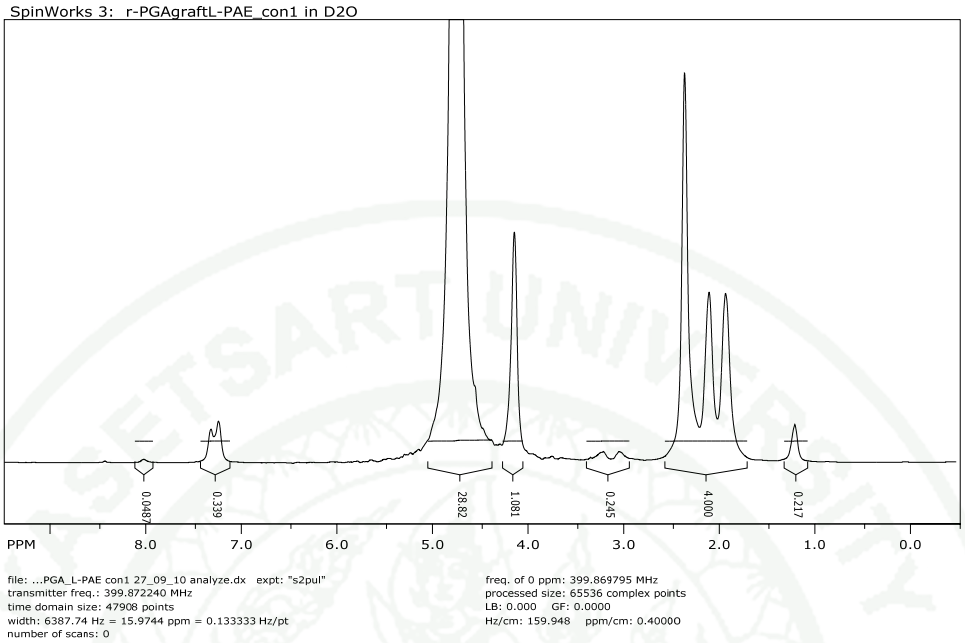

Appendix Figure A9 ^{1}H-NMR spectrum of γ-PGA-*graft*-L-PAE with grafting degree of 7%.

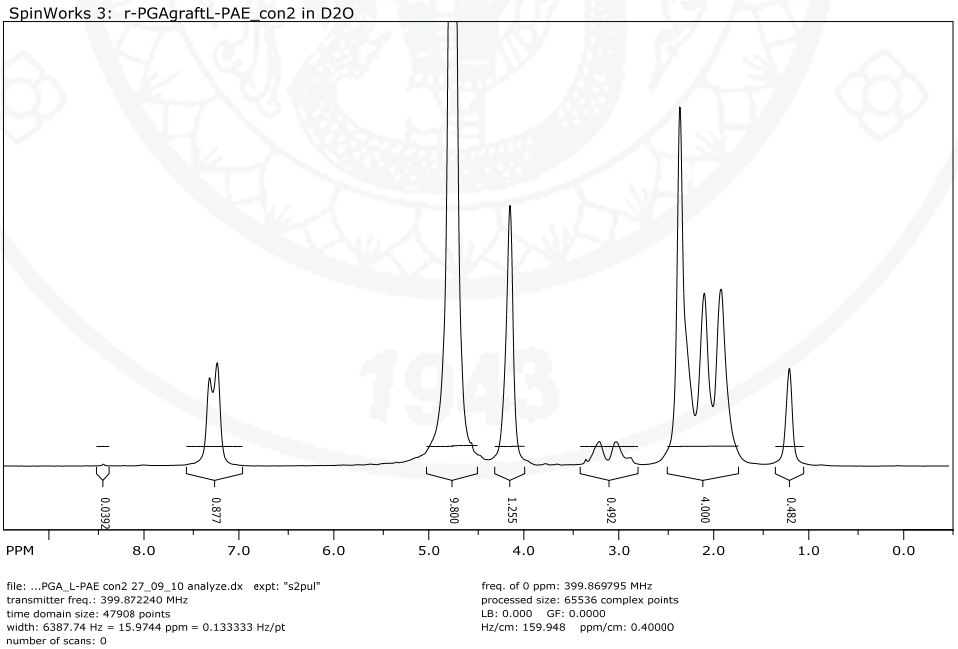

Appendix Figure A10 ^{1}H-NMR spectrum of γ-PGA-*graft*-L-PAE with grafting degree of 15%.

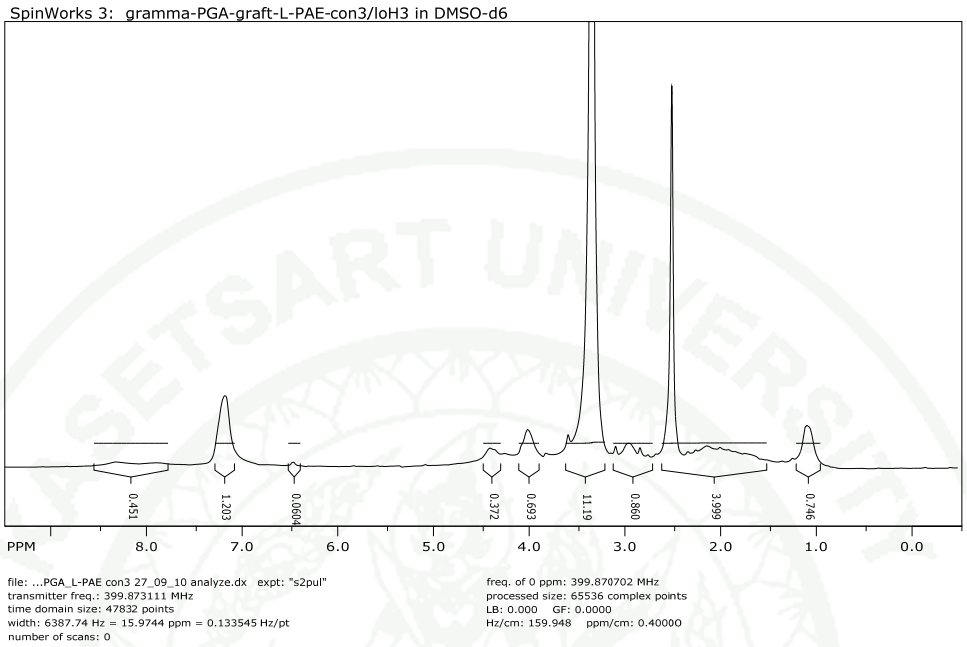

Appendix Figure A11 ^{1}H-NMR spectrum of γ-PGA-*graft*-L-PAE with grafting degree of 22%.

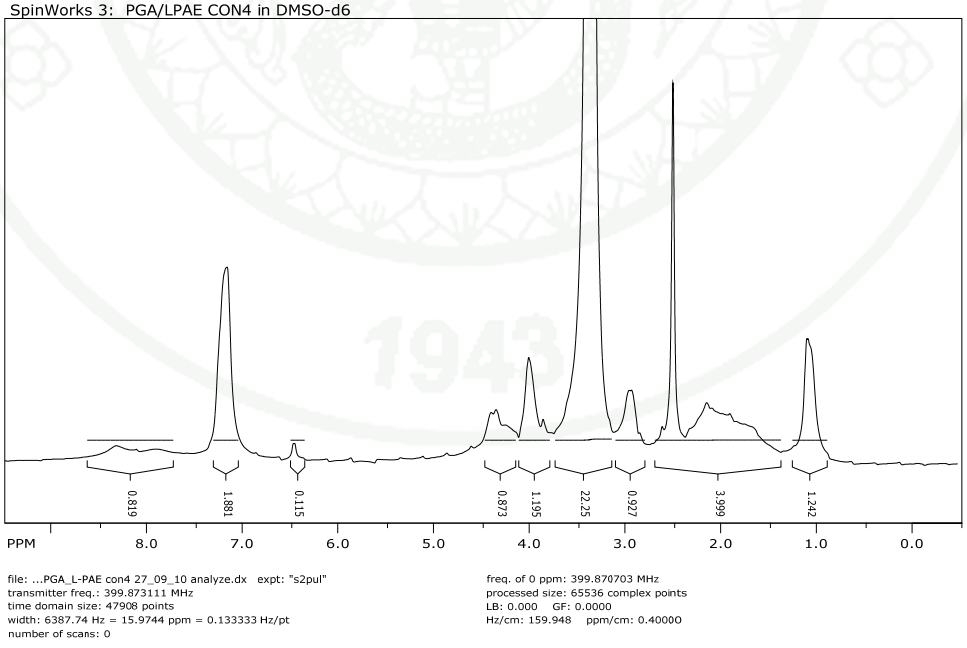

Appendix Figure A12 ^{1}H-NMR spectrum of γ-PGA-*graft*-L-PAE with grafting degree of 30%.

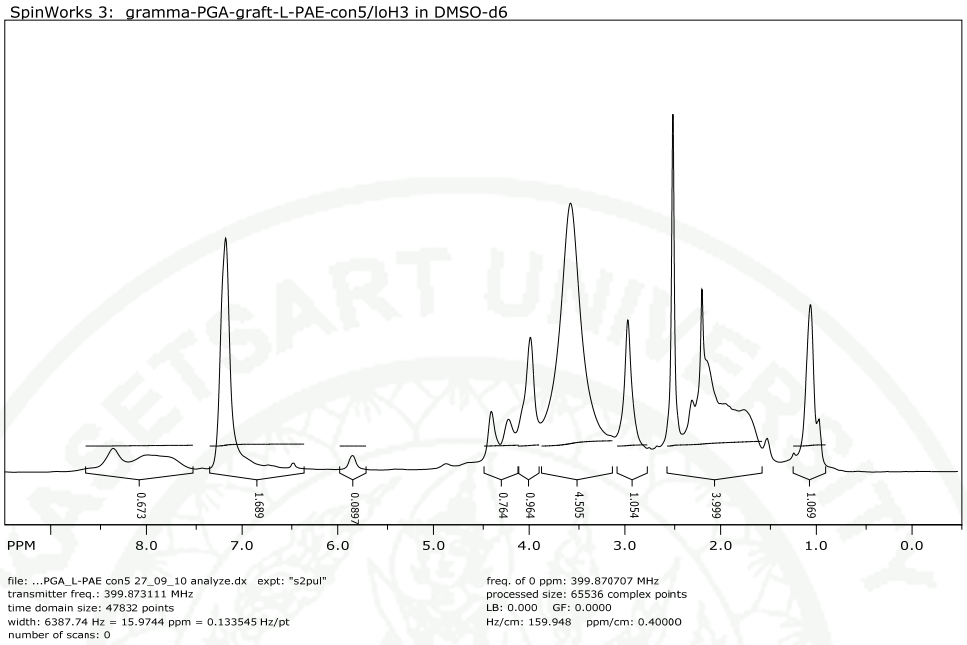

Appendix Figure A13 ^{1}H-NMR spectrum of γ-PGA-*graft*-L-PAE with grafting degree of 36%.

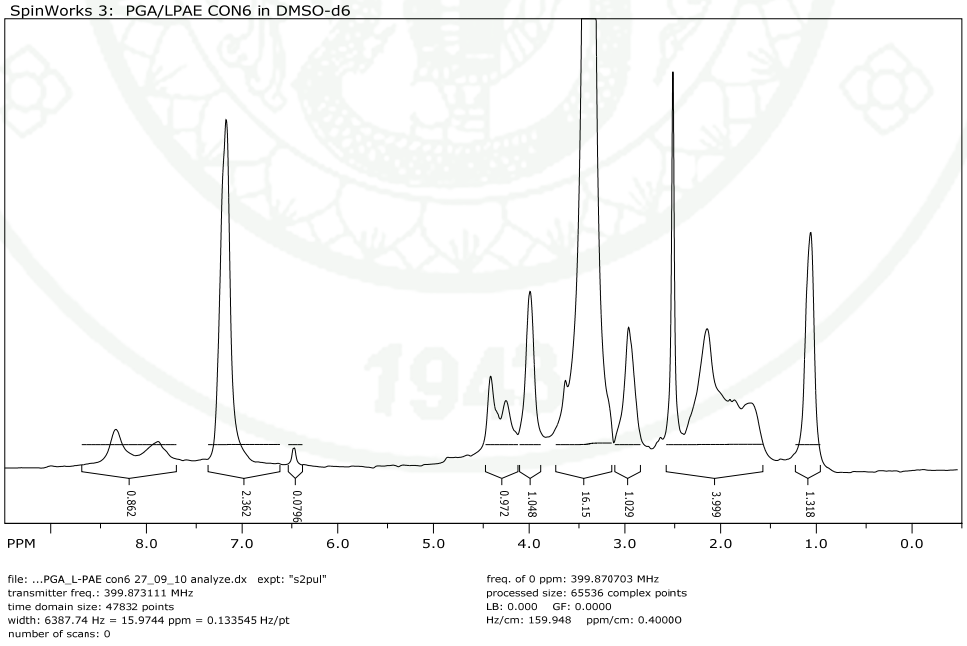

Appendix Figure A14 ^{1}H-NMR spectrum of γ-PGA-*graft*-L-PAE with grafting degree of 49%.

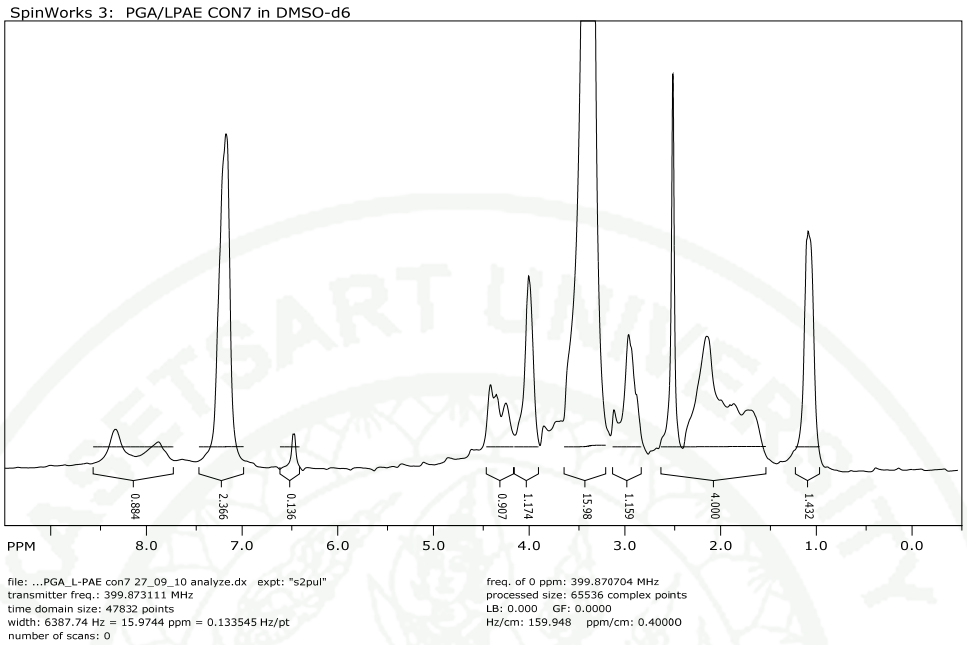

Appendix Figure A15 ^{1}H-NMR spectrum of γ-PGA-*graft*-L-PAE with grafting degree of 54%.

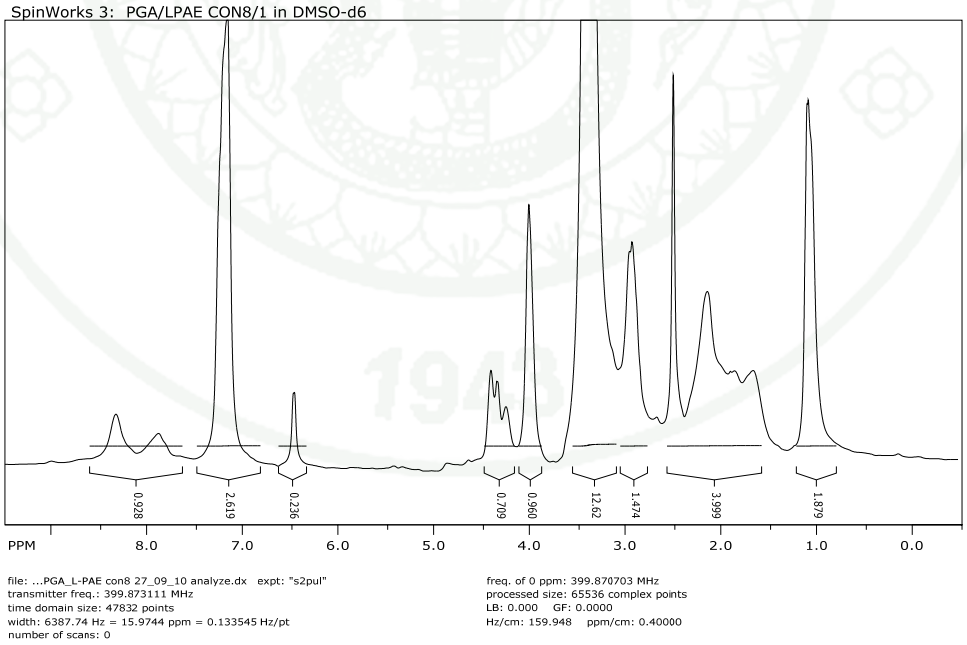

Appendix Figure A16 ^{1}H-NMR spectrum of γ-PGA-*graft*-L-PAE with grafting degree of 62%.

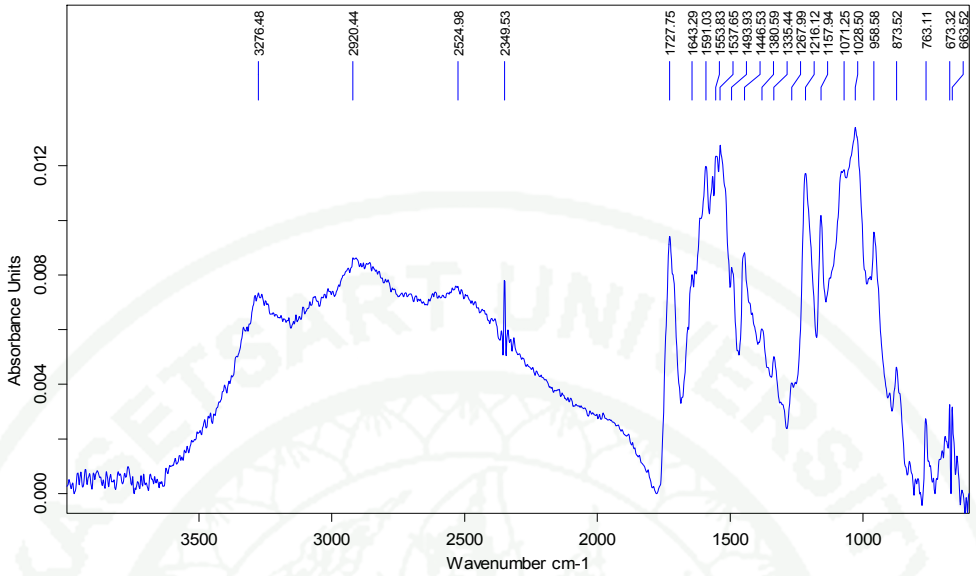

Appendix Figure A17 FT-IR spectrum of γ-PGA-*graft*-Mt-Bx at 15 min.

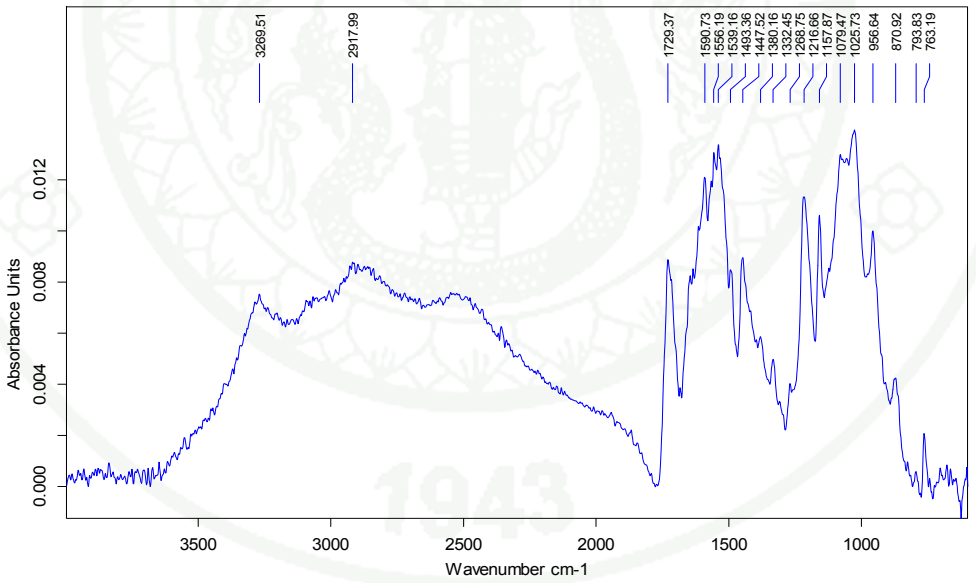

Appendix Figure A18 FT-IR spectrum of γ-PGA-*graft*-Mt-Bx at 30 min.

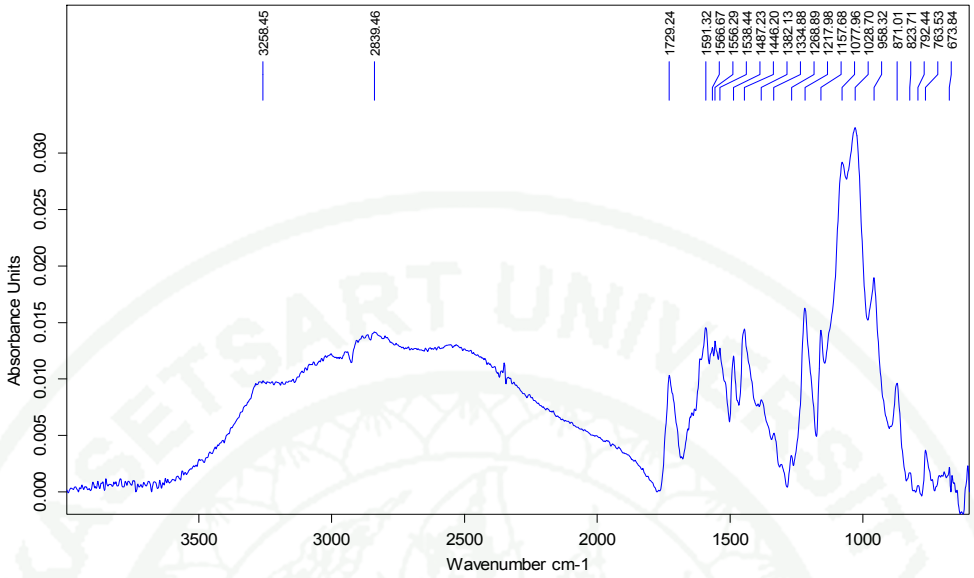

Appendix Figure A19 FT-IR spectrum of γ-PGA-*graft*-Mt-Bx at 1 h.

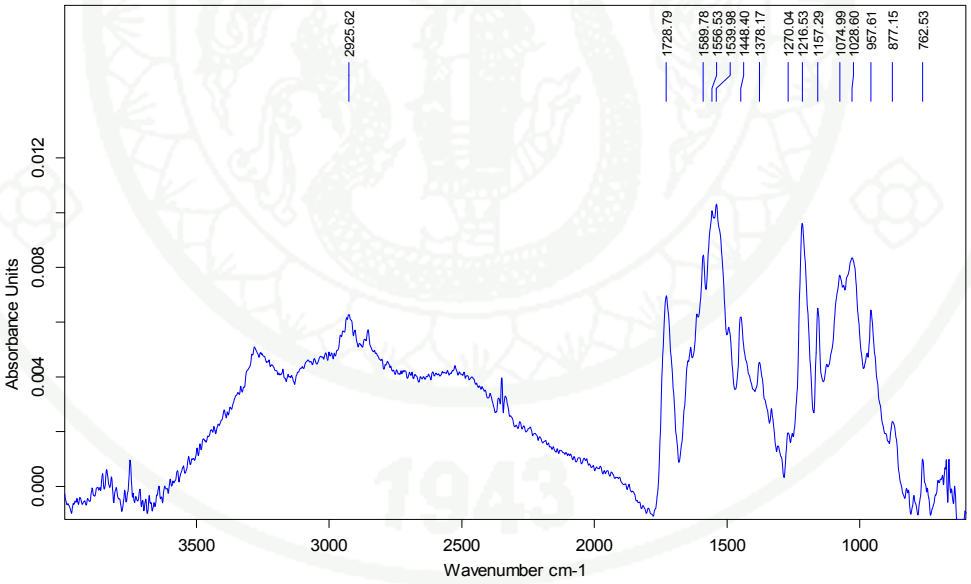

Appendix Figure A20 FT-IR spectrum of γ-PGA-*graft*-Mt-Bx at 2 h.

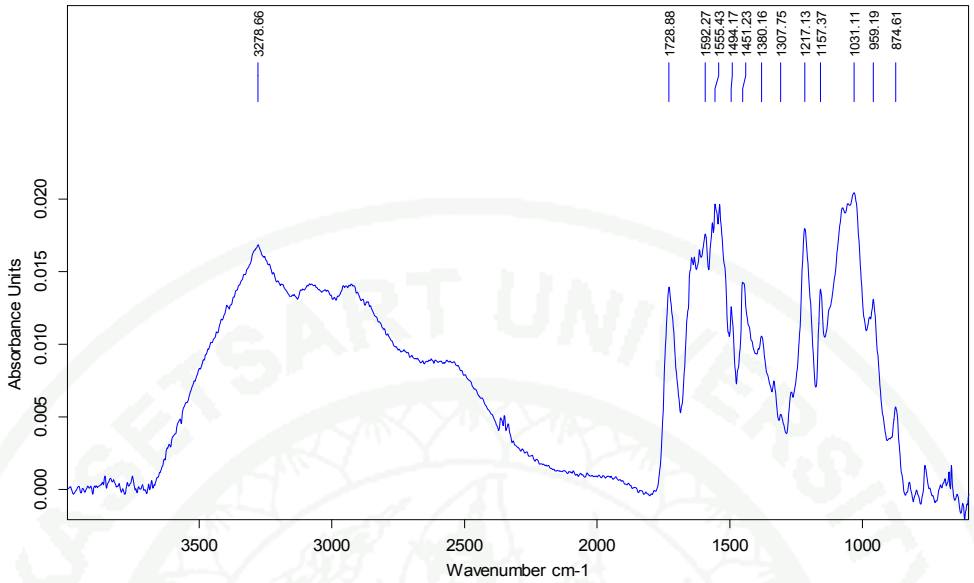

Appendix Figure A21 FT-IR spectrum of γ-PGA-*graft*-Mt-Bx at 4 h.

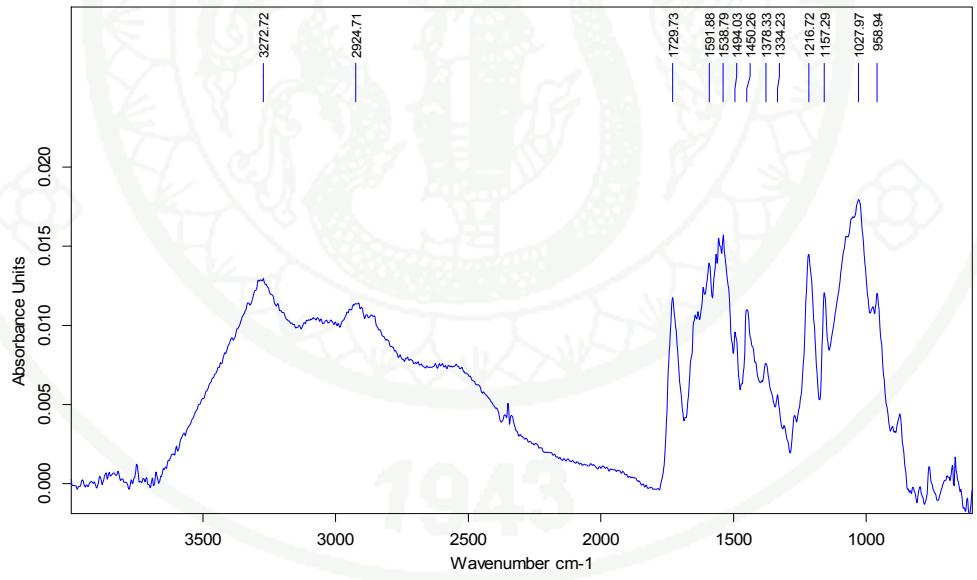

Appendix Figure A22 FT-IR spectrum of γ-PGA-*graft*-Mt-Bx at 6 h.

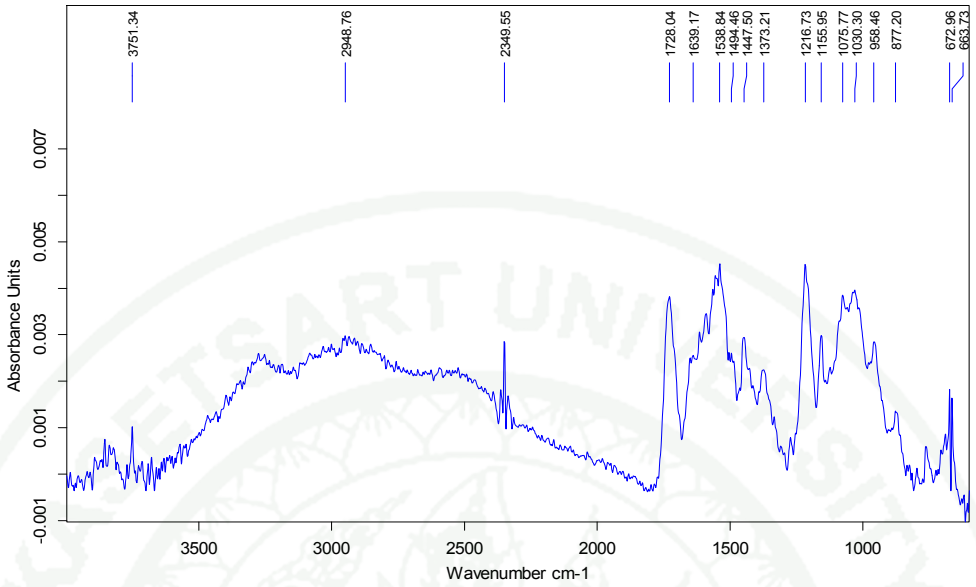

Appendix Figure A23 FT-IR spectrum of γ-PGA-*graft*-Mt-Bx at 8 h.

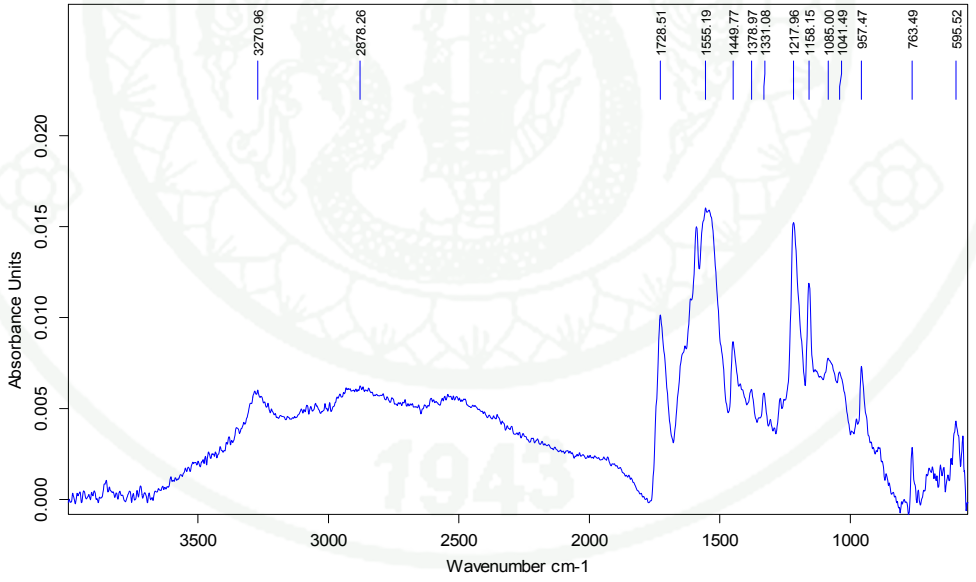

Appendix Figure A24 FT-IR spectrum of γ-PGA-*graft*-Et-Bx at 15 min.

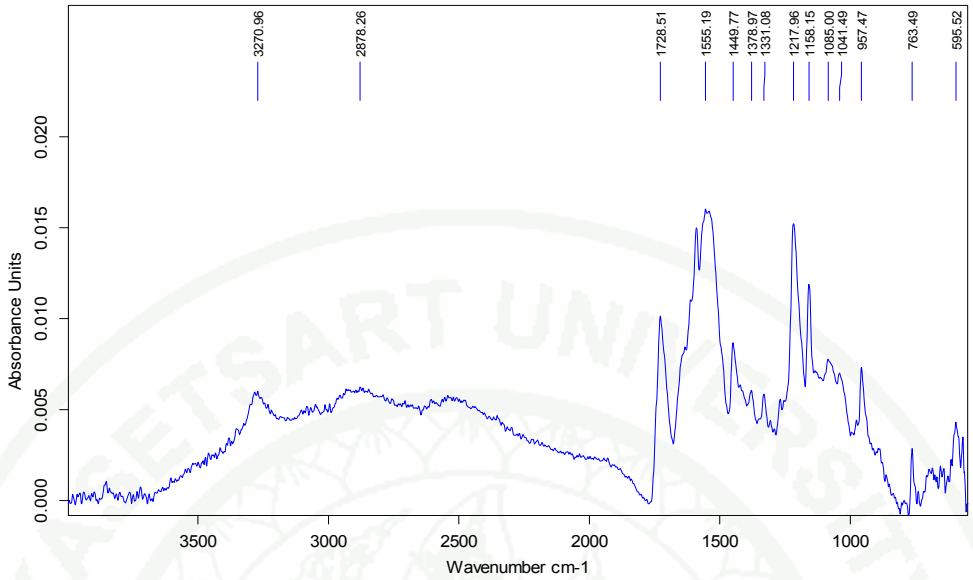

Appendix Figure A25 FT-IR spectrum of γ-PGA-*graft*-Et-Bx at 30 min.

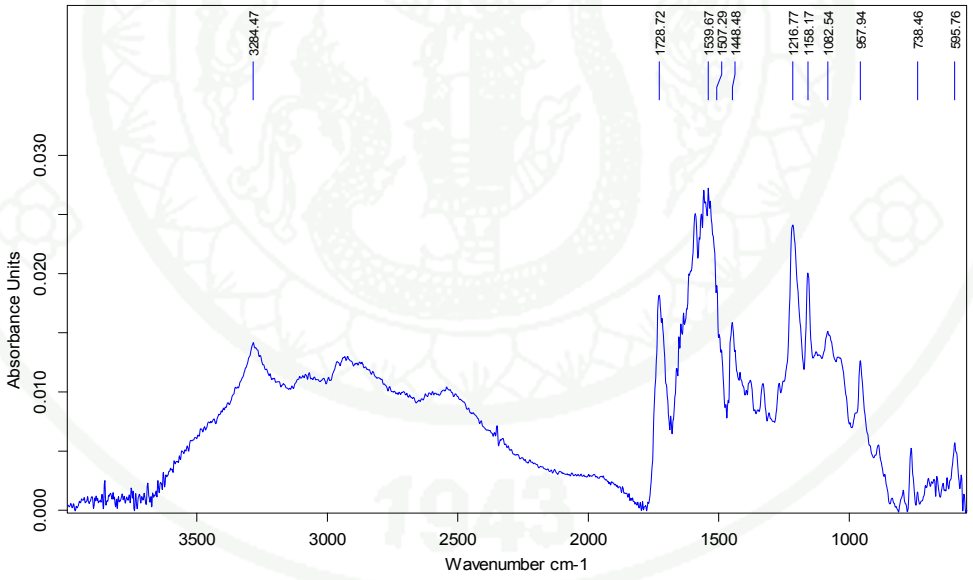

Appendix Figure A26 FT-IR spectrum of γ-PGA-*graft*-Et-Bx at 1 h.

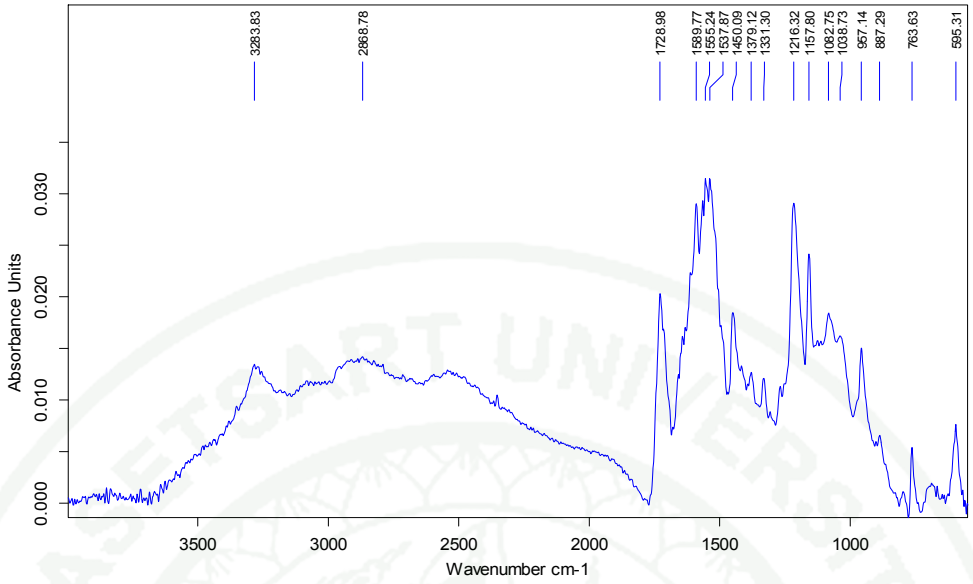

Appendix Figure A27 FT-IR spectrum of γ-PGA-*graft*-Et-Bx at 2 h.

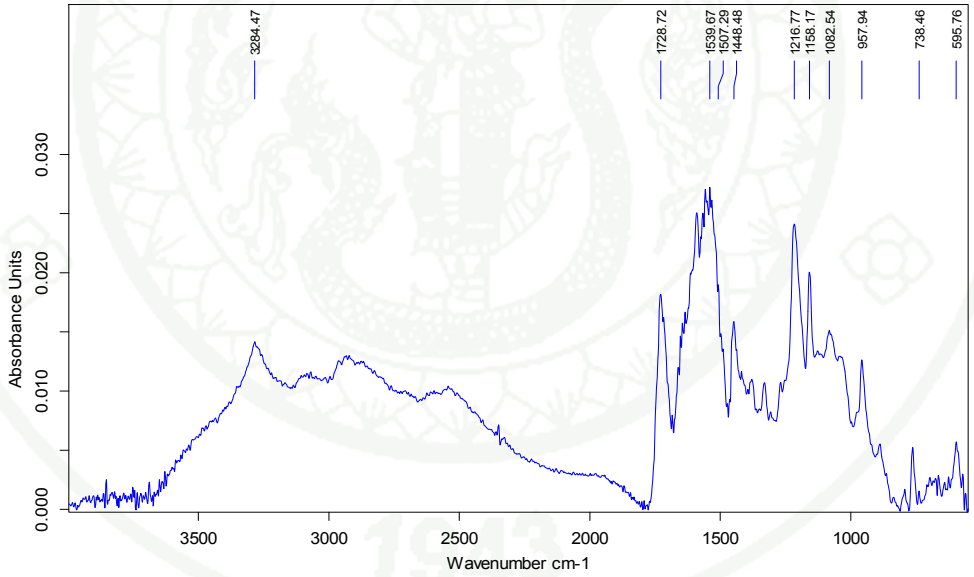

Appendix Figure A28 FT-IR spectrum of γ-PGA-*graft*-Et-Bx at 4 h.

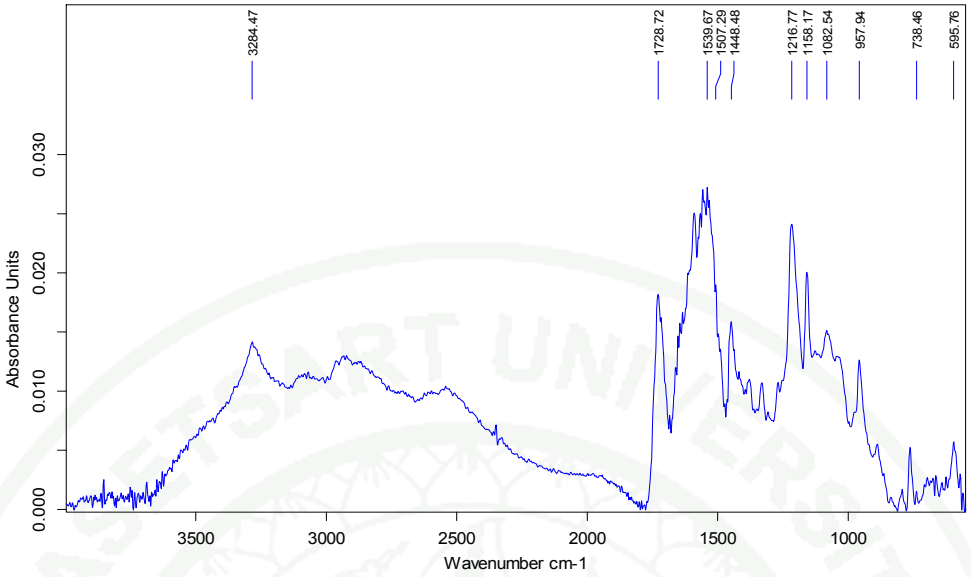

Appendix Figure A29 FT-IR spectrum of γ-PGA-*graft*-Et-Bx at 6 h.

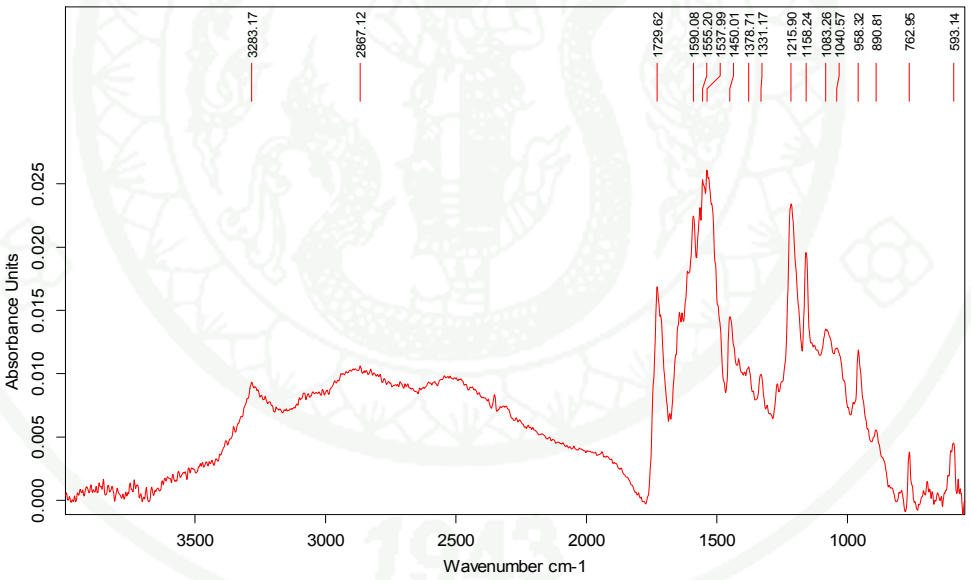

Appendix Figure A30 FT-IR spectrum of γ-PGA-*graft*-Et-Bx at 8 h.

Appendix B

Particle size

Appendix Table B1 Particle size of γ-PGA-*graft*-L-PAE (0.2 mg/mL) in water at room temperature.

Sample	Grafting degree	Size		PDI	
		mean	SD	mean	SD
1	**7±1**	393	186	0.52	0.09
2	**15±2**	245	281	0.61	0.31
3	**22±2**	30	0.4	0.80	0.02
4	**30±1**	66	31	0.74	0.27
5	**36±1**	38	21	0.44	0.15
6	**49±1**	58	1	0.17	0.02
7	**54±1**	129	35	0.25	0.02
8	**62±2**	97	18	0.26	0.06

Appendix Table B2 Particle size of γ-PGA-*graft*-L-PAE (0.2 mg/mL) in 4M NaCl at room temperature.

Sample	Grafting degree	Size		PDI	
		mean	SD	mean	SD
1	**7±1**	68	13	0.73	0.19
2	**15±2**	192	95	0.58	0.22
3	**22±2**	62	55	0.66	0.37
4	**30±1**	129	138	0.38	0.03
5	**36±1**	264	284	0.30	0.21
6	**49±1**	405	56	0.46	0.09
7	**54±1**	223	28	0.47	0.10
8	**62±2**	226	118	0.66	0.31

Appendix Table B3 Particle size of γ-PGA-*graft*-L-PAE (0.2 mg/mL) in 4M NaCl at 60°C.

Sample	Grafting degree	Size		PDI	
		mean	SD	mean	SD
4	**30±1**	746	0.29	0.29	0.01
5	**36±1**	871	0.45	0.45	0.14
6	**49±1**	1219	0.23	0.23	0.01

Appendix Table B4 Particle size of γ-PGA-*graft*-L-PAE (saturated solution) in water at room temperature.

Sample	Grafting degree	Size		PDI	
		mean	SD	mean	SD
1	**7±1**	27	4	0.85	0.02
2	**15±2**	144	74	0.71	0.34
3	**22±2**	32	5	0.92	0.15
4	**30±1**	42	17	0.78	0.32
5	**36±1**	35	3	0.54	0.02
6	**49±1**	68	0.3	0.16	0.01
7	**54±1**	81	1	0.15	0.02
8	**62±2**	83	6	0.21	0.05

Appendix Table B5 Particle size of γ-PGA-*graft*-L-PAE (saturated solution) in 4M NaCl at room temperature.

Sample	Grafting degree	Size		PDI	
		mean	SD	mean	SD
1	**7±1**	33	4	0.74	0.02
2	**15±2**	64	19	0.66	0.20
3	**22±2**	105	55	0.28	0.02
4	**30±1**	56	3	0.78	0.03
5	**36±1**	73	21	0.85	0.11
6	**49±1**	159	9	0.47	0.03
7	**54±1**	587	24	0.64	0.12
8	**62±2**	488	56	0.90	0.02

Appendix Table B6 Particle size of γ-PGA-*graft*-L-PAE (saturated solution) in 4M NaCl at 60°C.

Sample	Grafting degree	Size		PDI	
		mean	SD	mean	SD
4	**30±1**	839	201	0.34	0.02
5	**36±1**	1289	178	0.26	0.06
6	**49±1**	1278	317	0.25	0.04

Appendix C

Conference

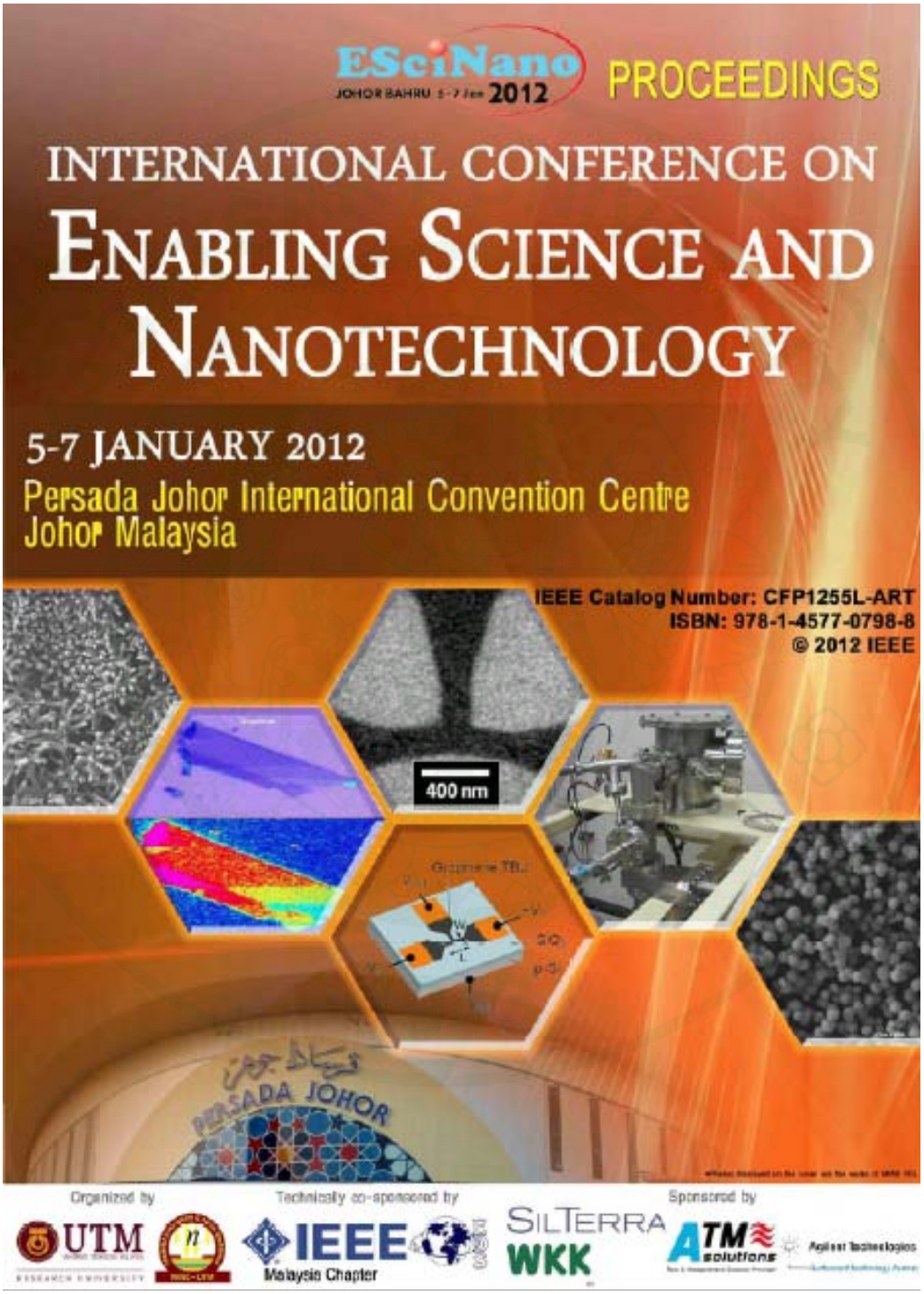

2012 International Conference on Enabling Science and Nanotechnology (ESciNano2012)

IEEE Catalog Number: CFP1255L-ART
ISBN: 978-1-4577-0798-8

Additional copies of this publication are available from:
Curran Associates, Inc.
57 Morehouse Lane
Red Hook, NY 12571 USA
Phone: (845) 758-0400
Fax: (845) 758-2633
E-mail: curran@proceedings.com

65	**Fabrication of p-ZnO/n-GaN diodes using a simple thermal evaporation technique** K.M.A. Saron and M.R. Hashim
67	**Development of a Novel Sensing Material,Poly(γ-Glutamic acid) grafted Benzoxazine (γ-PGA-g-Bzx), for Transition Metal (II) Ions** N. Choothong, A. Kaewvilai, A. Laobuthee and A. Lertworasirikul
68	**DFT calculations: Stress Dependence Structural and Band gap Study of Anatase and Rutile TiO_2** T. Mahmood , C. Cao, R. Ahmed, M. Ahmed and I. A. Zafar
70	**Synthesis of Nano-sized Alpha Alumina Using Solvothermal and Hydrothermal Methods: A Comparative study** M.Y.M. Sulaiman, W. Paulus and M. Muslim
72	**Applications of Image Processing (IP) Method on The Structure Measurements in Porous GaN.** A. Mahmood, N. M. Ahmed, A. Ramizy, Z. Hassan, Y. F. Kwong, C.L. Siang and M. B. Md Yunus
73	**Organic Thin-Film Transistors based on Naphthalene-Bis(dicarboximide) Polymer for n-Channel Organic Memory using Hole-Acceptor Layer** K. A. Mohamad, I. Saad and H. Fukuda
74	**Ohmic contacts to p-type doped ZnO** L.S. Chuah, S.S. Tneh, Z. Hassan, K. G. Saw and F. K. Yam
75	**The role of pulse time T_{on} on porous silicon as template for Au nanoparticles by using integrated electrochemical technique** T.S.T. Amran, M.R.Hashim, N.K.Ali, H.Yazid and R. Adnan
76	**Some Characterizations of Permanent Splicing Systems** F.W. Heng, N.H Sarmin and F. Karimi
77	**Characterization of p- and n-type GaN Thin Films Grown by Plasma-Assisted Molecular Beam Epitaxy** R. Radzali, N. Zainal, Y.F. Kwong and Z. Hassan
81	**Drive Current Boosting and Low Sub-Threshold Swing Obtained by δ_p^+ Layer in Double-Gate Tunnel FET** A. Chakraborty, Dr P.N Kondekar and M.K Yadav
82	**Cu-doped TiO_2 nanopowder synthesized by sonochemical process** N. Wongpisutpaisan, A. Ruangphanit N. Vittayakorn and W. Pecharapa
83	**Modification of Tantalum (V) Nitride with Zirconium Oxide for Photocatalytic Hydrogen Production under Visible Light Irradiation** L. Yuliati, K. Maeda, T. Takata, and K. Domen
84	**Photocatalytic Removal of Phenol under Visible Light Irradiation on Zinc Phthhalocyanine/Mesoporous Carbon Nitride** S.C Lee , H.O Lintang and L. Yuliati
85	**Optimized Vanadate Laser Performance at Variation of Crystal's Lengths** G. Krishnan, N.E Khamsan and N. Bidin

A Novel Colorimetric Sensing Material, Poly(γ-Glutamic acid)-*grafted*-3,4-Dihydro-3-(2′-ethyl hydroxyl)-6-ethyl-2*H*-benzoxazine (γ-PGA-*grafted*-ethyl-Bx), for Iron(III) Ions

Nu-orn Choothong, Attaphon Kaewvilai, Apirat Laobuthee** and Amornrat Lertworasirikul*

Department of Materials Engineering, Faculty of Engineering, Kasetsart University, Bangkok 10900, Thailand

* Corresponding author. fengarl@ku.ac.th, (A. Lertworasirikul); Tel.: +66-2-942-855-5 ext 2128

** Corresponding author. fengapl@ku.ac.th, (A. Laobuthee); Tel.: +66-2-942-855-5 ext 2132

A novel rapid ion colorimetric sensing material for Fe(III) ions was developed from poly(γ-glutamic acid) and 3,4-dihydro-3-(2′-ethyl hydroxyl)-6-ethyl-2*H*-benzoxazine (ethyl-Bx). The benzoxazine as an ionophore segment was grafted into γ-PGA backbone via the esterification reaction, which is a simple and effective reaction. The structure of γ-PGA-*grafted*-ethyl-Bx was characterized by using FTIR and ^{1}H-NMR. The most attainable degree of conversion was 25%. The γ-PGA-*grafted*-ethyl-Bx showed a highly selective and sensitive recognition toward Fe(III), which was clearly observable with the necked eye. The Fe(III) ions sensing property of γ-PGA-*grafted*-ethyl-Bx was further examined by using photometric titration method. After the interaction between the γ-PGA-*grafted*-ethyl-Bx and Fe(III) ions was formed, the solution of the polymer in dimethylsulfoxide was changed from clear and colorless to red color, resulting in the shift of the maximum wavelength from UV to visible range.

Keyword: γ-PGA, benzoxazine, transition metal ion, colorimetric sensing materials, photometric titration method.

Introduction

The iron is a common contaminant often present in the waste water from the industrial sites or iron smelter industries. In natural, iron is usually found in its

oxidized form as an iron(III) oxide, which is insoluble and non-degradable. The ingestion or consumption of iron is especially harmful to human by pain in the stomach. After ingestion, the iron passes deeper into the body and damages the internal organs, particularly the brain and the liver. The body goes into shock and death from liver failure. Despite the numerous water treatments, iron is still present in the water due to the dissolution of pipes and the solder in older buildings. Thus, many independent and government organizations have been concerned and set the limited permissible iron(III) level in waste water and drinking water. These factors demonstrate need for the development of rapid, simple and easily handle equipment for detecting iron(III) ions in residential and environment water samples.

The sensor technology is much simpler in an instrument and sample preparation. Many sensors for iron detection have been investigated (Wanga et al. 2001, Azad et al. 1985, Wang et al. 2010, Hassan et al. 2009, Zhang et al. 2010) but the selective colorimetric sensor (Gracia et al. 1997) has been attracted due to the excellent sensitivity, rapid response, the ability to do the detection in a non-destructive manner and cost-effective. The sensing method of colorimetric detection has been widely utilized for quantifying various molecules (Gracia et al. 1997, Robert et al. 1997, Maity et al. 2011, Liang et al. 2007, Abdolkarim et al. 2006). Most of the generated colorimetric sensors are based on the complex formation between the heavy metals and the ligand as a substrate (Sun et al. 2011, **Güler et al.** 2007, Song et al. 2002, Pedro et al. 2009).

Benzoxazines, heterocyclic compounds consisting of benzene and oxazine rings, were synthesized from *p*-substituted phenolic compounds, primary amines and para-formaldehyde via Mannich reaction (Holly and Cope 1944, Dunkers et al. 1996). Benzoxazines could form complex with rare earth alkali such as cerium(III), (Veranitisagul et al. 2011) and alkali earth heavy metal such as copper, magnesium, calcium, zinc and iron(III) (Oflidi et al. 2009, Panushkin et al. 2007, Apenysheva wt al. 2006, Fan et al. 1995, Michael et al. 2007, Rungsimanon et al. 2008) at nitrogen and oxygen positions. Due to their chemical structures, many researches have focused on their supramolecular structures and interactions with metal ions. In 2003, Laobuthee *et al*. (Laobuthee et al. 2003) found that intermolecular hydrogen bonding plays an important role and the host-guest formation was occurred via molecular assembly. It was noted that although the type of metal ion was changed, the host

always interacted at the same position. Similarly, Phongtamrug *et al*. (Phongtamrug et al. 2006) confirmed the host-guest property of benzoxazine via inclusion phenomena in 2006. The results suggest that the nitrogen atom and oxygen atom play an important role in interaction with alkali heavy metal by sharing their lone pare electrons. Therefore, benzoxazines are attracted for development to be a sensing material for metal ions.

Additionally, non-toxic and biodegradable materials have been applied for use in the field of bio-sensor during the past decades. (Gu et al. 2011, Dubuisson et al. 2009) Poly(γ-glutamic acid) is a natural components existing in a natto, a traditional Japanese food. It is produced by fermentation of soy bean by *Bacillus subtilis*. The properties of the poly(γ-glutamic acid) are water soluble, biodegradable and non-toxic. It is very useful in many fields such as drug delivery carrier and tissue engineering material (Takami et al. 2005, Sung et al. 2005). High proportion of carboxylic functional group in γ-PGA provides binding properties for metal ions. A number of studies using this polymer for the removal of metal ions from waste water have been reported. (Taniguchi et al. 2005, Taniguchi et al. 2005, Mark et al. 2006, Shih et al. 2003) Cross-linked poly(γ-glutamic acid) was found to be able to form the interaction with iron(III) ions. (Taniguchi et al. 2005)

This work has attempted to develop a novel sensing material for iron(III) ions by combining a chelating property of γ-PGA with the supramolecular and ion extraction properties of benzoxazine monomer. Here, 3,4-dihydro-3-(2′-ethyl hydroxyl)-6-ethyl-2*H*-benzoxazine is grafted into the poly(γ-glutamic acid) main chain via the esterification reaction. A selectivity and sensitivity as a colorimetric sensor for iron(III) ions is qualitatively and quantitatively studies by a photometric titration method.

Experimental

Materials

γ-PGA (poly(γ-glutamic acid), $\overline{M}_w$ = 170,000) was supplied from Wako (Japan). Ethyl-Benzoxazine (3,4-dihydro-3-(2′-ethyl hydroxyl)-6-ethyl-2*H*-benzoxazine) was synthesized as reported elsewhere (Bruke et al. 1949).

Acetronitrile (CH_3CN) was provided from Labscan (Thailand). Sulfuric acid from Carlo Erba was used as a catalyst. Dimethylsulfoxide (DMSO) was purchased from Sigma-Aldrich (Germany). Iron(III) nitrate salts ($Fe(NO_3)_3 \cdot 9H_2O$) was obtained from Ajax (New Zealand). All chemicals used in this work were analytical grade and used without further purification.

Instrument

Fourier transform infrared (FT-IR) spectra were recorded on an Alpha FT-IR spectrometer instrument from Bruker within the frequency range of 4000-600 cm^{-1} and resolution of 4 cm^{-1}. Proton nuclear magnetic resonance (^{1}H-NMR) spectra were measured on a Varian Mercury-400 spectrometer working at 400 MHz. Deuterated dimethylsulfoxide (DMSO-d6) was used as a solvent and tetramethylsilane (TMS) was used as an internal reference. UV-visible spectra and maximum absorbance were recorded on a Shimadzu UV-1700 spectrophotometer from 190 to 800 nm.

Preparation and characterization of γ-PGA-grafted-ethyl-Bx

γ-PGA-*grafted*-ethyl-Bx was prepared from γ-PGA and ethyl-benzoxazine monomer via esterification reaction. Synthesis schematic of the grafted copolymer was shown in Figure 1.

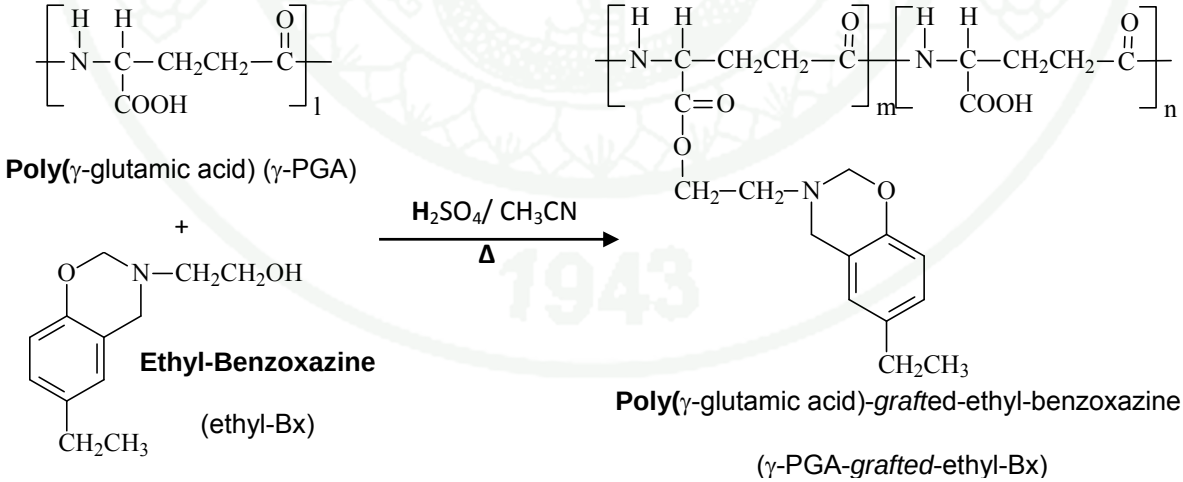

FIGURE 1. Synthesis schematic of γ-PGA-*grafted*-ethyl-Bx

γ-PGA (1.0 g, 2.0 mmol) dispersed in CH_3CN (100 ml) was prepared in a two-necked round bottoms flask equipped with a magnetic stirring bar, a condenser and a

dropping funnel. A catalytic amount of H_2SO_4 was added to the solution. The slurry was refluxed and stirred at 80°C for 1 h. The ethyl-Bx (1.5 g, 7.75 mmol) dissolved in CH_3CN (80 ml) was then drip-fed into the slurry. The mixture was further refluxed at 80°C for 2 h. Then, the yellow solid product was filtered, washed several times with distilled water and acetone and dried overnight in an oven at 60°C.

The grafted copolymer product was characterized by FT-IR and ^{1}H-NMR. The degree of grafting was calculated by ^{1}H-NMR.

Investigation on iron(III) ions responsive properties of γ-PGA-grafted-ethyl-Bx

The iron(III) ions responsive behavior was primary investigated in aqueous solution. The γ-PGA-*grafted*-ethyl-Bx powder (2.0 mg) was added in to the aqueous solution of iron(III) nitrate (5mM). The mixture was dramatically shaken for 5 minutes. After that the solution was detected by naked eye and UV-visible spectrophotometer.

The iron(III) ions responsive properties were qualitatively and quantitatively studies with the photometric titration method in a DMSO solution. Different volumes of 0.008 mmole of γ-PGA-*grafted*-ethyl-Bx in DMSO solutions (0.100, 0.200, 0.300, 0.400, 0.500, 0.600, 0.800, 1.000, 1.200, 1.400, 1.600, 1.800, 2.000, 2.500, 3.000, 3.500, 4.000, 4.500 and 5.000 ml) were prepared, and then each solution was added into 5.000 ml of DMSO solutions of the iron(III) nitrate (0.40 mmole). The mixed solutions were adjusted with DMSO to attain to a total volume of 10.000 ml. After the mixed solutions were left at room temperature for 30 min, they were measured for their by UV-visible attributes.

Results and Discussion

Preparation and characterization of γ-PGA-grafted-ethyl-Bx

The FT-IR spectrometer was used to examine the functional group of the starting materials (γ-PGA and ethyl-Bx) and the product. γ-PGA showed the characteristic peaks at 3283, 1640 and 1730 cm^{-1} (figure 2(a)). The first two positions related to the amide bond and the last position referred to a carbonyl group. The absorption peaks of ethyl-Bx at 1504, 1120 and 871 cm^{-1} referred to an oxazine ring

(trisubstituted on benzene), ether aromatic (Ar-O-C) and benzene ring out of plane, respectively (figure 2(b)). It was found that the characteristic peaks of the product appeared at 1733, 1517, 1164 and 901 cm^{-1} which correspond to the carbonyl bond, oxazine ring (trisubstituted on benzene), ether aromatic (Ar-O-C) and benzene ring out of plane, respectively (figure 2(c)).

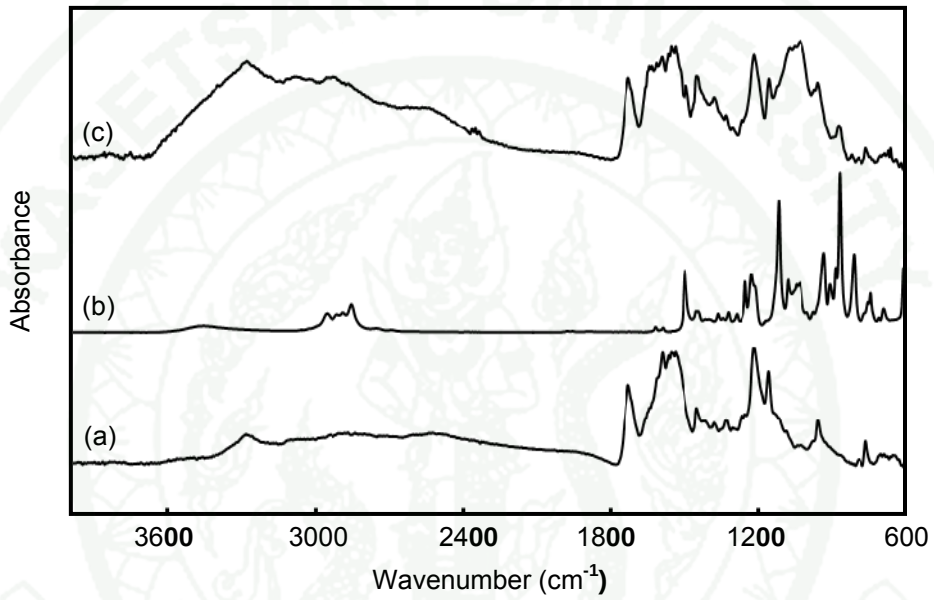

FIGURE 2. FT-IR spectra of γ-PGA (a), Bx (b) and γ-PGA-*grafted*-Bx (c)

The ^{1}H-NMR spectrum of γ-PGA-*grafted*-ethyl-Bx was shown in Figure 3. The signals of methylene protons (4H), methine proton (1H) and -NH amide proton (1H) from the γ-PGA backbone were shown at δ_H = 1.46-2.11, 2.11-2.41 and 8.04-8.28 ppm, respectively, while the signals of ethyl proton (5H), oxazine ring protons (2H) and aromatic protons (3H) from the ethyl-Bx attached to the carboxyl group of the γ-PGA backbone were shown at δ_H 0.97-1.21, 2.90-2.92 and 6.58-7.31 ppm, respectively. These results implied that the ethyl-Bx was successfully grafted into the γ-PGA backbone.

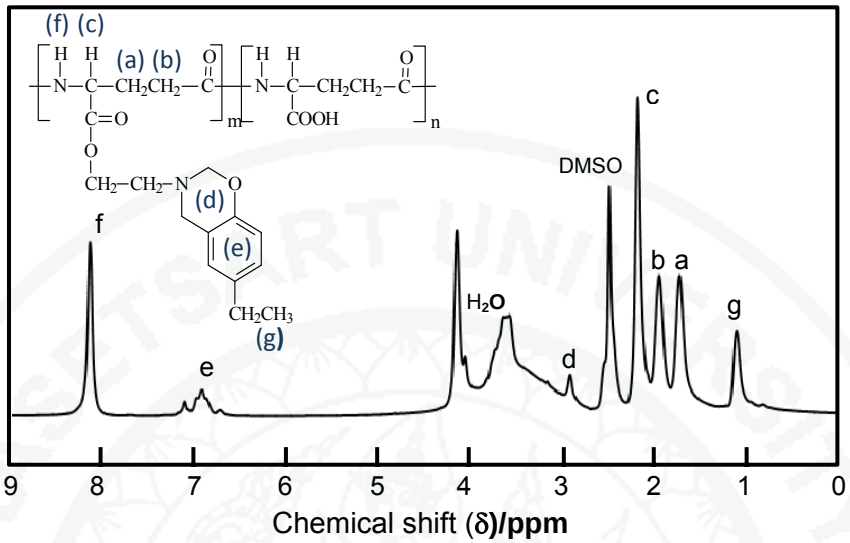

FIGURE 3. ^{1}H-NMR spectrum of γ-PGA-*grafted*-ethyl-Bx in DMSO-d6

The integration ratio of the amide proton (8.04-8.28 ppm) of γ-PGA and the aromatic proton (6.58-7.31 ppm) of ethyl-Bx was evaluated in the order to calculate the degree of grafting. The degree of ethyl-Bx grafting was found to be 25%. The characterization results of γ-PGA, ethyl-Bx and the product are summarized as follows:

Ethyl-Bx: FT-IR (KBr, cm^{-1}): 3600-2900 (br, OH), 2877 (s, CH), 1500 (oxazine ring), 1226 (s, CN), 1126 (s, CO), 1027 (s, Ar-O-C), 870 (s, CH) ;^{1}H NMR (400 MHz, $CDCl_3$, ppm): δ_H 2.21 (3H, s, Ar-**CH_3**), 2.93 (2H, t, **CH_2**CH_2OH J_2 = 3.11 Hz), 3.84 (2H, t, CH_2**CH_2**OH J_2 = 3.11 Hz), 4.33 (2H, s, Ar-**CH_2**-N), 4.83 (2H, s, O-**CH_2**-N), 6.70 (H, d, **Ar-H**, J_3 = 2.34 Hz), 6.71. (H, s, **Ar-H**), 6.77 (H, d, **Ar-H**, J_3 = 2.34 Hz). ESI-MS (m/z): 194 (M+1).

γ-PGA: FT-IR: 3283 (br, OH), 3000-2200 (br, CH), 1730 (s, C=O (carboxy)), 1640 (s, C=O (amide)), 1225 (s, C-O); ^{1}H NMR (400 MHz, DMSO-d_6, ppm): δ_H 1.75, 1.95 (2H(diastereotropic hydrogens), t, **CH_2**CH_2C=O J_2 = 6.90 Hz), 2.20 (2H, t, CH_2**CH_2**C=O J_2 = 6.90 Hz), 4.14 (H, s, NH**CH**CH_2), 8.13 (H, d, **NH**, J_3 = 5.91 Hz).

γ-PGA-*grafted*-ethyl-Bx: FT-IR: 3600-3200 (br, OH), 2978-2450 (br, CH), 1727 (s, C=O (carboxy)), 1613 (s, C=O (amide)), 1494 (oxazine ring), 1225 (s, C-O),

1073 (s, CO), 878 (s, CH); ^{1}H NMR (400 MHz, DMSO-d_6, ppm): δ_H 1.78 (2H, t, CH_2**CH_2**C=O J_2 = 5.84 Hz), 2.00 (2H, t, **CH_2**CH_2C=O J_2 = 5.84 Hz), 2.12 (3H s, Ar-**CH_3**), 2.23 (H, d, NH**CH**CH_2 J_3 = 7.88 Hz), 2.94 (2H, s, O-**CH_2**-N), 6.87 (H, d, **Ar-H**, J_4 = 12.6 Hz), 7.09 (H, d, Ar-H, J_4 = 12.6 Hz), 7.16 (H, s, **Ar-H**),8.16(H, d, **NH**, J_5 = 7.35 Hz).

Investigation on iron(III) ions responsive properties of γ-PGA-grafted-ethyl-Bx

The iron(III) ions responsive properties of γ-PGA-*grafted*-ethyl-Bx were primary investigated with naked eye (figure 4). After the γ-PGA-*grafted*-ethyl-Bx was added into the aqueous solution of iron(III) nitrate, color of the solution was changed from clear to purple. This color transition phenomenon was further examined confirmed by using UV-visible spectrophotometer.

γ-PGA-*grafted*-ethyl-Bx **Aqueous solution of iron(III) nitrate** γ-PGA-*grafted*-ethyl-Bx-iron(III) complex in anaqueous solution

FIGURE 4. The color transition of aqueous solution of iron(III) nitrate after mixing with γ-PGA-*grafted*-ethyl-Bx

Figure 5(a) showed UV spectrum of an aqueous solution of iron(III) nitrate. The maximum absorbance was observed at 294 nm. The maximum absorption peak was shifted to 520 nm after the γ-PGA-*grafted*-ethyl-Bx was added into the solution Figure 5(b). This result indicated that γ-PGA-*grafted*-ethyl-Bx formed complex with the iron(III) ions resulting in color transition of the solution.

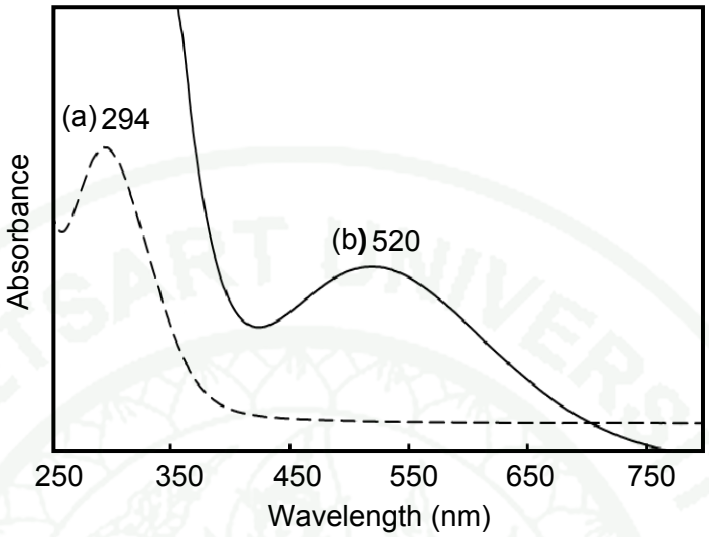

FIGURE 5. UV-visible absorption spectra of an aqueous solution of iron(III) nitrate (a), and mixture of γ-PGA-*grafted*-ethyl-Bx and iron(III) nitrate in an aqueous solution (b)

Iron(III) ions responsive properties of γ-PGA-*grafted*-ethyl-Bx was additionally observed in DMSO solution. The solution of γ-PGA-*grafted*-ethyl-Bx in DMSO solution was mixed with iron(III) nitrate in DMSO solution. Then color of the mixture was immediately changed from clear to red (figure 6). This color transition phenomenon was further confirmed by using UV-visible spectrophotometer.

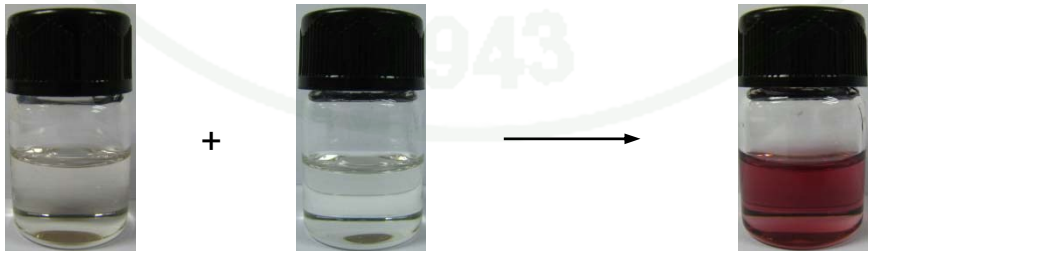

FIGURE 6. Color transition of the DMSO solution of the iron(III) ion after γ-PGA-*grafted*-ethyl-Bx solution was added

Figure 7 showed UV spectra of solution of γ-PGA-grafted-ethyl-Bx in DMSO, iron(III) nitrate in DMSO and the mixed solution of γ-PGA-*grafted*-ethyl-Bx and iron(III) nitrate in DMSO. The maximum absorption peak was shifted to 503 nm after the complex between the γ-PGA-grafted-ethyl-Bx and iron(III) ions was formed. The obtained results indicated that γ-PGA-grafted-ethyl-Bx showed sensitivity to iron(III) ions in both water and DMSO dolutions.

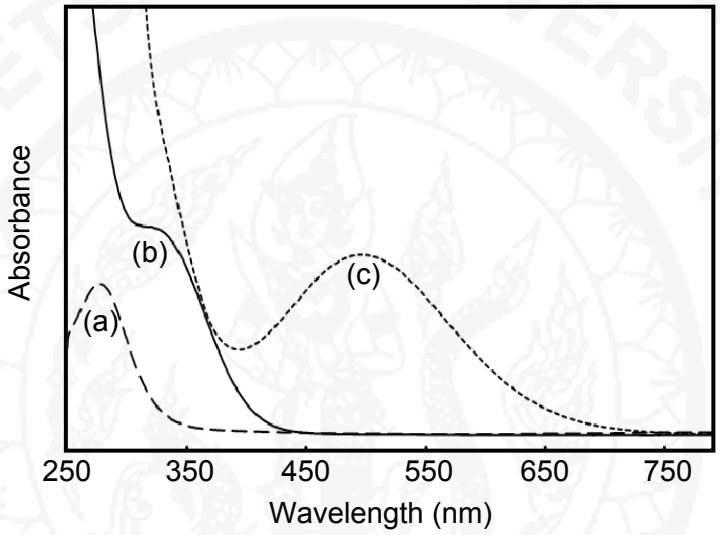

FIGURE 7. UV-Vis absorption spectra of solution of γ-PGA-*grafted*-ethyl-Bx in DMSO (a), iron(III) nitrate in DMSO (b), and mixture of γ-PGA -*grafted*-ethyl-Bx and iron(III) nitrate in DMSO solution (c)

The qualitative analysis to determine a ratio of the polymer to iron(III) ions in the complex was carried out by using a photometric titration method. The solution of the γ-PGA-*grafted*-ethyl-Bx and iron(III) ions were prepared by using DMSO as a solvent. In this study, different amount of the polymer solution was added into the iron(III) ions solution. The ratio of γ-PGA-*grafted*-ethyl-Bx complexed with iron(III) ions was evaluated from the absorbance at the maximum wavelength (λmax) of the complex at 501 nm. Figure 8 showed the result obtained from the titration method. It was found that the absorbance increase as quantity of the polymer in the solution increased at the beginning, and then it is started to be constant after the polymer

solution was add more than 1.63 ml. Calculation based on these results revealed that the ratio of γ-PGA-*grafted*-ethyl-Bx to the iron(III) ion was 1:154.

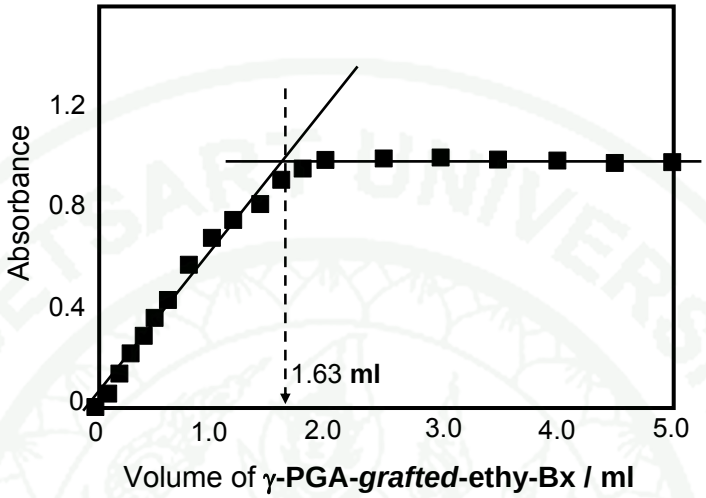

FIGURE 8. Relationship between absorbance at 501 nm and volume of γ-PGA-*grafted*-ethyl-Bx solution (0.008 mmole) from photometric titration method.

Conclusions

Color transition based sensor for iron(III) ions was developed in this study by grafting 3,4-Dihydro-3-(2″-ethyl hydroxyl)-6-ethyl-2*H*-benzoxazine (ethyl-Bx) into γ-PGA backbone. The grafting degree was approximately 25%. This grafted copolymer showed sensitive response toward iron(III) ions in both aqueous and DMSO solutions. The response of the γ-PGA-*grafted*-ethyl-Bx to iron(III) nitrate can be observed from the color transition. The color was changed from clear to purple in aqueous solution and changed from clear to red in DMSO solution. The stoichiometric ratio of γ-PGA-*grafted*-ethyl-Bx to the iron(III) ion estimated from the photometric titration method was found to be 1:154

Acknowledgments

The authors would like to acknowledge the financial support from The Joint Research Program of National Research Council of Thailand (NRCT) and Japan

Society for the Promotion of Science (JSPS), the center of advanced studies in Industrial Technology and Faculty of Engineering, Kasetsart University and The graduate school Kasetsart University.

References

Abdolkarim, A.; Masoud, A. M.; Abolhasan, N.; Mohammad, A. K.; Ali, K.-N.; Mohammad, N. S. R. Speciation of iron(II), iron(III) and full-range pH monitoring using paptode: A simple colorimetric method as an appropriate alternative for optodes. Sensors and Actuators B: Chemical. 2006, 113, 857-865.

Apenysheva, T. E.; Bukov, N. N.; Sklyar, A. A.; Bolotin, S. N.; Pushkareva, K. S. Structures of copper(II) complexes with dihydrobenzoxazine derivatives in chloroform. Russion Journal of Inorganic Chemistry, 2006, 32, 335-338.

Azad, T. F.; Alan, T. Application of a reducing column for metal speciation by flow injection analysis spectrophotometric determination of iron(III) and simultaneous determination of iron(II) and total iron. Analytica Chimica Acta. 1985, 167, 225-231.

Bruke, P.W. 3,4-dihydro-1,3,2H-benzoxazines. Reaction of *p*-substituted phenols with N,N-dimethylolamine. Journal of the American Chemical Society 1949, 71, 609-612.

Dubuisson, E.; Monnier, V.; Menez, N.-S.; Boury, B.; Usson, Y.; Pansu, R. B.; Ibanez, A. Brilliant molecular nanocrystals emerging from sol–gel thin films: towards a new generation of fluorescent biochips. Nanotechnology, 2009, 20, 315301.

Dunkers, J.; Zarate, E. A.; Ishida, H. Crystal structure and hydrogen bonding characteristics of N,N-bis(3,5-dimethyl-2-hydroxybenzyl)methyl amine, a benzoxazine dimer. Journal of Physical Chemistry 1996, 100, 13514-13520.

Fan, J.-Y.; Sun, D.; Yu, H.; Kerwin, S. M.; Hueley, L. H. Self-assembly of a quinobenzoxazine-Mg2+ complex on DNA: a new paradigm for the structure of a drug-DNA complex and implications for the structure of the quinolone

bacterial gyrase-DNA complex. Journal of Medicinal Chemistry, 1995, 38, 408-424.

Gracia, de J.; Saraviab, M.L.M.F.S.; Aratijob, A.N.; Limab, J.L.F.C.; Vallec, d. M.; Pochd, M. Evaluation of natural computation techniques in the modelling and optimization of a sequential injection flow system for calorimetric iron(III) determination. Analytica Chimica Acta. 1997, 348, 143-150.

Gu, T.; Zhang, Y.; Deng, F.; Zhang, J.; Hasebe, Y. Direct electrochemistry of glucose oxidase and biosensing for glucose based on DNA/chitosan film. Journal of Environmental Sciences, 2011, 23, S66–S69.

Güler, E.; Demet, U.; Güler, S.; Şükrü, K**.** A novel iron(III) selective membrane electrode based on benzo-18-crown-6 crown ether and its applications. Journal of Membrane Science. 2007, 288, 36-40.

Hassan, A. Z.; Mohammad, R. A.; Mohammad, R. G. Monitoring of iron (III) ions with a Fe^{3+} PVC membrane sensor based on 4,4'-dimethoxybenzil bisthiosemicarbazone. Journal of the Chilean Chemical Society. 2009, 54, 186-190.

Holly, F. W.; Cope, A. C. Condensation products of aldehydes and ketones with o-aminobenzyl alcohol and o-hydroxybenzylamine. Journal of the American Chemical Society 1944, 66, 1875-1879.

Laobuthee, A.; Ishida, H.; Chirachanchai, S. Metal ion guest responsive benzoxazine dimers and inclusion phenomena of cyclic derivatives. Journal of Inclusion Phenomena and Macrocyclic Chemistry, 2003, 47, 179-185.

Liang, Z.Q.; Wang, C.X.; Yang, J.X.; Gao, H.W.; Tian, Y.P.; Tao, X.T.; Jiang, M.H. A highly selective colorimetric chemosensor for detecting the respective amounts of iron(II) and iron(III) ions in water. New Journal of Chemistry. 2007, 31, 906-910.

Maity, D.; Govindaraju, T. Highly selective colorimetric chemosensor for Co^{2+}. Inorganic Chemistry. 2011, 50, 11282-11284.

Mark, S. S.; Crusberg, T. C.; Dacunha, C. M.; Di Iorio, A. A. A heavy metal biotrap for wastewater remediation using poly-γ-glutamic acid. Biotechnology Progress, 2006, 22, 523-531.

Michael, M. B.; Mark, R. D.; Sean, M. K. The novel bis(brnzoxazine) cytotoxic natural product UK-1 is a magnesium ion-dependent DNA binding agent and inhibitor of human topoisomerase II. Bioorganic Chemistry,2007, 27, 326-337.

Oflidi, A. I.; Apenysheva, T. E.; Pushkaryova, K. S.; Frolov, V. Yu.; Bolotin, S. N.; Kolokolov, F. A.; Panyyushkin, V. T. Synthesis of copper(II) coordination compounds with benzoxazine derivatives. Russion Journal of Inorganic Chemistry, 2009, 54, 69-72.

Ogawa, Y.; Hosoyama, H.; Hamoto, M.; Motai, H. Purification and properties of γ-Glutamyltranspeptidase from Bacillus subtilis (natto). Agricultural and Biological Chemistry. 1991, 55, 2971-2977.

Panushkin, V. T.; Apenysheva, T. E.; Sokol, V. I.; Sergienko, V. S.; Pushkareva, K. S.; Bolotin, S. N.; Kolokolov, F. A.; Gromachevskaya, E. V.; Borogavko, A. A.; Kosulina, T. P. The copper(II) acetate complex with 2-(2-hydroxyphenyl)-4,4-diphenyl-1,2-dihydro-4H-3,1-benzoxazine. Russion Journal of Inorganic Chemistry, 2007, 33, 674-679.

Pedro, M.-N.; Laurent, A. B.; Avelino, C.; Hermenegildo, G. Dual-response colorimetric sensor array for the identification of amines in water based on supramolecular host–guest complexation. Tetrahedron Letters. 2009, 50, 2301-2304.

Phongtamrug , S.; Chirachanchai, S.; Tashiro, K. Supramolecular structure of N,N-Bis(s-hydroxybenzyl) alkylamine: from hydrogen bond assembly to coordination network in guest acceptance. Macromolecular Symposium, 2006, 242, 40-48.

Robert, E.; James, J. S.; Robert, C. M.; Robert, L. L.; Chad, A. M. Selective colorimetric detection of polynucleotides based on the distance-dependent optical properties of gold nanoparticles. Science. 1997, 277, 1078-1081.

Rungsimanon, Th.; Laobuthee, A.; Miyata, M.; Chirachanchai, S. [1+1] and [2+2] crown ethers derived from N,N-bis(2-hydroxyalkylbenzyl) alkalamine and their inclusion phenomena with metal ions. Journal of Inclusion Phenomena and Macrocyclic Chemistry, 2008, 62, 333-338.

Shih, I.L.; Van, Y.-Ts.; Sau, Y.Y. Antifreeze activities of poly(γ-glutamic acid) produced by *Bacillus licheniformis*. Biotechnology Letters, 2003, 25, 1709-1712.

Song, J.; Cheng, Q.; Zhu, Sh.; Stevens, C. R. "smart" materials for biosensing devices: cell-mimicking supramolecular assemblies and colorimetric detection of pathogenic agents. Biomedical micro devices. 2002, 4, 213-221.

Sun, J.; Ge, J.; Liu, W.; Fan, Zh.; Zhang, H.; Wang, P. Highly sensitive and selective colorimetric visualization of streptomycin in raw milk using Au nanoparticles supramolecular assembly. Chemical Communications. 2011, 47, 9888-9890.

Sung, M. H.; Park, C.; Kim, C. J.; Poo, H.; Soda, K.; Ashiuchi, M. Natural and edible biopolymer poly-γ-glutamic acid: synthesis, production, and applications. The Chemical Record. 2005, 5, 352-366.

Takami, A.; Tatsuo, K.; Toshiyuki, K.; Mitsuru, A. Preparation and characterization of biodegradable nanoparticles based on poly(γ-glutamic acid) with L-phenylalanine as a protein carrier. Journal of Controlled Release. 2005, 108, 226– 236.

Taniguchi, M.; Kato, K.; Shimauchi, A.;Ping, X.; Nakayama, Fujita, K.-J.; Tanaka, T.; Tarui, Y.; Hirasawa, E. Proposal for wastewater treatment by applying flocculating activity of cross-linked poly-γ-glutamic acid. Journal of Bioscience and Bioengineering, 2005, 99, 245-251.

Taniguchi, M.; Kato, K.; Matsui, O.; Nakayama, H.; Usuki, Y.; Ichimura, A.; Fujita, K.-I.; Tanaka, T.; Tarui, Y.; Hirasawa, E. Flocculating activity of cross-linked poly-γ-glutamic acid against bentonite and *Escherichia coli* suspension pretreated with $FeCl_3$ and its interaction with Fe^{3+}. Journal of Bioscience and Bioengineering, 2005, 100, 207-211.

Veranitisagul, Ch.; Kaewvilai, A.; Sangngern, S.; Wattanathana, W.; Suramitr, S.; Koonsaeng, N.; Laobuthee, A. Novel recovery of nano-structured ceria (CeO2) from Ce(III)-benzoxazine dimer complexs via thermal decomposition. International Journal of Molecular Sciences, 2011, 12, 4365-4377.

Wang, B.; Hai, J.; Liu, Z.; Wang, Q.; Yang, Z.; Sun, S. Selective detection of iron(III) by rhodamine-modified Fe_3O_4 nanoparticles. Angewandte Chemie. 2010, 49, 4576-4579.

Wanga, Q.; Tana, C. Terbium hybrid particles with spherical shape as luminescent probe for detection of Cu^{2+} and Fe^{3+} in water. Analytica Chimica Acta. 2001, 708, 111-115.

Zhang, M.; Zheng, B.; Yuan, H.; Xiao, Dan. A spectrofluorimetric sensor based on grape skin tissue for determination of iron(III). Bulletin of the Chemical Society of Ethiopia. 2010, 24, 31-37.

CIRRICULUM VITAE

NAME **:** Miss Nuorn Choothong

BIRTH DATE **:** September 8, 1984

BIRTH PLACE **:** Prachaupkhirikhan, Thailand

EDUCATION **:**

YEAR	**INSTITUTE**
2009	Silapakorn University

DEGREE/DIPLOMA

B.Eng. (Engineering Petrochemicals And Polymeric Materials)